AD_____

Award Number:

W81XWH-06-1-0320

TITLE:

Understanding the mechanisms through which Matrix Metalloproteinases (MMPs) contribute to Breast Cancer-associated Osteolytic lesions

PRINCIPAL INVESTIGATOR:

Sophie Thiolloy

CONTRACTING ORGANIZATION:

Vanderbilt University Medical Center
Nashville, TN 37203-6869

REPORT DATE: March 2009

TYPE OF REPORT:

Annual Summary

PREPARED FOR: U.S. Army Medical Research and Materiel Command
Fort Detrick, Maryland 21702-5012

DISTRIBUTION STATEMENT:

X Approved for public release; distribution unlimited

Form Approved
OMB No. 0704-0188

1. REPORT DATE *(DD-MM-YYYY)*	**2. REPORT TYPE**	**3. DATES COVERED** *(From - To)*
01-03-2009	Annual Summary	15 Feb 2006 - 14 Feb 2009

4. TITLE AND SUBTITLE
Understanding the mechanisms through which Matrix Metalloproteinases (MMPs) contribute to Breast Cancer-associated Osteolytic lesions

5a. CONTRACT NUMBER
W81XWH-06-1-0320

5b. GRANT NUMBER

5c. PROGRAM ELEMENT NUMBER

6. AUTHOR(S)
Thiolloy Sophie

5d. PROJECT NUMBER

5e. TASK NUMBER

5f. WORK UNIT NUMBER

7. PERFORMING ORGANIZATION NAME(S) AND ADDRESS(ES)
Vanderbilt University Medical Center

Nashville, TN 37203-6869

8. PERFORMING ORGANIZATION REPORT NUMBER

9. SPONSORING / MONITORING AGENCY NAME(S) AND ADDRESS(ES)
U.S. Army Medical Research and Materiel Command
Fort Detrick, MD 21702-5012

10. SPONSOR/MONITOR'S ACRONYM(S)

11. SPONSOR/MONITOR'S REPORT NUMBER(S)

12. DISTRIBUTION / AVAILABILITY STATEMENT
Approved for public release; distribution unlimited

13. SUPPLEMENTARY NOTES

14. ABSTRACT
Bone metastasis is a common event during breast cancer (BC) progression. Matrix Metalloproteinases (MMPs) are often overexpressed in BC and play an important role in tumor progression. Metastatic BC is primarly osteolytic and we hypothesize that specific host derived MMPs contribute to the growth and development of osteolytic lesions. In an intratibial model that recapitulates breast induced osteolysis, we demonstrated that host MMP-2 and MMP-7 are required for mammary tumor growth in the bone and the development of osteolytic lesions. However MMP-9 does not affect tumor growth and bone resorption in our model of mammary tumor-associated bone lesions. Osteoclast-derived MMP-7 mediates its effect through the processing of RANKL into its soluble form which increases osteoclast precursor cell recruitment and activation. Osteoblast-derived MMP-2 impacts mammary tumor survival in the bone microenvironment by controlling levels of active TGF-β via the processing of its latency protein, LTBP-3, novel substrate for MMP-2. In conclusion, drugs targeting specifically MMP-2 and MMP-7 could be used in combination with currently used therapies to improve treatment of BC-associated with osteolytic lesions.

15. SUBJECT TERMS
Breast cancer, Matrix Metalloproteinases, osteolysis, RANKL, TGF-beta

16. SECURITY CLASSIFICATION OF:			**17. LIMITATION OF ABSTRACT**	**18. NUMBER OF PAGES**	**19a. NAME OF RESPONSIBLE PERSON**
a. REPORT	**b. ABSTRACT**	**c. THIS PAGE**			USMARMC
U	U	U	UU	83	**19b. TELEPHONE NUMBER** *(include area code)*

Table of Contents

Page

Introduction

In the United States, 80% of the women who will succumb to breast cancer, this year, will have evidence of bone metastasis(Coleman and Rubens, 1987). The process of breast to bone metastasis illustrates the "seed and soil theory" which suggests that certain tumors spread to specific organs depending on the complexity of the interactions between the tumor cells (seed) and their environment (soil)(Paget, 1989). The skeleton is a common site for metastasis in many cancers such as breast, lungs or prostate cancer. Breast to bone cancer metastases are typically osteolytic and induce bone destruction(Mundy, 2002).

The MMPs are a family of enzymes that degrade the extracellular matrix and a variety of signaling molecules and cell surface receptors such as osteopontin, TNF-α, TGF-β and RANKL(Agnihotri et al., 2001; Haro et al., 2000; Lynch et al., 2005). Thus, MMPs, by cleaving and/or solubilizing these functional factors, can modify the communication between tumor cells and the host microenvironment(Lynch and Matrisian, 2002). In the normal bone stroma, a number of MMPs have been detected in osteoclasts, the cells responsible for bone resorption, including MMP-3, -7, -9, -13 and –14(Engsig et al., 2000). Our understanding of the contribution of specific MMPs to pathological conditions such as breast cancer induced osteolysis is limited. The use of broad spectrum MMP inhibitors can decrease and even prevent breast tumor induced osteolysis in animal models(Lee et al., 2001; Nemeth et al., 2002; Winding et al., 2002). However, these broad spectrum inhibitors have dose-limiting side effects which limit their usefulness (Coussens et al., 2002). The contribution of specific MMPs to the observed tumor growth and osteolysis remains to be determined. In the current project, we are investigating the role of specific MMPs in mammary tumor growth induced osteolysis and determining the molecular mechanisms through which specific MMPs contribute to this process.

Project

Accomplishment

Task 1. *Determination of the contribution of stromal MMP-2, -3, -7 and -9 to mammary tumor growth and osteolysis in the in vivo tumor:bone microenvironment.*

- **a.** Intra-tibial injection of luciferase tagged PLB1 (forms primary tumors, induces bone destruction and forms lung metastases) cells studies in MMP deficient (MMP-2, -3, -7 and -9) and wild-type FVB mice (months 1-24): familiarization with real time imaging modalities such as Xenogen's IVIS system for monitoring luciferase activity (months 1-6).
- **b.** Generation of *in situ* hybridization protocols for MMPs in bone tissue (months 7-30).
- **c.** Histological analysis of wild-type and MMP deficient mice intra-tibially injected with PLB1 cells (months 3-30) and immunohistochemistry and cytochemistry for the localization of tumor cells, bone cells and immune cells in sections from intra-tibially implanted tumors.
- **d.** Collation of the data and publications of the results (months 27- 36).

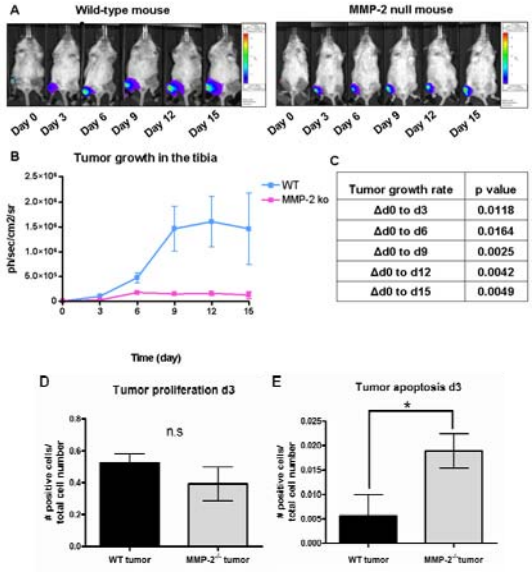

Figure 1. *Stromal MMP-2 increases mammary tumor growth in the bone.* We injected PLB1 luciferase cells into the tibia of FVB wild-type (n=11) or MMP-2 null mice (n=10) and image them over time (days 0, 3, 6, 9, 12, 15) using the IVIS system from Xenogen (A). The bioluminescent signal was quantified using the living image software (B). The tumor growth rate for each time point in the two groups of animals was calculated (C). Tumor proliferation and apoptosis were assessed by immunohistochemistry for MCM2 and active caspase-3 respectively (D and E).

Our initial studies have focused on MMP-2 and MMP-9. To assess if stromal MMP-2 affects mammary tumor growth in the bone, we injected the murine breast cancer PLB1 cells into

the tibias of wild-type (n=11) or MMP-2 deficient (n=10) FVB mice. This cell line has been isolated from the polyoma middle T antigen (PyMT) FVB mice. These mice develop spontaneous mammary tumors that recapitulate the pathology of human breast cancer(Lin et al., 2003). Using this cell line allows for the use of fully immune competent FVB mice representing a more accurate human scenario. After injection of the PLB1 cells tagged with luciferase, the growth of the tumor was quantified every 3 days by a retro-orbital injection of luciferin (105ng/kg). Photoemission from the tumor was quantified with the Xenogen IVIS^{TM} imaging system (**Figure 1**). From day 3 onwards, we observed a significant difference in the tumor growth rate in the MMP-2 null mice compared to the wild-type animal ($p<0.02$, Student's *t* Test). We confirmed this tumor growth effect with an independent cell line 4T1 cells expressing luciferase in immunocompromised Rag2 null wild-type and MMP-2 null C57Bl/6 mice.

In order to investigate further the effect of host MMP-2 on tumor growth, we assessed tumor proliferation and apoptosis by using a flow cytometry approach. PLB1 cells expressing green fluorescent protein (GFP) were injected into wild-type and MMP-2 deficient mice. Tumor and bone marrow cells were isolated from the tibia and processed for cytometry analysis to determine tumor proliferation using phospho histone H3 and apoptosis by using cleaved caspase-3. However, PLB1 cells retain a level of GFP *in vivo* below the detection capacity of the flow cytometer. Therefore, we decided to use a histochemical approach and use MCM2 as a marker of proliferation and cleaved caspase-3 as an indicator of apoptosis. After 3 days post-surgery, tumor injected limbs were harvested and processed for histochemical staining for tumor proliferation and apoptosis. Tumor proliferation was not different between tumor injected MMP-2 deficient mice compared to wild-type controls, however, tumor apoptosis was significantly increased in MMP-2 null mice compared to control mice (**Figure 1**). These results suggest that host derived MMP-2 impacts mammary tumor growth in the bone by contributing to tumor survival as early as 3 days post-injection.

To determine the role of host MMP-2 in mammary tumor induced osteolysis *in vivo*, trabecular bone volume was assessed using a high resolution micro-computer tomography (µCT) and histomorphometry at 9 days after surgery (**Figure 2A and C**). Tumor injected tibia of wild-type mice presented a significant lower ratio of trabecular bone volume compared to the sham injected limb ($p<0.005$). However tumor bearing limbs of MMP-2 null animals did not show any difference compared to sham injected limbs in terms of bone resorption. More interestingly, MMP-2 deficient mice presented a significant higher ratio of trabecular bone volume to tissue volume (BV/TV) compared to the wild-type controls ($p<0.05$). In other words, MMP-2 deficient mice presented a lesser extent of bone resorption induced by the presence of the mammary tumor compared to the wild-type control animals. X-rays analysis revealed that MMP-2 deficient mice showed a significant lower tumor burden compared to wild-type controls ($p=0.0016$, **Figure 2B**). Finally the ratio of osteoclast number per unit of length of trabecular bone was assessed in tumor and sham injected tibias by histomorphometry, MMP-2 deficient mice bearing tumor presented a significant decreased number of osteoclasts compared to the controls ($p<0.05$, **Figure 2D**). Taken together, we demonstrated that host-derived MMP-2 impacts mammary tumor growth in

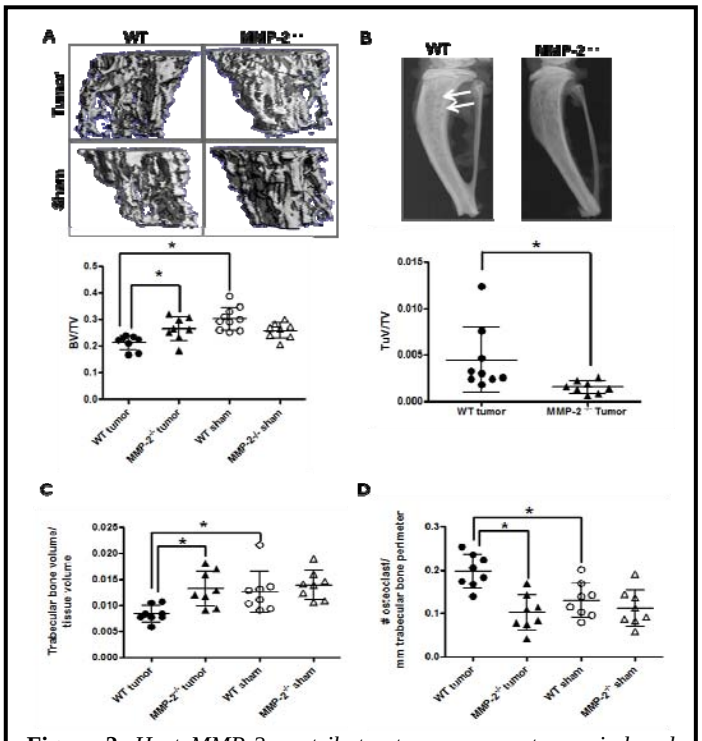

Figure 2. *Host MMP-2 contributes to mammary tumor induced bone resorption.* PLB1 luciferase cells were injected intratibially into FVB wild-type or MMP-2 null mice. At day 9 after injection, the animals were sacrificed and histological analyses were performed. (A and C) The ratio of BV/TV was determined using µCT and histomorphometry analyses on tumor and sham injected tibias. (B) Using X-ray analysis, the ratio of TuV/TV was assessed in tumor bearing limbs. Arrows indicate lytic lesion in the bone. (D) The ratio of osteoclast number per unit of length of trabecular bone was assessed by histomorphomtery in tumor and sham injected tibias.

the bone by enhancing tumor survival as early as 3 days after injection. Furthermore, stromal MMP-2 contributes to tumor induced osteolysis.

We also investigated the contributions of host derived MMP-9 in tumor growth and bone resorption in our *in vivo* model. We injected PLB1-luciferase cells into the tibia of FVB wild-type and MMP-9 null mice and tumor growth into the tibia was followed using bioluminescent imaging for 9 days. Immunofluorescent stainings for MMP-9 and TRAcP showed that multinucleated TRAcP positive osteoclasts present at the tumor:bone interface are the major source of MMP-9 (**Figure 3A**). Although, mature osteoclasts seem to be the main source of MMP-9, no difference was observed in the growth of the tumor between MMP- 9 deficient mice and control mice (**Figure 3B**). Using µCT and analysis trabecular bone volume was assessed in the tumor and sham injected limb at the end point of the study in agreement with the tumor growth data (**Figure 3A-B**). We concluded from this study that host-derived MMP-9 does not affect either mammary tumor growth or bone resorption upon intratibial injection. However, the limitations of our mouse model itself prevented us from addressing the potential contributions of stromal MMP-9 in earlier steps of metastasis such as survival in the blood stream or extravasation into a secondary site.

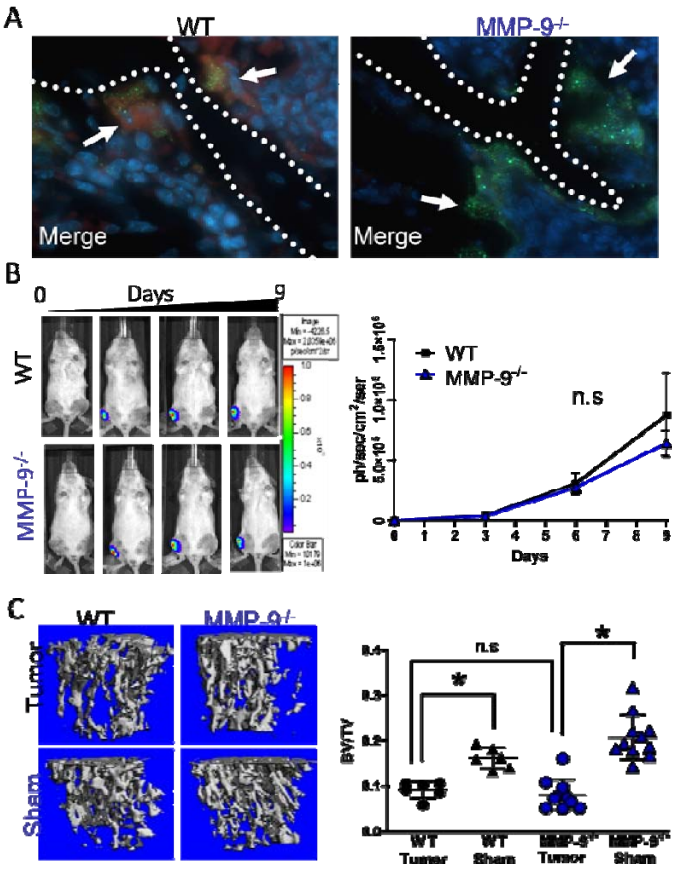

Figure 3. *Host MMP-9 does not significantly contribute to mammary tumor progression in the bone.* (A) Representative photomicroraphs (630X magnification) of MMP-9 (red) localization merged with TRAcP (green) localization in WT and MMP-9$^{-/-}$ animals. DAPI (blue) was used as a nuclear stain. Arrows indicate osteoclasts while dashed line represents the tumor: bone interface. (B) PLB1-Luc cells were injected intratibially into syngeneic FVB wild type or MMP-9 null, luminescence was measured over a 9 day period. (C) Representative µCT scans and quantification of BV/TV of tumor bearing and sham injected limbs of WT and MMP-9-/- animals

As MMP-7 deficient mice were not available in FVB background, we investigated the contributions of MMP-7 in tumor growth in the bone in the immunodeficient Rag2 deficient C57BL/6 mice, lacking mature B and T cells. PLB1-Luciferase cells were injected into the tibia of wild-type and MMP-7 deficient mice. Co-immunofluorescent stainings for MMP-7 and TRAcP showed that mature osteoclasts are the main source of MMP-7 in tumor bearing limbs (**Figure 4A**). Upon intratibial injection of the PLB1-luciferase cells, a significant slower tumor growth rate was observed in the MMP-7 null Rag2 null mice compared to the control mice (**Figure 4B**). To investigate further the effect of host derived MMP-7 on tumor growth, tumor proliferation and apoptosis were determined by immunohistochemical staining for respectively, phopho histone H3 and cleaved caspase-3, at 9 days post-surgery that was the end point of the study (**Figure 4C-D**). MMP-7 deficient mice bearing tumor showed no difference in terms of tumor proliferation; however levels of tumor apoptosis were significantly higher in MMP-7 null mice compared to the wild-type controls, suggesting a contribution of host MMP-7 to tumor survival in the bone.

We also assessed the contributions of host derived MMP-7 to tumor induced osteolysis in our model at 9 days after intratibial injection. By µCT and histomorphometry, the MMP-7 deficient mice showed a significant lower extent of bone resorption in the tumor bearing limbs compared to wild-type animals (**Figure 5A-B**). Tumor burden assessed by X-rays was also significantly lower in the tumor injected legs of MMP-7 animals compared to the controls (**Figure 5C**).

The second part of this project was focused on determining the mechanism through which host-derived MMP-7 and MMP-2 contribute to tumor survival and bone resorption.

Task 2. *Identification of the mechanism by which specific host derived MMPs contribute to breast tumor induced osteolysis using an ex vivo approach.*

- **a.** Generation and characterization of the *ex vivo* calvaria model (months 1-6).
- **b.** Isolation of MMP deficient calvaria and histological assessment of tumor induced bone destruction. MMP deficient animals to use will be identified in Task 1, part a (months 6-32).
- **c.** Collation of the data and publication of results (months 34-36)

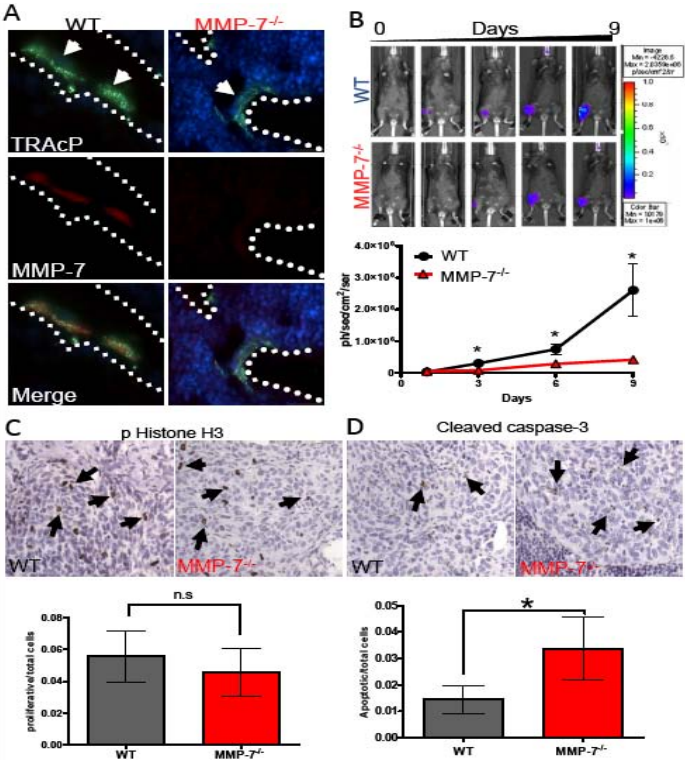

Figure 4. *Host MMP-7 contributes to mammary tumor induced osteolysis.* (A) Representative photomicroraphs of MMP-7 (red) localization merged with TRAP (green) localization in WT and MMP-7$^{-/-}$ animals. DAPI (blue) was used as a nuclear stain. Arrows indicate osteoclasts while dashed line represents the tumor: bone interface. (B) PLB1-Luc cells were injected intratibially into syngeneic FVB wild type or MMP-7 deficient mice; luminescence was measured over a 9 day period. (C and D), tumor proliferation and apoptosis were assessed by immunohistochemical staining for phospho histone H3 and cleaved

The execution of this task relied on the use of an *ex vivo* calvaria model described by Ohshiba *et al*, 2003(Ohshiba et al., 2003). We focused our initial effort on understanding how MMP-2 contributes to mammary tumor induced osteolysis since such a significant effect had been observed in task 1. MMP-2 deficient mice showed a difference in the amount of trabecular bone loss as well as a decrease in the number of mature osteoclasts. Thus we investigated the potential role of host MMP-2 in osteoclast function and migration as our observations in the MMP-2 deficient mice could be due to a failure of the osteoclasts MMP-2 null osteoclasts to act properly. Unfortunately, the *ex vivo* calvaria model did not recapitulate the observed effects i*n vivo* with respect to tumor induced osteolysis. Therefore, we took *in vitro* as well as *in vivo* approaches to test the role of host derived MMP-2 in osteoclast migration and function. Impaired osteoclast function in MMP-2 deficient mice and subsequent decreased bone resorption could induce a decrease in mammary tumor growth in the bone. As osteoclasts derive from the monocyte/macrophage lineage, we determined if the differences in tumor growth and bone resorption observed were due to a difference in the immune cell populations. We established by FACS the immunotype of both groups of mice in the presence and absence of tumor. We used specific immune markers such Gr-1 (neutrophils), B220 (B cells), CD4 (T cells), F4/80 (activated macrophages) and CD11b (monocytes). No striking difference was observed in the different immune cell populations between the MMP-2 null mice and the controls. Therefore, the impaired bone resorption induced by mammary tumor growth in MMP-2 deficient mice was not caused by a decreased in the osteoclast precursor cell population. Furthermore, CD11b positive osteoclast precursors cells isolated from MMP-2 deficient mice did not show any difference in terms of migration, differentiation into mature osteoclast and resorption of dentin compared to osteoclast precursor cells derived from wild-type mice (data not shown). We concluded that MMP-2 deficient osteoclast precursor cells were as potent as wild-type osteoclast precursor cells in migration and differentiation and furthermore, MMP-2 null osteoclasts are as functional as wild-type control cells. Thus, the lower extent of bone resorption observed in MMP-2 deficient mice in presence of the tumor is unlikely to be caused by a defect in osteoclast function.

Since we observed an effect of host MMP-2 in tumor growth and survival, we then focused on factors in the bone that can control tumor growth such as TGF-β or insulin growth factor (IGF). TGF-β is stored in the bone matrix as a large latent complex (LTBP-LAP-TGF-β). Successive processing by proteases including several MMPs induce the release of first LAP-TGF-β (small latent TGF-β complex) and ultimately active TGF-β (Dubois et al., 1995; Saharinen et al., 1999). Studies have demonstrated that MMP-2 has the ability to release both the small latent complex and active TGF-β (Dallas et al., 2002; Yu and Stamenkovic, 2000). We determined the levels of LAP-TGF-β and phospho-Smad2 in the lysates of tumor bearing limbs of MMP-2 deficient and wild-type mice, 3 days post-surgery. MMP-2 deficient mice bearing tumor presented a higher level of LAP-TGF-β and a decreased level of phospho-Smad2 compared to the wild-type controls (**Figure 6A-B**). This indicates a decreased level of activation of the TGF-β signaling pathway in the MMP-2 null mice compared to the controls. Therefore, we concluded that absence of host-derived MMP-2 impacts the activation of TGF-β in the bone microenvironment which ultimately affects the TGF-β pathway in the tumor. Dallas and colleagues have demonstrated that MMP-2 and MMP-9 are able to cleave LTBP-1 inducing the release of the small latent form of TGF-β and therefore regulating the availability of TGF-β in the bone environment (Dallas et al., 2002). LTBP-3, another member of the LTBP family, has been linked to bone development; LTBP-3 deficient mice present growth retardation, an abnormal cranio-facial development and develop osteoclerosis and osteoarthritis (Dabovic et al., 2002; Dabovic et al., 2005). Based on these data, we hypothesis that host MMP-2 is important for the release of TGF-β through the cleavage of LTBP-3 from the large latent complex. As no recombinant LTBP-3 protein and specific antibody are commercially available, we obtained from Dr Daniel Rifkin, New York University School of Medicine, mouse LTBP-3 and TGF-β1 expression plasmids. To assess the susceptibility of LTBP-3 for proteolytic processing, the conditioned medium of COS-7 cells overexpressing the large latent complex of LTBP-3 and LAP-TGF-β was subjected to digestion with recombinant active MMP-2 (**Figure 7A**). The molecular weight of the complex was reduced from ~240 kDa to ~230-220 kDa in the presence of recombinant active MMP-2, a processing event that has been previously reported to be the result of plasmin cleavage (**Figure 7A**) (Penttinen et al., 2002). These data demonstrate for the first time that

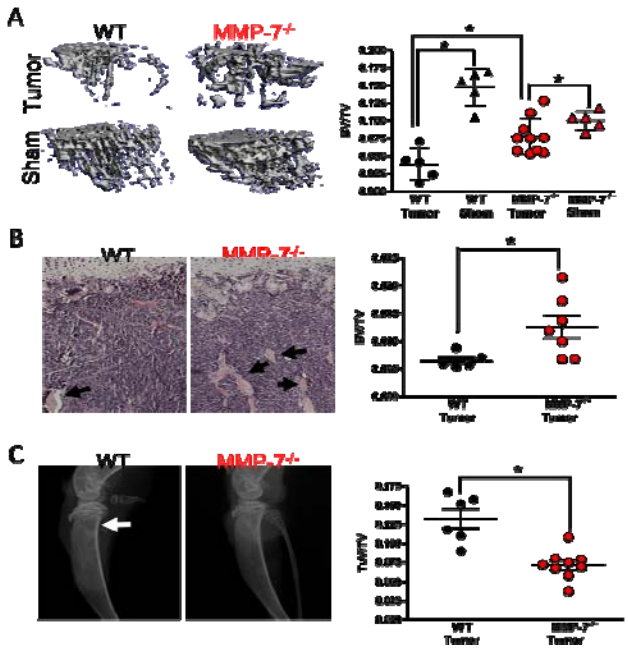

Figure 5. *Tumor mediated osteolysis is attenuated in the absence of host derived MMP-7.* (A) Representative μCT scans of trabecular bone from tumor and sham injected limbs of WT and MMP-7$^{-/-}$ mice. (B) Representative H&E stained photomicrographs of tumor bearing tibias from WT and MMP-7$^{-/-}$ mice. Arrows indicate trabecular bone. The BV/TV ratio was determined in sections of tumor injected tibias from WT and MMP-7 deficient mice. (C) Representative radiographic images from tumor injected WT and MMP-7$^{-/-}$ mice at day 9. Arrow indicates lytic tumor lesions. The ratios of TuV/TV were assessed for WT and MMP-7$^{-/-}$ animals.

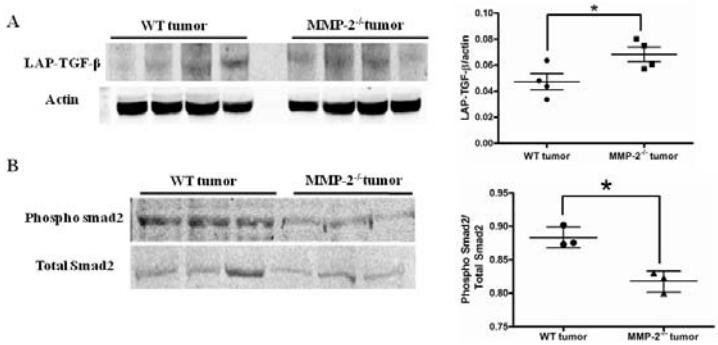

Figure 6. *Increased level of latent TGF-β inducing a decreased pathway activation in MMP-2 null mice bearing tumor.* Wild-type and MMP-2 null mice were injected with PLB1-luciferase cells and tumor and sham injected tibias were harvested 3 days post surgery. (A) Western blot for LAP and actin proteins were perform on lysates, quantifications of the bands were performed using the Li-Cors Odyssey imaging system, results were expressed as ratio of LAP signal over actin signal. (B) Western blot for phosho and total Smad2 proteins were performed on lysates, the results were expressed as ratio of phospho Smad2 signal over total Smad2 signal. All western blot analyses were performed on two different set of samples (n=3 to 4 mice for each group).

MMP-2 has the ability to process the latency binding protein of TGF-β responsible for sequestering TGF-β in the bone matrix.

The ability of TGF-β to promote tumor survival and growth of the PyMT-Luc cells was assessed in a soft agar colony formation assay. Treatment of the tumor cells with TGF-β significantly increased the number of colonies but not the size of the colonies compared to the control condition (**Figure 7B**). To assess the possibility that TGF-β could mediate tumor survival in conditioned media from osteoblast, neutralizing TGF-β antibody, 2G7, was used to treat cell culture media harvested from wild type and MMP-2 deficient primary osteoblasts. Blocking of TGF-β in conditioned media of wild type osteoblasts significantly reduced tumor metabolic activity (**Figure 7C**). These data support the hypothesis that osteoblast-derived MMP-2 regulates the levels of TGF-β in the tumor-bone microenvironment, ultimately impacting tumor cell survival.

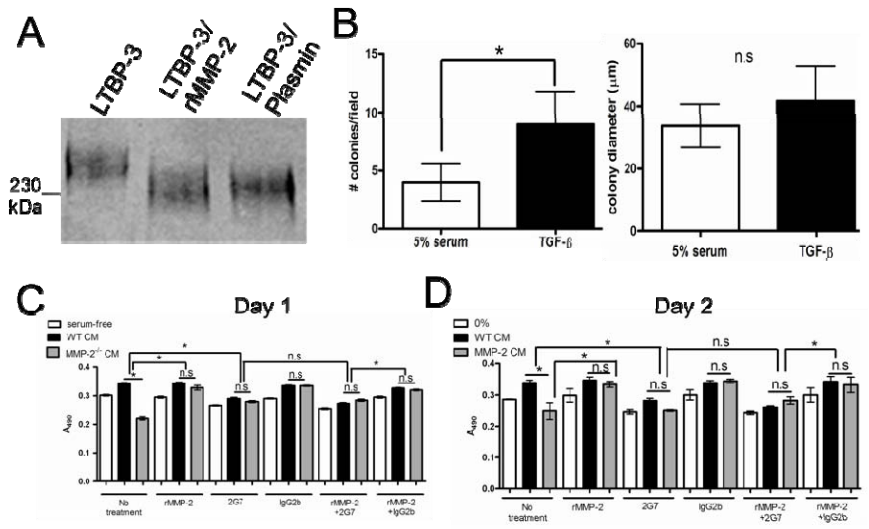

Figure 4. Osteoblast-derived TGF-β mediates tumor survival. **A:** Cleavage assay of LTBP-3 by recombinant MMP-2 or plasmin. **B** Tumor survival and growth in presence of WT CM, MMP-$2^{-/-}$ CM or 1 ng/ml TGF-β was determined by soft agar colony formation assay. Number of colonies and colony diameter were reported for each condition. PyMT-Luc cells were treated with conditioned media from wild type (WT CM)or MMP-2 null (MMP-$2^{-/-}$ CM)osteoblasts. Ability of the tumor cells to proliferate and survive was assessed by MTT and soft agar colony formation assays. **C and D:** Metabolic activity of PyMT-Luc cells treated with WT CM or MMP-$2^{-/-}$ CM in presence of 2G7 (TGF-β neutralizing antibody), IgG2b (control antibody) or recombinant MMP-2 (rMMP-2) was assessed by MTT assay. Data are mean ± SD. Asterisk indicates $p<0.05$ and n.s indicates non significance.

Given that MMP-2 has been shown to impact osteoblast function and that our human and mouse tissues samples showed an osteoblast localization of MMP-2, we determined if osteoblast-derived MMP-2 could mediate tumor growth and survival. The ability of conditioned media from wild type and MMP-2 deficient primary osteoblast to modulate PyMT-Luc cells growth and survival was assessed using MTT growth and soft agar colony formation assays (**Figure 8A**). Conditioned media derived from wild type primary osteoblasts induced significant higher metabolic activity of tumor cells and a statistical higher number of tumor colonies compared to tumor cells incubated with conditioned media from MMP-2 deficient osteoblasts (Figure 4A). However, no difference was observed in the average size of the colonies between the two conditions, suggesting that the absence of MMP-2 in osteoblasts affects tumor survival but not tumor growth which is in agreement with our *in vivo* data (**Figure 8B**). To confirm that osteoblast-derived MMP-2 mediates this phenomenon, recombinant MMP-2 was added to conditioned media from MMP-2 deficient primary osteoblasts prior to treatment of PyMT-Luc cells. Addition of exogenous MMP-2 to

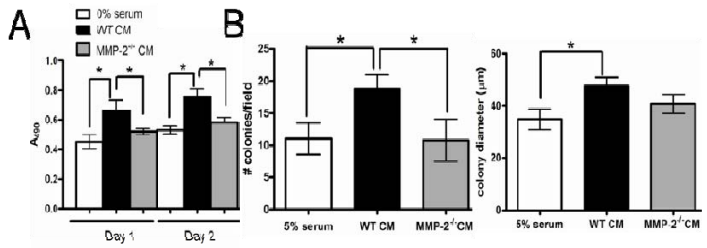

Figure 4. Osteoblast-derived MMP-2 mediate tumor survival. PyMT-Luc cells were treated with conditioned media from wild type (WT CM)or MMP-2 null (MMP-$2^{-/-}$ CM)osteoblasts. Ability of the tumor cells to proliferate and survive was assessed by MTT and soft agar colony formation assays. **AF:** Metabolic activity of PyMT-Luc cells treated with WT CM or MMP-$2^{-/-}$ CM was assessed by MTT assay. **B:** Tumor survival and growth in presence of WT CM, MMP-$2^{-/-}$ CM was determined by soft agar colony formation assay. Number of colonies and colony diameter were reported for each condition. **C:** Cleavage assay of LTBP-3 by recombinant MMP-2 or plasmin. Data are mean ± SD. Asterisk indicates $p<0.05$ and n.s indicates non significance.

conditioned media from MMP-2 deficient osteoblasts rescued the tumor survival phenotype (**Figure 7C and D**). Therefore, these results demonstrate for the first time that osteoblast-derived MMP-2 influences tumor cell survival.

Based on our observations of a decrease in bone resorption in the MMP-7 deficient mice bearing tumor and the osteoclasts being a major source of MMP-7, we investigated the molecular mechanism through which osteoclast-derived MMP-7 contributes to tumor induced osteolysis. The pH in the resorption pit created by the active osteoclasts is acidic (pH<4) and given the functionality of MMP-7 at more neutral pH, it is greatly unlikely that host MMP-7 directly contributes to bone resorption. However, numerous studies have demonstrated that MMPs could influence cell-cell communication by processing numbers of signaling molecules such as growth factors, cytokines, chemokines including RANKL. Therefore, we investigated the possibility that MMP-7 solublization of RANKL would be relevant in our model. Soluble RANKL was significantly decreased in the tumor bearing lysates of MMP-7 deficient mice compared to the controls (**Figure 9A**). It is interesting to note that soluble RANKL levels in the tumor bearing samples were higher than the sham injected limbs showing that RANKL is still processed in MMP-7 null mice as many studies have demonstrated that other proteases could cleave RANKL such as MMP-1, -3, a disintegrin and metalloprotease-17 (ADAM-17) and serine protease cathepsin G (Lum et al., 1999; Lynch et al., 2005; Schlondorff et al., 2001; Wilson et al., 2008). We confirmed these results by immunoprecipitation of total RANKL on lysates of tumor bearing limbs of wild-type and MMP-7 deficient mice and western blotting for soluble RANKL. MMP-7 deficient mice injected with tumor presented significantly lower levels of soluble RANKL compared to wild-type controls (**Figure 9B**). As RANKL is a key factor for osteoclast recruitment and maturation, we assessed the number of mature osteoclasts present at the tumor-bone interface in both wild-type and MMP-7 deficient tibia bearing tumor by histomorphometry. A significant decrease in osteoclast number was observed in MMP-7 null mice compared to the wild-type controls (**Figure 9C**). These data suggest that MMP-7 mediates mammary tumor induced osteolysis via the solubilization of RANKL and the recruitment and activation of osteoclasts that in turn promote the release of factors from the bone matrix that are critical for tumor survival.

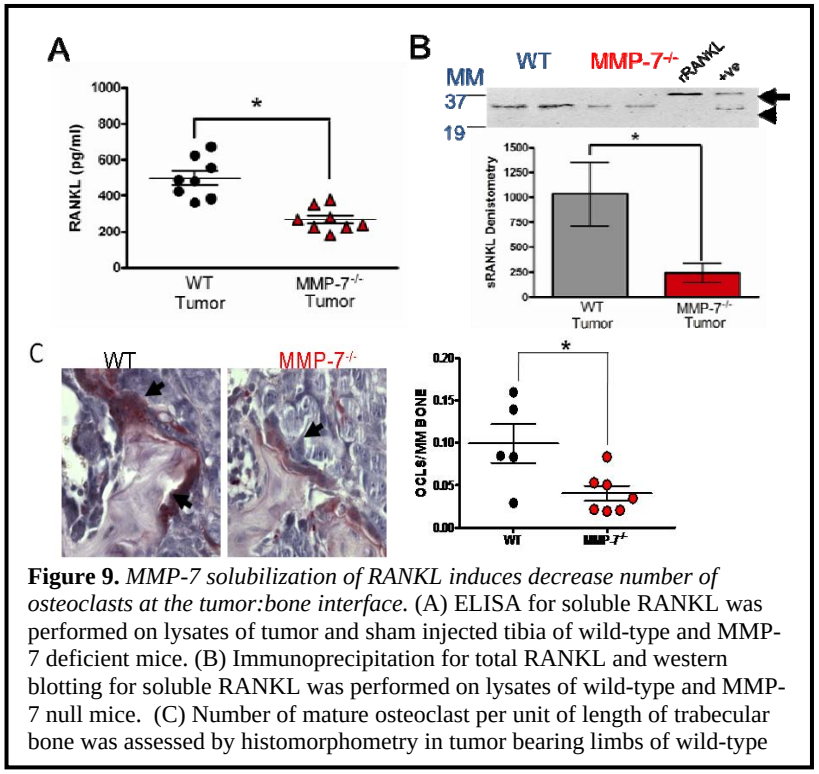

Figure 9. *MMP-7 solubilization of RANKL induces decrease number of osteoclasts at the tumor:bone interface.* (A) ELISA for soluble RANKL was performed on lysates of tumor and sham injected tibia of wild-type and MMP-7 deficient mice. (B) Immunoprecipitation for total RANKL and western blotting for soluble RANKL was performed on lysates of wild-type and MMP-7 null mice. (C) Number of mature osteoclast per unit of length of trabecular bone was assessed by histomorphometry in tumor bearing limbs of wild-type

Key research accomplishement

- Mature osteoclasts at the tumor-bone interface are a rich source of MMP-7 and MMP-9.
- Osteoclast-derived MMP-7 impacts mammary tumor growth and tumor induced osteolysis. (First time observation)
    - Molecular mechanism: solublization of membrane-bound RANKL by MMP-7 that mediates maturation/activation of osteoclast precursor cells.
- Osteoclast-derived MMP-9 does not contribute to both mammary tumor growth and bone resorption.
- Osteoblasts are a rich source of MMP-2.

- Osteoblast-derived MMP-2 impacts mammary tumor growth by enhancing tumor survival. (First report to show this)
- Host-MMP-2 impacts mammary tumor-induced osteolysis. (First report)
- MMP-2 can modulate the release of active TGF-β via the processing of its latency protein, LTBP-3. (First report)
- Osteoblast-derived MMP-2 and osteoblast-derived TGF-β mediate mammary tumor survival. (First report)

Reportables outcomes:

- **American Society of Matrix Biology biennial meeting**, October 2006, poster presentation
"Stromal MMP-2 promotes mammary tumor-induced osteolysis *in vivo*"
Sophie Thiolloy, Conor C. Lynch, Michelle D. Martin, Barbara Fingleton, Lynn M. Matrisian

- **6th Annual Host -tumor Interactions and Cancer Biology joint retreat**, November 2006, oral presentation, Oral talk award (1st place)
"Stromal MMP-2 contributes to mammary tumor induced osteolysis *in vivo* "
Sophie Thiolloy, Conor C. Lynch, Michelle D. Martin, Barbara Fingleton and Lynn M. Matrisian

- **Cancer Induced Bone Disease meeting,** San Antonio, December 2006, poster presentation
"Stromal MMP-2 promotes mammary tumor-induced osteolysis *in vivo* "
Sophie Thiolloy, Conor C. Lynch, Michelle D. Martin, Barbara Fingleton, and Lynn M. Matrisian

- **7th Annual Host -tumor Interactions and Cancer Biology joint retreat**, November 2007, 2 poster presentations
"The *in vivo* impact of host MMP-2 to mammary tumor induced osteolysis"
Sophie Thiolloy, Conor C. Lynch, Barbara Fingleton, Lynn M. Matrisian
"The differential contributions of host MMP-7 and MMP-9 on mammary tumor induced osteolysis"
Sophie Thiolloy, Ginger E. Holt, Jennifer Halpern, Herbert S. Schwartz, Gregory R. Mundy, Lynn M. Matrisian and Conor C. Lynch
- **5th ERA of hope meeting**, Baltimore, June 2008, poster presentation
"Contributions of host MMP-2 and MMP-9 to mammary tumor-induced osteolysis"
Sophie Thiolloy, Conor C. Lynch, James Edwards, David K. Flaherty, Barbara Fingleton, Gregory R. Mundy, Lynn M. Matrisian
- **6th Cancer Induced Bone Disease meeting**, Edinburg, Scotland, July 2008, poster presentation, travel award
"Contributions of host MMP-2 and MMP-9 to mammary tumor-induced osteolysis"
Sophie Thiolloy, Conor C. Lynch, James Edwards, David K. Flaherty, Barbara Fingleton, Gregory R. Mundy, Lynn M. Matrisian

Publications:

- "Osteoclast derived matrix metalloproteinase-7 but not matrix metalloproteinase-9 contributes to tumor induced osteolysis" Sophie Thiolloy, Jennifer Halpern, Ginger E. Holt, Herbert S. Schwartz, Gregory R. Mundy, Lynn M. Matrisian and Conor C. Lynch. Cancer Research, EPub.
- "An Osteoblast-derived protease controls TGF-beta release and tumor cell survival in the bone microenvironment", Sophie Thiolloy, James Edwards, Barbara Fingleton, Daniel B. Rifkin, Gregory R. Mundy, Lynn M. Matrisian and Conor C. Lynch. In submission.

Conclusions and future directions

Over the first year of our studies, we showed the significant importance of stromal MMP-2 in the growth of mammary tumor cells in bone. We demonstrated that stromal MMP-2 contributes to the growth and the survival of the tumor cell in the bone and does not affect the activation of osteoclasts. Over the second year, we developed molecular tools such as wild-type and MMP-2 null FVB GFP expressing mice and a cell line expressing both luciferase and DsRed2 to investigate further the role of host-derived MMP-2 in mammary tumor survival in the bone. We also determined that stromal MMP-7 contributes to mammary tumor growth in the bone and osteolysis *in vivo*. Although MMP-2 and MMP-9 have several common substrates, we have determined that in our model of mammary tumor induced osteolysis, MMP-9 does not contribute to the growth of the tumor and the bone resorption. During the last year of the fellowship, we established that osteoclast-derived MMP-7 impacts mammary tumor growth and osteolysis *in vivo* through the release of soluble RANKL from its membrane bound form. Furthermore, we demonstrated that osteoblast-derived MMP-2 impacts mammary tumor survival in the bone microenvironment by controlling the levels of active TGF-β via the process of its latency protein, LTBP-3, novel substrate for MMP-2. Therefore, novel therapeutic agents focusing on major components of the 'vicious cycle' will improve the current treatment options offered to breast cancer patients with lytic bone metastases. Development of specific MMP-2 and MMP-7 inhibitors or therapies that target their substrates would benefit patients whose response to bisphosphonates and other traditional treatment strategies are unsatisfactory. Alternatively, these new therapeutic agents may also be useful as adjuvants in combination with bisphosphonates, denosumab (specific RANKL antibody), hormonal therapies or other treatments offered, to hopefully lead to the eradication of breast-to-bone metastasis.

Bibliography

Agnihotri, R., Crawford, H. C., Haro, H., Matrisian, L. M., Havrda, M. C., and Liaw, L. (2001). Osteopontin, a novel substrate for matrix metalloproteinase-3 (stromelysin-1) and matrix metalloproteinase-7 (matrilysin). J Biol Chem *276*, 28261-28267.

Coleman, R. E., and Rubens, R. D. (1987). The clinical course of bone metastases from breast cancer. Br J Cancer *55*, 61-66.

Coussens, L. M., Fingleton, B., and Matrisian, L. M. (2002). Matrix metalloproteinase inhibitors and cancer: trials and tribulations. Science *295*, 2387-2392.

Dabovic, B., Chen, Y., Colarossi, C., Zambuto, L., Obata, H., and Rifkin, D. B. (2002). Bone defects in latent TGF-beta binding protein (Ltbp)-3 null mice; a role for Ltbp in TGF-beta presentation. J Endocrinol *175*, 129-141.

Dabovic, B., Levasseur, R., Zambuto, L., Chen, Y., Karsenty, G., and Rifkin, D. B. (2005). Osteopetrosis-like phenotype in latent TGF-beta binding protein 3 deficient mice. Bone *37*, 25-31.

Dallas, S. L., Rosser, J. L., Mundy, G. R., and Bonewald, L. F. (2002). Proteolysis of latent transforming growth factor-beta (TGF-beta)-binding protein-1 by osteoclasts. A cellular mechanism for release of TGF-beta from bone matrix. J Biol Chem *277*, 21352-21360.

Dubois, C. M., Laprise, M. H., Blanchette, F., Gentry, L. E., and Leduc, R. (1995). Processing of transforming growth factor beta 1 precursor by human furin convertase. J Biol Chem *270*, 10618-10624.

Engsig, M. T., Chen, Q. J., Vu, T. H., Pedersen, A. C., Therkidsen, B., Lund, L. R., Henriksen, K., Lenhard, T., Foged, N. T., Werb, Z., and Delaisse, J. M. (2000). Matrix metalloproteinase 9 and vascular endothelial growth factor are essential for osteoclast recruitment into developing long bones. J Cell Biol *151*, 879-889.

Haro, H., Crawford, H. C., Fingleton, B., Shinomiya, K., Spengler, D. M., and Matrisian, L. M. (2000). Matrix metalloproteinase-7-dependent release of tumor necrosis factor-alpha in a model of herniated disc resorption. J Clin Invest *105*, 143-150.

Lee, J., Weber, M., Mejia, S., Bone, E., Watson, P., and Orr, W. (2001). A matrix metalloproteinase inhibitor, batimastat, retards the development of osteolytic bone metastases by MDA-MB-231 human breast cancer cells in Balb C nu/nu mice. Eur J Cancer *37*, 106-113.

Lin, E. Y., Jones, J. G., Li, P., Zhu, L., Whitney, K. D., Muller, W. J., and Pollard, J. W. (2003). Progression to malignancy in the polyoma middle T oncoprotein mouse breast cancer model provides a reliable model for human diseases. Am J Pathol *163*, 2113-2126.
Lum, L., Wong, B. R., Josien, R., Becherer, J. D., Erdjument-Bromage, H., Schlondorff, J., Tempst, P., Choi, Y., and Blobel, C. P. (1999). Evidence for a role of a tumor necrosis factor-alpha (TNF-alpha)- converting enzyme-like protease in shedding of TRANCE, a TNF family member involved in osteoclastogenesis and dendritic cell survival. Journal Biological Chemistry *274*, 13613-13618.
Lynch, C. C., Hikosaka, A., Acuff, H. B., Martin, M. D., Kawai, N., Singh, R. K., Vargo-Gogola, T. C., Begtrup, J. L., Peterson, T. E., Fingleton, B., *et al.* (2005). MMP-7 promotes prostate cancer-induced osteolysis via the solubilization of RANKL. Cancer Cell *7*, 485-496.
Lynch, C. C., and Matrisian, L. M. (2002). Matrix metalloproteinases in tumor-host cell communication. Differentiation *70*, 561-573.
Mundy, G. R. (2002). Metastasis to bone: causes, consequences and therapeutic opportunities. Nat Rev Cancer *2*, 584-593.
Nemeth, J. A., Yousif, R., Herzog, M., Che, M., Upadhyay, J., Shekarriz, B., Bhagat, S., Mullins, C., Fridman, R., and Cher, M. L. (2002). Matrix metalloproteinase activity, bone matrix turnover, and tumor cell proliferation in prostate cancer bone metastasis. J Natl Cancer Inst *94*, 17-25.
Ohshiba, T., Miyaura, C., Inada, M., and Ito, A. (2003). Role of RANKL-induced osteoclast formation and MMP-dependent matrix degradation in bone destruction by breast cancer metastasis. Br J Cancer *88*, 1318-1326.
Paget, S. (1989). The distribution of secondary growths in cancer of the breast. 1889. Cancer Metastasis Rev *8*, 98-101.
Penttinen, C., Saharinen, J., Weikkolainen, K., Hyytiainen, M., and Keski-Oja, J. (2002). Secretion of human latent TGF-beta-binding protein-3 (LTBP-3) is dependent on co-expression of TGF-beta. J Cell Sci *115*, 3457-3468.
Saharinen, J., Hyytiainen, M., Taipale, J., and Keski-Oja, J. (1999). Latent transforming growth factor-beta binding proteins (LTBPs)--structural extracellular matrix proteins for targeting TGF-beta action 2. Cytokine Growth Factor Rev *10*, 99-117.
Schlondorff, J., Lum, L., and Blobel, C. P. (2001). Biochemical and pharmacological criteria define two shedding activities for TRANCE/OPGL that are distinct from the tumor necrosis factor alpha convertase. Journal Biological Chemistry *276*, 14665-14674.
Wilson, T. J., Nannuru, K. C., Futakuchi, M., Sadanandam, A., and Singh, R. K. (2008). Cathepsin G enhances mammary tumor-induced osteolysis by generating soluble receptor activator of nuclear factor-kappaB ligand. Cancer Res *68*, 5803-5811.
Winding, B., NicAmhlaoibh, R., Misander, H., Hoegh-Andersen, P., Andersen, T. L., Holst-Hansen, C., Heegaard, A. M., Foged, N. T., Brunner, N., and Delaisse, J. M. (2002). Synthetic matrix metalloproteinase inhibitors inhibit growth of established breast cancer osteolytic lesions and prolong survival in mice. Clin Cancer Res *8*, 1932-1939.
Yu, Q., and Stamenkovic, I. (2000). Cell surface-localized matrix metalloproteinase-9 proteolytically activates TGF-beta and promotes tumor invasion and angiogenesis. Genes and Development *14*, 163-176.

Title: Osteoclast derived matrix metalloproteinase-7 but not matrix metalloproteinase-9 contributes to tumor induced osteolysis

Authors: Sophie Thiolloy[1], Jennifer Halpern[2], Ginger E. Holt[2,] Herbert S. Schwartz[2], Gregory R. Mundy[3], Lynn M. Matrisian[2] and Conor C. Lynch [*1,2]

Author affiliations: [1]Department of Cancer Biology, [2]Department of Orthopaedics and Rehabilitation and [3]Vanderbilt Center for Bone Biology, Vanderbilt University, Nashville, TN. 37232. USA

Author e-mails: sophie.thiolloy@vanderbilt.edu; jennifer.halpern@vanderbilt.edu; ginger.e.holt@vanderbilt.edu; herbert.s.schwartz@vanderbilt.edu; gregory.r.mundy@vanderbilt.edu; lynn.matrisian@vanderbilt.edu; conor.lynch@vanderbilt.edu

[*]**Corresponding Author:** Dr. Conor C. Lynch, Department Of Orthopaedics and Rehabilitation, Vanderbilt University Medical Center East, South Tower, Suite 4200, Nashville, TN, 37232-8774. Tel: 615-343-5729. Fax: 615-343-1028. e-mail: conor.lynch@vanderbilt.edu

Running Title: Osteoclast derived MMP-7 promotes mammary tumor induced osteolysis

Key words: breast to bone metastasis, osteoclasts, osteolysis, matrix metalloproteinase, MMP-7, MMP-9, receptor activator of nuclear kappa B ligand, RANKL.

Abstract

The matrix metalloproteinases, MMP-2, -3, -7, -9 and -13 are highly expressed in the tumor-bone microenvironment and of these, MMP-7 and MMP-9 were found to be localized to bone resorbing osteoclasts in human breast to bone metastases. In a bid to define the roles of host derived MMP-7 and MMP-9 in the tumor-bone microenvironment, the tibia of MMP-7 and MMP-9 null mice were injected with an osteolytic luciferase tagged mammary tumor cell lines. Our data demonstrates that osteoclast derived MMP-7 significantly contributes to tumor growth and tumor induced osteolysis while osteoclast derived MMP-9 had no impact on these processes. MMP-7 is capable of processing a number of non-matrix molecules to soluble active forms that have profound effects on cell-cell communication such as RANKL, a crucial mediator of osteoclast precursor recruitment and maturation. Therefore, the ability of osteoclast derived MMP-7 to promote RANKL solubilization in the tumor-bone microenvironment was explored. Results revealed that levels of soluble RANKL were significantly lower in the MMP-7 null mice compared to wild type controls. In keeping with this observation, MMP-7 null mice had significantly fewer osteoclast numbers at the tumor-bone interface compared to the wild-type controls. In summary, we propose that the solubilization of RANKL by MMP-7 is a potential mechanism through which MMP-7 mediates mammary tumor induced osteolysis. Our studies indicate that the selective inhibition of MMP-7 in the tumor-bone microenvironment may be of benefit for the treatment of lytic breast to bone metastases.

Introduction

Bone metastasis is a common event during breast cancer progression with the resultant lesions often being osteolytic (1). In the bone microenvironment, metastatic breast cancer cells hijack the normal bone remodeling process to induce aberrant activation of bone resorbing osteoclasts (2). Increased bone resorption results in the release of sequestered growth factors from the bone matrix such as transforming growth factor β (TGFβ) and insulin like growth factors (IGFs). These factors subsequently promote tumor survival and growth thus completing what has aptly been described as the vicious cycle of tumor induced osteolysis (3).

Osteoclasts are critical for the completion of the vicious cycle since they are the principal cells involved in the direct resorption of the mineralized bone matrix. Therefore, understanding how osteoclast precursors are recruited to areas requiring bone remodeling and understanding the mechanisms involved in controlling their maturation and activation is key for the development of new therapies that can effectively stop the vicious cycle. In order to resorb bone, the osteoclast forms a resorptive seal on the mineralized bone matrix after retraction of the osteoblast canopy (4). Acidification of the resorption zone, in combination with collagenolysis, leads to the demineralization and degradation of the bone matrix respectively (5). Osteoclasts express a variety of proteases including the cysteine protease, cathepsin-K and matrix metalloproteinases (MMPs) (6). While cathepsin-K activity is critical for bone resorption (7), the role of osteoclast derived MMPs is less clear. The MMPs are a family of enzymatic proteins that are often overexpressed in the tumor microenvironment (8).

Collectively, MMPs are capable of degrading the entire extracellular matrix (ECM) but more recently, MMPs have been implicated as important mediators of cell-cell communication by virtue of their ability to process multiple non-matrix molecules such as cytokines and growth factors to soluble forms resulting in either enhanced or attenuated activities (9).

In the context of the tumor-bone microenvironment, pre-clinical animals studies have demonstrated the efficacy of broad spectrum MMP inhibitors (MMPIs) in preventing tumor growth and tumor induced osteolysis (10-12). However, the failure of MMPIs in human clinical trials prevents their application for the treatment of bone metastases (13). A main conclusion derived from these trials was the necessity for defining the precise roles of individual MMPs in disease processes that would allow for the generation of highly selective MMP inhibitors. To this end, we have assessed the expression of MMPs in human clinical samples of osteolytic breast to bone metastasis. While the expression of many MMPs was noted throughout the tumor/stroma, MMP-7 and MMP-9 were highly localized to bone resorbing osteoclasts. Given the importance of the osteoclasts in driving the vicious cycle, the current study focused on determining if and how these osteoclast derived MMPs impacted tumor induced osteolysis.

Materials and Methods

Reagents

All experiments involving animals were conducted after review and approval by the office of animal welfare at Vanderbilt University. De-identified human samples of frank

osteolytic breast to bone metastasis (n=11) were collected by curettage with IRB approval from Vanderbilt University from 2005 to 2008. Double null immunocompromised recombinase activating gene-2 (RAG-2) and MMP-7 mice were generated as previously described (14). Wild type and MMP-9 null mice in the FVB/N-Tg background were kindly provided by Dr. Lisa Coussens, Dept. of Pathology, University of California San Francisco. A luciferase expressing syngeneic FVB mammary tumor cell line derived from the polyoma virus middle T model of mammary tumorigenesis, designated PyMT-Luc, was isolated in our laboratory and maintained as previously described (15). A luciferase tagged 4T1 mammary tumor cell line (16) was kindly provided by Dr. Swati Biswas of the Vanderbilt Center for Bone Biology. All reagents were obtained from Sigma-Aldrich except where specified.

Intratibial injection and in vivo quantitation of tumor growth

PyMT-Luc and 4T1-Luc tumor cells (10^5) in a 10µl volume of sterile phosphate buffered saline (PBS) were injected into the tibia of anesthetized immunocompetent or immunocompromised 6 week old mice that were wild type or null for MMP-7 or MMP-9. The contralateral limb was injected with 10µl of PBS alone and acted as a sham injected control. The IVIS™ system (Caliper Life Sciences) was used to detect luminescence from PyMT-Luc cells after intratibial injection. Firefly luciferin (120mg/kg in sterile PBS, Gold Biotechnology, Inc.) was delivered retro-orbitally 1 to 2 minutes prior imaging. Mice were imaged at 24 hours and every 3 days after surgery until day 9 which was previously determined to be the time point prior to tumor breach of the cortical bone in wild type control mice. Living Image™ software (Calipers Life Sciences)

was used to quantify the luminescence intensity in the tumor bearing limb over time. Mice were sacrificed at 9 days post-surgery and both the tumor injected and contralateral control tibiae were harvested. All animal studies were independently repeated at least twice.

Histology

Fresh human breast-to-bone metastases, tumor and sham injected mouse tibiae were fixed overnight in 10% buffered formalin and decalcified for 3 weeks in 14% EDTA at pH 7.4 with changes every 48-72 hours. Tissues were embedded in paraffin and 5µm thick sections were cut. For MMP-7, MMP-9 and tartrate resistant acid phosphatase (TRAcP) localization, the following technique was employed. Sections were rehydrated through a series of ethanols and then rinsed in tris buffered saline (TBS; 10mM Tris at pH 7.4, 150mM NaCl) with Tween-20 (0.05%). For antigen retrieval, slides were immersed in a 20µg/ml solution of proteinase K according to the manufacturer's instructions for 10 minutes at room temperature. Following washing in TBS, tissue sections were blocked using standard blocking criteria for 1 hour at room temperature. MMP-7 (17) or MMP-9 (Oncogene, Cat. No. AB3-IM37L) antibodies at a dilution of 1:100 were added in blocking solution overnight at 4^{o}C. Slides were washed extensively in TBST prior to the addition of a species specific fluorescently labeled secondary antibody (Alexafluor 568nm, Invitrogen) diluted 1:1,000 in blocking solution for 1 hour at room temperature. Slides were washed in TBS and then equilibrated in an acetate buffer as described (18). The ELF97 TRAcP stain (Invitrogen, Cat. No. 6601) was diluted 1:1,000 in acetate buffer and slides were incubated for 15 minutes at room temperature. Following

washing, slides were aqueously mounted in media (Biomeda Corp) containing 2μM DAPI (4´,6 diamidino-2-phenylindole) for nuclear localization.

TRAcP was also detected using a traditional colorimetric kit according to the manufacturer's instructions (Sigma-Aldrich, Cat. No. 387A). Gross anatomy of the mouse tibiae was assessed by hematoxylin and eosin (H&E) staining. Proliferation (anti-phospho Histone H3, Millipore, Cat. No. 06-570) and apoptosis (anti-Caspase-3, Cell Signaling, Cat. No. 9662) were assessed by immunohistochemistry as previously described (14).

Micro computed tomography (μCT), X-ray and histomorphometric analyses

For gross analysis of trabecular bone volume, formalin fixed tibiae were scanned at an isotropic voxel size of 12μm using a microCT40 (SCANCO Medical). The tissue volume (TV) was derived from generating a contour around the metaphyseal trabecular bone that excluded the cortices. The area of measurement began at least 0.2mm below the growth plate and was extended by 0.12mm. The bone volume (BV) included all bone tissue that had a material density greater than 438.7 mgHA/cm^3. These analyses allowed for the calculation of the BV/TV ratio. The same threshold setting for bone tissue was used for all samples. Radiographic images (Faxitron X-ray Corp) were obtained using an energy of 35kV and an exposure time of 8 seconds. The tumor volume (TuV) was calculated as a function of the total tissue volume (TV) of the tibial medullary canal using Metamorph® software (Molecular Devices). For histomorphometry, three non-serial sections of tumor bearing limbs were H&E stained

to assess the ratio of BV/TV or with TRAcP to assess osteoclast number per mm of bone at the tumor-bone interface using Metamorph®.

Immunoprecipitation, immunoblotting and ELISA

Tumor and sham injected tibias from wild type or MMP null animals were harvested 9 days post-injection and flash frozen in liquid nitrogen. Tissue homogenates were generated by mortar and pestle and total protein was subsequently extracted using a standard protein lysis buffer containing a complete protease inhibitor cocktail (Roche, Cat. No. 11836145001). Protein concentration in isolated samples was quantitated using a bicinchoninic acid (BCA) assay as per manufacturer's instructions (Pierce, Cat. No. 23227). For immunoprecipitation and quantitation of soluble RANKL in the tumor bone microenvironments, equal concentrations of total protein (1mg) in 1ml of PBS were pre-cleared with 10µl of protein-G-sepharose beads (Amersham Biosciences) for one hour at 4^{o}C. Pre-cleared lysates were then incubated with 2µg of antibody directed to the N-terminus of RANKL (sc-7628, Santa Cruz Biotechnology) for 1 hour at 4^{o}C. with rocking prior to the addition of 10µl of protein-G-sepharose beads. Subsequently, 10µl of protein G-sepharose beads were added to the samples and the bead-antibody-protein complexes were allowed to form overnight at 4^{o}C. A nutator was used during all steps for agitation. The complexes were washed extensively (100mM NaCl, 50mM Tris-HCl, pH7.5, 0.5% NP-40) and then boiled in sample buffer (10% SDS, 0.5M Tris-HCl pH 6.8, 30% glycerol, 1% β-mercaptoethanol and 0.02% bromophenol blue) for 10 minutes prior to loading on to a 15% SDS-PAGE gel. Recombinant RANKL (462-TR-010/CF, RnD Systems, Minneapolis, MN) or MMP-7 solubilized RANKL (10µg recombinant

RANKL incubated with 100ng active MMP-7 (cat # 444270, Calbiochem, LaJolla, CA) for 1 hour at 37^{o}C) as previously described (14))were added as positive controls for the molecular weight of MMP solubilized RANKL. Proteins were transferred to nitrocellulose membranes and blocked for 1 hour at room temperature (5% milk powder in 1xTBS; 5mM Tris-HCL pH 7.4,). The blots were then panned with an antibody directed to the N-terminus of RANKL (1: 1,000 dilution; Cat # 804-243-C100, Axxora LLC in 5% milk in 1XTBST (TBS with 0.05% Tween 20)) overnight with rocking at 4^{o}C. The following day, blots were washed extensively with 1xTBST prior to the addition of a secondary infra-red labeled anti-mouse antibody (1: 5,000 dilution in 1xTBST-Cat# 610-132-121, Rockland Inc.) for 1 hour at room temperature. After washing in 1xTBST, blots were developed and bands of interest were quantitated using the Odyssey system (LI-COR Biosciences, Lincoln, NE). ELISA was also used for the quantitation of soluble RANKL in samples according to the manufacturer's instructions (Quantikine, R&D Systems, Cat. No. MTR00).

Statistical analyses

For *in vivo* data, statistical analysis was performed using Anova and Bonferroni multiple comparison tests. *In vitro*, statistical significance was analyzed using a student's t test. A value of $p < 0.05$ was considered significant. Data are presented as mean ± standard deviation (SD).

Results

MMP-7 and MMP-9 are expressed by osteoclasts in human breast to bone metastases

Previous observations using an animal model of tumor-bone interaction identified several MMPs as being highly expressed at the tumor-bone interface compared to the tumor area alone, namely MMP-2, -3, -7, -9 and -13 ((14) and unpublished observations). The expression of these MMPs was examined in human cases of frank breast to bone metastasis (n=11). Interestingly, MMP-7 and MMP-9 were largely localized to the majority of mature TRAcP positive multinucleated osteoclasts at the tumor-bone interface in human samples containing areas of osteolysis (10 of 11 samples) (Fig. 1*A-C* and supplemental Fig. S1 and S2). Other cells in the stromal compartment stained positively for MMP-7 and MMP-9 but remarkably, the tumor cells were negative for these metalloproteinases. MMP-2, -3 and -13 were also detected but their expression was diffuse throughout the tumor/stroma compartment (data not shown). Since osteoclasts are the principal cells involved in bone resorption, we examined whether the ablation of host derived MMP-7 or MMP-9 would impact the vicious cycle in terms of mammary tumor growth and/or mammary tumor induced osteolysis.

Host derived MMP-9 does not contribute to tumor growth or tumor induced osteolysis.

MMP-9 has previously been reported to be localized to osteoclasts and MMP-9 null animals have been identified as having a delay in osteoclast recruitment during the

development of long bones (19). Therefore, we initially tested the role of host derived MMP-9 in tumor growth or tumor induced osteolysis. Consistent with our observations in human samples, bone resorbing osteoclasts in wild type mice were positive for MMP-9 expression by immunofluorescent staining while as expected, MMP-9 was not detected in MMP-9 null osteoclasts (Fig. 2*A*). Since MMP-9 null animals have a transient developmental bone phenotype, we determined the baseline trabecular bone volume as a function of tissue volume (BV/TV) in wild type and MMP-9 null animals at 6 weeks of age which was the proposed time-point for introduction of the PyMT-Luc tumor cells. No difference in the BV/TV between the wild-type and MMP-9 null animals was observed (Fig. S3*A*).

To assess the contribution of host MMP-9 in mammary tumor growth in the bone microenvironment, the PyMT-Luc tumor cells, in which MMP-9 expression is undetectable *in vivo* (20), were injected into the tibia of syngeneic FVB wild-type or MMP-9 null mice. Surprisingly, quantitation of the bioluminescent signal from the tumor cells showed no difference in the tumor growth rate between the MMP-9 null and wild type control mice (Fig. 2*B*). With respect to tumor induced osteolysis, analysis of the BV/TV ratio by high resolution μCT demonstrated that the tumor injected tibias of wild-type and MMP-9 null were significantly lower ($p<0.05$) than their respective sham injected control counterparts (Fig. 2*C*). However, a direct comparison of the BV/TV ratios between the wild-type and MMP-9 null tumor injected limbs revealed no difference in BV/TV ratios (Fig. 2*C*). Furthermore, no differences in tumor growth as assessed by phospho histone H3 for proliferation and cleaved caspase-3

immunohistochemistry for apoptosis, trabecular bone volume and osteoclasts/mm bone by histomorphometry were observed between the wild type and MMP-9 null groups (data not shown). These experiments, with similar sized groups were repeated on several occasions with similar results. These results using the intratibial model suggest that host MMP-9 does not contribute to mammary tumor growth in the bone or tumor induced osteolysis and are consistent with studies examining the role of host MMP-9 in the prostate cancer-bone microenvironment (21).

Host MMP-7 contributes to mammary tumor growth in the bone microenvironment

This is the first report to document the expression of MMP-7 in human breast to bone metastases and in human osteoclasts (Fig. 1), although MMP-7 has previously been identified in rodent osteoclasts by our group (14). Recapitulating observations in human clinical samples, MMP-7 expression was identified in wild type murine osteoclasts and not in MMP-7 null osteoclasts (Fig. 3*A*). Given that MMP-7 expression by osteoclasts is a relatively recent observation, studies into defining roles for MMP-7 in skeletal development have not been explored thus far. Therefore, prior to testing the impact of host derived MMP-7 on the vicious cycle, the trabecular bone volume in non-injected 6 week old immunocompromised wild type and MMP-7 null animals was examined using high resolution µCT. Our results revealed no significant difference in the BV/TV ratio between wild type and MMP-7 null animals suggesting that at this time point, MMP-7 null animals do not display an obvious bone phenotype in comparison to the wild type controls (Fig. S3*B*).

To determine the contribution of host MMP-7 to mammary tumor growth in the bone microenvironment, PyMT-Luc cells were injected into 6 week old wild-type or MMP-7 null mice. Quantitation of the bioluminescent signal from the PyMT-Luc cells demonstrated a significant decrease in the tumor growth rate in MMP-7 null mice compared to the wild type controls (Fig. 3*B*). These experiments with similar sized groups in terms of animal numbers were independently repeated on four occasions and similar observations were noted. To further investigate the potential role of MMP-7 in tumor growth, tumor proliferation and apoptosis were assessed by immunohistochemistry for phospho-histone H3 and cleaved caspase-3, respectively, in multiple sections from at least five animals per group (Fig. 3*C* and *D*). Surprisingly, no difference in tumor proliferation was observed between the wild type and MMP-7 null groups, however, tumor apoptosis was significantly higher in MMP-7 null mice compared to the wild type controls ($p<0.05$). Similar findings with respect to the impact of host MMP-7 on tumor growth using the 4T1-Luc cell line were also observed (Fig. S4*A*-*C*). These results suggest that host-derived MMP-7 significantly contributes to mammary tumor growth in the bone by enhancing tumor cell survival.

Host derived MMP-7 contributes to mammary tumor induced osteolysis

The vicious cycle of tumor-bone interaction suggests that tumor growth/survival is dependent on osteoclast mediated bone resorption. Since MMP-7 is primarily localized to bone resorbing osteoclasts in the tumor-bone microenvironment, we assessed whether a lack of MMP-7 in osteoclasts impacted tumor induced osteolysis. Analysis of the BV/TV ratios from wild type and MMP-7 null tumor injected tibias using μCT (Fig.

4*A*) and histomorphometry (Fig. 4*B*) revealed that the MMP-7 null group had a significantly higher amount of trabecular bone which is in keeping with our tumor growth data, i.e. less tumor growth in the MMP-7 null animal would lead to less osteolysis. X-ray analysis also revealed a significantly lower tumor volume in the MMP-7 null animals compared to wild type controls (Fig. 4*C*). Studies using the 4T1-Luc cell line also demonstrated that host derived MMP-7 also significantly impacted tumor induced osteolysis (Figure S5A and B). These results demonstrate that host derived MMP-7 significantly impacts mammary tumor induced osteolysis.

MMP-7 mediates RANKL solubilization in the tumor-bone microenvironment

Next, we explored the potential molecular mechanism through which osteoclast derived MMP-7 was impacting tumor induced osteolysis. Given the acidity of the resorption lacunae (pH<4) and the neutral activity profile of MMP-7, we suggest that MMP-7 does not function in direct bone matrix degradation but in the processing of factors that impact cell-cell communication within the tumor-bone microenvironment. MMP-7 has previously been shown to process a number of growth factors and cytokines to soluble active forms including members of the tumor necrosis factor family (TNF), TNF-α, Fas ligand (FasL) and RANKL (14, 22, 23). RANKL is essential for osteoclastogenesis and is a potent chemotactic molecule for monocytes and osteoclast precursor cells (24, 25). Therefore, we investigated if MMP-7 solubilization of RANKL was relevant in our model.

ELISA analysis revealed lower levels of total RANKL (membrane bound and soluble) in the tumor injected tibias of MMP-7 null mice compared to wild type control

mice (Fig. 5*A*) while no difference was observed in the sham injected control counterparts of each group (data not shown). Similar levels of osteoprotegerin (OPG), a soluble decoy receptor of RANKL, were found in the wild-type and MMP-7 null animals and were not present at a high enough concentration to interfere with the detection of RANKL by ELISA (data not shown). Immunoprecipitation and immunoblotting for soluble RANKL revealed significantly lower levels of soluble RANKL in PyMT-Luc or 4T1-Luc tumor injected MMP-7 null animals compared to wild type controls as assessed by densitometry (Fig. 5*B*; $p<0.001$ and Fig S5*C*; $p<0.001$).

Interestingly, soluble RANKL could still be detected in the tumor bearing limbs of MMP-7 null animals. This suggests that RANKL solubilization is still occurring in the absence of MMP-7. We and others have previously identified that other metalloproteinases such as MMP-1, -3, -14, a disintegrin and metalloprotease-17 (ADAM-17) and the serine protease cathepsin G are capable of processing RANKL to a soluble active form and therefore, these proteases may also be playing a role in the solubilization of RANKL in our model (14, 26-28). However, since the levels of RANKL are significantly lower in the MMP-7 null mice, we suggest that MMP-7 is the dominant protease involved in RANKL solubilization.

Next, since a decrease in the amount of soluble RANKL was detected in the tumor bearing limbs of the MMP-7 null animals, we asked if there was concomitant decrease in the number of osteoclasts in the MMP-7 null tumor-bone microenvironment. We observed significantly lower numbers of TRAcP positive multinucleated osteoclasts per unit length of tumor-bone interface in the MMP-7 null animals compared to the wild-

type controls (Fig. 5*C*). Significantly lower numbers of osteoclasts were also recorded in MMP-7 deficient animals injected with 4T1-Luc cells compared to wild type controls (Fig. S5*D*). Given the importance of RANKL in mediating osteoclastogenesis, these data suggest that MMP-7 mediates mammary tumor induced osteolysis by impacting the availability of a key factor for osteoclastogenesis, RANKL.

Discussion

Understanding the molecular mechanisms that control the vicious cycle is key for the development of new therapeutics that will be effective not only in treating bone metastases but also in curing them. In the current study, we found that in human cases of breast to bone metastasis, osteoclasts were a rich source of MMP-7 and MMP-9. Interestingly, our studies using two unrelated osteolytic inducing tumor cell lines (PyMT-Luc and 4T1-Luc) revealed that only MMP-7 appeared to contribute to mammary tumor growth and tumor induced osteolysis in the bone microenvironment. Furthermore, our data suggests that MMP-7 solubilization of the osteoclastogenic factor RANKL is the principal molecular mechanism underlying these observations. Previously, we have identified that MMP-7 processing of RANKL results in the generation of an active soluble form that can promote osteoclast maturation and activation (14). Therefore, in the context of the breast to bone metastases we hypothesize that in the absence of MMP-7 solubilized RANKL, there is a resultant decrease in osteoclast maturation and

bone resorption at the tumor-bone interface that in turn results in a decrease in bone derived growth factors that impact tumor growth (Fig. 6).

Our results how an osteoclast derived protease, MMP-7, can promote osteoclast activation in the tumor-bone microenvironment by generating an active soluble form of the osteoclastogenic factor, RANKL and suggest that selective inhibition of MMP-7 may be of benefit for the treatment of lytic metastases. Several studies support the rationale for the development of selective MMP inhibitors for the treatment of bone metastases. To this end, broad spectrum MMP inhibitors such as batimastat have been identified as being effective in preventing tumor growth and tumor induced osteolysis in the bone environment using animal models (10-12). However, conclusions from human clinical trials with the same inhibitors identified the necessity for highly selective MMPIs that lack the deleterious side effects of broad spectrum inhibitors prior to their application in clinical settings (13). This requires an understanding of the precise roles of MMPs in the context of particular diseases and in this regard, our studies suggest MMP-7 as an attractive target for the treatment of lytic metastases.

While MMP-7 solubilization of RANKL is predicted here to be a mechanism underlying our observations, MMP-7 may contribute via other mechanisms. For example, MMP-7 processing of apoptotic factors such as Fas ligand in the tumor-microenvironment may directly impact tumor survival (22). In addition, the direct processing of the bone matrix by MMP-7 may be a possibility. Acidification and cathepsin-K secretion into osteoclast resorption lacunae allows for the demineralization and collagenolysis of the bone matrix respectively (6). By a process known as

transcytosis, the osteoclast mediates the removal of bone products from the area of bone undergoing resorption (29). Given the punctate localization of MMP-7 by immunofluorescent staining (Fig. 1*A* and 3*A*) it is tempting to speculate that MMP-7 contributes to the further processing of bone matrix components such as osteopontin (30), or the release of growth factors from bone matrix components such as TGFβ (31) and IGFs (32), within these transcytotic vesicles. The expression of MMP-7 from other cellular sources may also be a possibility. In the tumor-bone microenvironment, we observed that MMP-7 expression was largely confined to osteoclasts. However, MMP-7 has also been shown to be expressed by macrophages and given the role of macrophages in tumor induced osteolysis, the contribution of macrophage derived MMP-7 in our model or in humans cannot be discounted (33, 34).

Given the apparent role of MMP-7 in osteoclast function in the pathological setting of tumor induced osteolysis, it is surprising that MMP-7 null animals appear to have a normal skeletal phenotype. Data presented here using μCT scan analysis demonstrate a similar BV/TV ratio between MMP-7 null and wild type control mice at 6 weeks of age. While a role for MMP-7 in bone development has not been explored, a number of reports have revealed that the phenotype of the MMP-7 null animals is often apparent in response to injury/challenges or disease. For example, in non-pathological conditions such as herniated disc resorption, macrophage derived MMP-7 is critical for the resorption of the herniated disc and in mammary and prostate involution, MMP-7 processing of FasL is important for initiating apoptosis (22, 23, 35). More often, phenotypes in the MMP-7 null animals have been observed in pathological conditions

such as pancreatitis, colon tumorigenesis, mammary gland tumorigenesis and in innate defense wherein MMP-7 null animals show significant delays in disease progression or in response to infection (36-39). Therefore, although MMP-7 null mice lack an apparent skeletal phenotype, in the context of tumor-bone microenvironment, it is clear based on the results in the current study that host MMP-7 plays an important role in osteoclast biology. In addition, our observations defining a role for MMP-7 in bone diseases are consistent with previous reports that implicate roles for host MMP-7 in prostate cancer induced osteolysis, osteoarthritis and cartilage/periarticular bone destruction (14, 40, 41).

Although MMP-9 was localized to human and murine osteoclasts, the ablation of host MMP-9 did not appear to impact PyMT-Luc tumor growth and bone resorption compared to the wild-type controls. Analogous results were obtained by Nabha et al., using the same intratibial model but in the context of prostate cancer progression in the bone (21). Given the importance of MMP-9 in osteoclast migration and recruitment in developing long bones (19), these results were surprising. It appears that in the tumor-bone microenvironment, MMP-9 is not critical for osteoclast function. The possibility that tumor-derived MMP-9 could overcome the absence of host MMP-9 exists in our model, however, *in vivo* studies by our group have demonstrated that MMP-9 expression by the PyMT-Luc tumor cells is not detectable (20). Therefore, the ability of tumor derived MMP-9 to circumvent the loss of host derived MMP-9 and impact tumor progression in the bone is unlikely. However, due to functional overlap amongst members of the MMP

family, MMPs produced by osteoclasts and other stromal cells in the tumor microenvironment may compensate for the absence of host MMP-9.

While our data points towards MMP-9 as not being critical for mammary tumor growth or induced osteolysis, it is important to note that MMP-9 could contribute to other steps of metastasis that are not taken into account with the intratibial model. These include extravasation from the sinusoidal vasculature in the bone and initial survival, the latter of which has been shown to be an important role for host derived MMP-9 in early lung metastasis (42). Furthermore, MMP-9 has been implicated in tumor angiogenesis by mediating the release of matrix sequestered vascular endothelial growth factor (VEGF) (43). In the context of the prostate tumor-bone microenvironment, Nabha and colleagues demonstrated a decrease in angiogenesis in MMP-9 null animals compared to wild type controls (21). Therefore, the selective inhibition of MMP-9 may still prove useful in preventing the establishment and angiogenesis of bone metastases.

In conclusion, this study demonstrates that osteoclast derived MMP-7, but not MMP-9, significantly contributes to tumor induced osteolysis by impacting osteoclast recruitment/differentiation. We suggest that MMP-7 mediated solubilization of RANKL is a potential mechanism underlying this observation. Our data supports the rationale for the generation of selective MMP inhibitors for the treatment of osteolytic bone metastases and implies that the development of such reagents would expand the therapeutic options available to patients suffering with this incurable disease.

Acknowledgements

We would like to thank James Edwards and Steve Munoz of the Vanderbilt Bone Center for their expertise. This research was supported by NIH: 1 R01 CA84360 (LMM) and Susan G. Komen Foundation: PDF 02 1394 (CCL) CCL and ST are supported by the Department of Defense under award number W81XWH-07-1-0208 and BC051038 respectively. Views and opinions of, and endorsements by the author(s) do not reflect those of the US Army or the Department of Defense.

References

1. Coleman RE, Rubens RD. The clinical course of bone metastases from breast cancer. British Journal of Cancer 1987; 55: 61-6.

2. Mundy GR. Metastasis to bone: causes, consequences and therapeutic opportunities. Nature Reviews Cancer 2002; 2: 584-93.

3. Chirgwin JM, Guise TA. Molecular mechanisms of tumor-bone interactions in osteolytic metastases. Crit RevEukaryotGene Expr 2000; 10: 159-78.

4. Compston JE. Bone marrow and bone: a functional unit. J Endocrinol 2002; 173: 387-94.

5. Delaisse JM, Engsig MT, Everts V, et al. Proteinases in bone resorption: obvious and less obvious roles. Clinica Chimica Acta 2000; 291: 223-34.

6. Delaisse JM, Andersen TL, Engsig MT, Henriksen K, Troen T, Blavier L. Matrix metalloproteinases (MMP) and cathepsin K contribute differently to osteoclastic activities. Microscopy Research and Technique 2003; 61: 504-13.

7. Saftig P, Hunziker E, Wehmeyer O, et al. Impaired osteoclastic bone resorption leads to osteopetrosis in cathepsin-K-deficient mice. Proc Natl Acad Sci U S A 1998; 95: 13453-8.

8. Chambers AF, Matrisian LM. Changing views of the role of matrix metalloproteinases in metastasis. Journal National Cancer Institute 1997; 89: 1260-70.

9. Lynch CC, Matrisian LM. Matrix metalloproteinases in tumor-host cell communication. Differentiation 2002; 70: 561-73.

10. Lee J, Weber M, Mejia S, Bone E, Watson P, Orr W. A matrix metalloproteinase inhibitor, batimastat, retards the development of osteolytic bone metastases by MDA-MB-231 human breast cancer cells in Balb C nu/nu mice. European Journal of Cancer 2001; 37: 106-13.

11. Winding B, NicAmhlaoibh R, Misander H, et al. Synthetic matrix metalloproteinase inhibitors inhibit growth of established breast cancer osteolytic lesions and prolong survival in mice. Clinical Cancer Research 2002; 8: 1932-9.

12. Nemeth JA, Yousif R, Herzog M, et al. Matrix metalloproteinase activity, bone matrix turnover, and tumor cell proliferation in prostate cancer bone metastasis. Journal National Cancer Institute 2002; 94: 17-25.

13. Coussens LM, Fingleton B, Matrisian LM. Matrix metalloproteinase inhibitors and cancer: trials and tribulations. Science 2002; 295: 2387-92.

14. Lynch CC, Hikosaka A, Acuff HB, et al. MMP-7 promotes prostate cancer-induced osteolysis via the solubilization of RANKL. Cancer Cell 2005; 7: 485-96.

15. Halpern J, Lynch CC, Fleming J, et al. The application of a murine bone bioreactor as a model of tumor: bone interaction. Clin Exp Metastasis 2006; 23: 345-56.

16. Aslakson CJ, Miller FR. Selective events in the metastatic process defined by analysis of the sequential dissemination of subpopulations of a mouse mammary tumor. Cancer Res 1992; 52: 1399-405.

17. Fingleton B, Powell WC, Crawford HC, Couchman JR, Matrisian LM. A rat monoclonal antibody that recognizes pro- and active MMP-7 indicates polarized expression in vivo. Hybridoma (Larchmt) 2007; 26: 22-7.

18. Filgueira L. Fluorescence-based staining for tartrate-resistant acidic phosphatase (TRAP) in osteoclasts combined with other fluorescent dyes and protocols. J Histochem Cytochem 2004; 52: 411-4.

19. Engsig MT, Chen QJ, Vu TH, et al. Matrix metalloproteinase 9 and vascular endothelial growth factor are essential for osteoclast recruitment into developing long bones. Journal of Cell Biology 2000; 151: 879-90.

20. Martin M, Carter K, Thiolloy S, Lynch CC, Matrisian L, Fingleton B. Effect of ablation or inhibition of stromal matrix metalloproteinase-9 on lung metastasis in a breast cancer model is dependent on genetic background Cancer Res 2008; 68: E-Pub ahead of print.

21. Nabha SM, Bonfil RD, Yamamoto HA, et al. Host matrix metalloproteinase-9 contributes to tumor vascularization without affecting tumor growth in a model of prostate cancer bone metastasis. Clin Exp Metastasis 2006; 23: 335-44.

22. Powell WC, Fingleton B, Wilson CL, Boothby M, Matrisian LM. The metalloproteinase matrilysin (MMP-7) proteolytically generates active soluble Fas ligand and potentiates epithelial cell apoptosis. Current Biology 1999; 9: 1441-7.

23. Haro H, Crawford HC, Fingleton B, Shinomiya K, Spengler DM, Matrisian LM. Matrix metalloproteinase-7-dependent release of tumor necrosis factor-alpha in a model of herniated disc resorption. Journal of Clinical Investigation 2000; 105: 143-50.

24. Kong YY, Yoshida H, Sarosi I, et al. OPGL is a key regulator of osteoclastogenesis, lymphocyte development and lymph-node organogenesis. Nature 1999; 397: 315-23.

25. Breuil V, Schmid-Antomarchi H, Schmid-Alliana A, Rezzonico R, Euller-Ziegler L, Rossi B. The receptor activator of nuclear factor (NF)-kappaB ligand (RANKL) is a new chemotactic factor for human monocytes. Faseb J 2003; 17: 1751-3.

26. Lum L, Wong BR, Josien R, et al. Evidence for a role of a tumor necrosis factor-alpha (TNF-alpha)-converting enzyme-like protease in shedding of TRANCE, a TNF family member involved in osteoclastogenesis and dendritic cell survival. J Biol Chem 1999; 274: 13613-8.

27. Schlondorff J, Lum L, Blobel CP. Biochemical and pharmacological criteria define two shedding activities for TRANCE/OPGL that are distinct from the tumor necrosis factor alpha convertase. J Biol Chem 2001; 276: 14665-74.

28. Wilson TJ, Nannuru KC, Futakuchi M, Sadanandam A, Singh RK. Cathepsin G enhances mammary tumor-induced osteolysis by generating soluble receptor activator of nuclear factor-kappaB ligand. Cancer Res 2008; 68: 5803-11.

29. Blair HC. How the osteoclast degrades bone. Bioessays 1998; 20: 837-46.

30. Agnihotri R, Crawford HC, Haro H, Matrisian LM, Havrda MC, Liaw L. Osteopontin, a novel substrate for matrix metalloproteinase-3 (stromelysin-1) and matrix metalloproteinase-7 (matrilysin). Journal Biological Chemistry 2001; 276: 28261-7.

31. Imai K, Hiramatsu A, Fukushima D, Pierschbacher MD, Okada Y. Degradation of decorin by matrix metalloproteinases: identification of the cleavage sites, kinetic analyses and transforming growth factor-beta 1 release. Biochemical Journal 1997; 322: 809-14.

32. Miyamoto S, Yano K, Sugimoto S, et al. Matrix metalloproteinase-7 facilitates insulin-like growth factor bioavailability through its proteinase activity on insulin-like growth factor binding protein 3. Cancer Research 2004; 64: 665-71.

33. Burke B, Giannoudis A, Corke KP, et al. Hypoxia-induced gene expression in human macrophages: implications for ischemic tissues and hypoxia-regulated gene therapy. American Journal of Pathology 2003; 163: 1233-43.

34. Athanasou NA, Sabokbar A. Human osteoclast ontogeny and pathological bone resorption. Histol Histopathol 1999; 14: 635-47.

35. Fingleton B, Vargo-Gogola T, Crawford HC, Matrisian LM. Matrilysin [MMP-7] expression selects for cells with reduced sensitivity to apoptosis. Neoplasia 2001; 3: 459-68.

36. Sawey ET, Johnson JA, Crawford HC. Matrix metalloproteinase 7 controls pancreatic acinar cell transdifferentiation by activating the Notch signaling pathway. Proc Natl Acad Sci U S A 2007; 104: 19327-32.

37. Wilson CL, Heppner KJ, Labosky PA, Hogan BL, Matrisian LM. Intestinal tumorigenesis is suppressed in mice lacking the metalloproteinase matrilysin. Proc Natl Acad Sci U S A 1997; 94: 1402-7.

38. Wilson CL, Ouellette AJ, Satchell DP, et al. Regulation of intestinal alpha-defensin activation by the metalloproteinase matrilysin in innate host defense. Science 1999; 286: 113-7.

39. Rudolph-Owen LA, Matrisian LM. Matrix metalloproteinases in remodeling of the normal and neoplastic mammary gland. J Mammary Gland Biol Neoplasia 1998; 3: 177-89.

40. Gjertsson I, Innocenti M, Matrisian LM, Tarkowski A. Metalloproteinase-7 contributes to joint destruction in Staphylococcus aureus induced arthritis. Microb Pathog 2005; 38: 97-105.

41. Ohta S, Imai K, Yamashita K, Matsumoto T, Azumano I, Okada Y. Expression of matrix metalloproteinase 7 (matrilysin) in human osteoarthritic cartilage. Laboratory Investigation 1998; 78: 79-87.

42. Acuff HB, Carter KJ, Fingleton B, Gorden DL, Matrisian LM. Matrix metalloproteinase-9 from bone marrow-derived cells contributes to survival but not growth of tumor cells in the lung microenvironment 1. Cancer Research 2006; 66: 259-66.

43. Bergers G, Brekken R, McMahon G, et al. Matrix metalloproteinase-9 triggers the angiogenic switch during carcinogenesis. Nature Cell Biology 2000; 2: 737-44.

Figure Legends.

Figure 1. MMP-7 and MMP-9 localization in human breast to bone metastases (n=11). **A-C:** Fluorescent TRAcP staining (green) was used to localize osteoclasts (arrows) while immunofluorescence was used to localize MMP-7 and MMP-9 (red). DAPI (blue) was used as a nuclear stain. Murine or rat IgG was used as a negative control. Dashed line represents the tumor-bone interface. Scale bars are 50μm.

Figure 2. Host MMP-9 does not impact mammary tumor growth or osteolysis in the bone microenvironment. **A:** Representative photomicrographs of MMP-9 (red) localization merged with TRAcP (green) localization in WT and MMP-$9^{-/-}$ animals. DAPI (blue) was used as a nuclear stain. Arrows indicate osteoclasts while dashed line represents the tumorbone interface. Scale bars are 50μm. **B:** PyMT-Luc cells were injected intratibially into syngeneic FVB wild type (WT; n=6) or MMP-9 null (MMP-$9^{-/-}$; n=11). The contralateral limb received a sham injection of saline. Luminescence was measured over a nine day period. Quantitation of tumor growth in WT and MMP-$9^{-/-}$ animals. **C:** Representative μCT scans of trabecular bone from tumor bearing and sham injected limbs of WT and MMP-$9^{-/-}$ animals. μCT was also used to calculate the ratio of trabecular bone volume to tissue volume (BV/TV) for tumor injected and sham injected wild type and MMP-$9^{-/-}$ mice. Data are mean ± SD. Asterisk denotes that $p<0.05$ while n.s. indicates a non-significant p value.

Figure 3. Host MMP-7 contributes to mammary tumor growth in the bone microenvironment. **A:** Representative photomicrographs of MMP-7 (red) immunofluorescent localization merged with TRAcP (green) localization in WT and MMP-$7^{-/-}$ animals. DAPI (blue) was used as nuclear stain. Arrows indicate osteoclasts

while dashed line represents the tumor-bone interface. **B:** PyMT-Luc cells were injected intratibially into RAG-2 null (WT; n=5) or MMP-7 null (MMP-$7^{-/-}$; n=10). The contralateral limb received a sham injection of saline. Luciferase activity was measured over a nine day period and used as a measure of tumor growth. **C-D:** Proliferative or apoptotic cells (arrows) in representative sections of WT and MMP-$7^{-/-}$ injected tibias were identified by immunostaining of phospho Histone H3 (pHistone H3) or cleaved caspase-3 respectively. The number of positively stained cells per total number of cells was calculated. Scale bars represent 50μm in all photomicrographs. Data are mean ± SD. Asterisk denotes that $p<0.05$ while n.s. indicates a non-significant p value.

Figure 4. Tumor mediated osteolysis is attenuated in the absence of host derived MMP-7. **A:** μCT scans of trabecular bone from tumor bearing and sham injected limbs of WT and MMP-$7^{-/-}$ animals allowed for the calculation of the BV/TV ratio. **B:** Representative H&E stained photomicrographs of tumor bearing tibias from WT and MMP-$7^{-/-}$ animals. Arrows indicate trabecular bone. Scale bars are 100 μm. The ratio of trabecular bone volume (BV) to tissue volume (TV) was determined several non-serial sections of tumor injected tibias obtained from WT (n=5) and MMP-7 null animals (n=7). **C:** Representative radiographic images from tumor injected WT and MMP-$7^{-/-}$ animals at day 9. Arrow indicates lytic tumor lesions in the wild type animals. The tumor volume (TuV) over tissue volume (TV) for tumor injected limbs of WT and MMP-$7^{-/-}$ animals was assessed. Data are mean ± SD. Asterisk denotes that $p<0.05$ while n.s. indicates a non-significant p value.

Figure 5. MMP-7 solubilization of RANKL in the tumor-bone microenvironment. **A:** ELISA analysis of soluble RANKL levels in lysates from tumor injected tibias obtained from WT (n=8) or MMP-$7^{-/-}$ (n=8) animals. **B:** Immunoprecipitation using antibodies directed toward the N-terminus of RANKL for the detection of soluble RANKL in tumor bearing tibias of WT and MMP-$7^{-/-}$ animals. MM refers to the molecular weight marker in kDa. Unglycosylated full length recombinant RANKL (arrow) was used as a positive control. In addition, MMP-7 solubilized RANKL (arrow head) served as a further positive control (+ve). Densitometry was performed on the level of soluble RANKL in PyMT-Luc bearing limbs derived from wild type (n=11) and MMP-$7^{-/-}$ null (n=12) mice. Data are mean ± SD. Asterisk denotes that $p<0.05$. **C:** TRAcP (red) positive, multinucleated (blue) osteoclasts (arrows) at the tumor-bone interface in WT and MMP-$7^{-/-}$ animals. The number of osteoclasts at the tumor-bone interface were determined in multiple non-serial sections of tumor injected tibias obtained from WT (n=5) and MMP-$7^{-/-}$ (n=7) animals. Scale bars are 100µm. Data are mean ± SD. Asterisk denotes that $p<0.05$ while n.s. indicates a non-significant p value.

Figure 6. Hypothetical mechanism of osteoclast derived MMP-7 action in the mammary tumor-bone microenvironment. **A:** Metastatic tumor cells through the secretion of factors such as parathyroid hormone related peptide (PTHrP), stimulate osteoblasts to express full length membrane bound RANKL. **B:** Osteoclasts express MMP-7 which can process membrane bound RANKL to a soluble active form. **C:** Soluble RANKL has been shown to be chemotactic for osteoclast precursors (25). In addition to acting as a potential

chemotactic molecule, soluble RANKL stimulates can stimulate the maturation and activation of osteoclast precursors. **D:** Activated osteoclasts in turn execute bone resorption leading to the release of growth factors such as TGFβ and IGFs that promote tumor growth in the bone microenvironment.

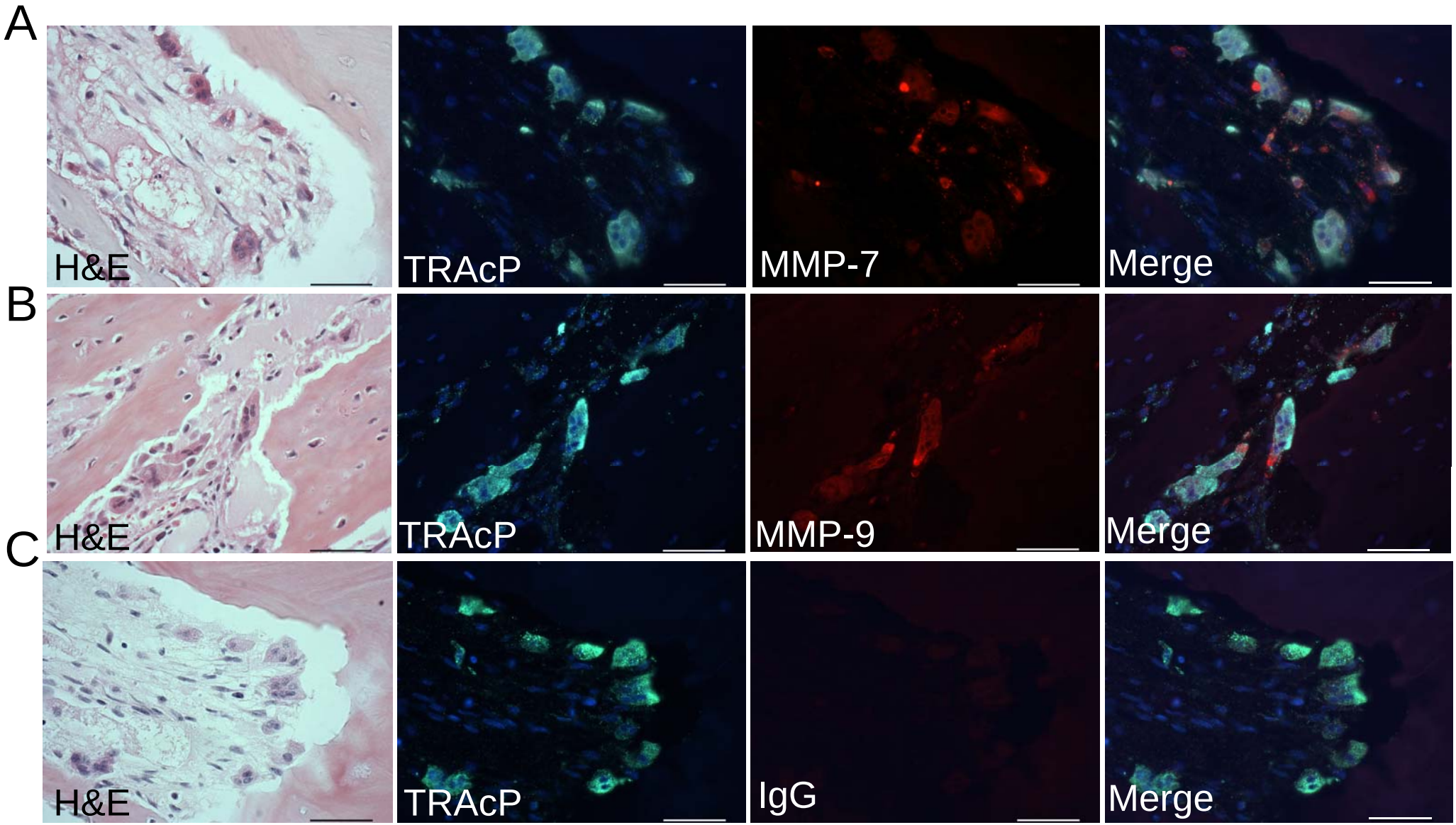
A
H&E
TRAcP
MMP-7
Merge
B
H&E
TRAcP
MMP-9
Merge
C
H&E
TRAcP
IgG
Merge

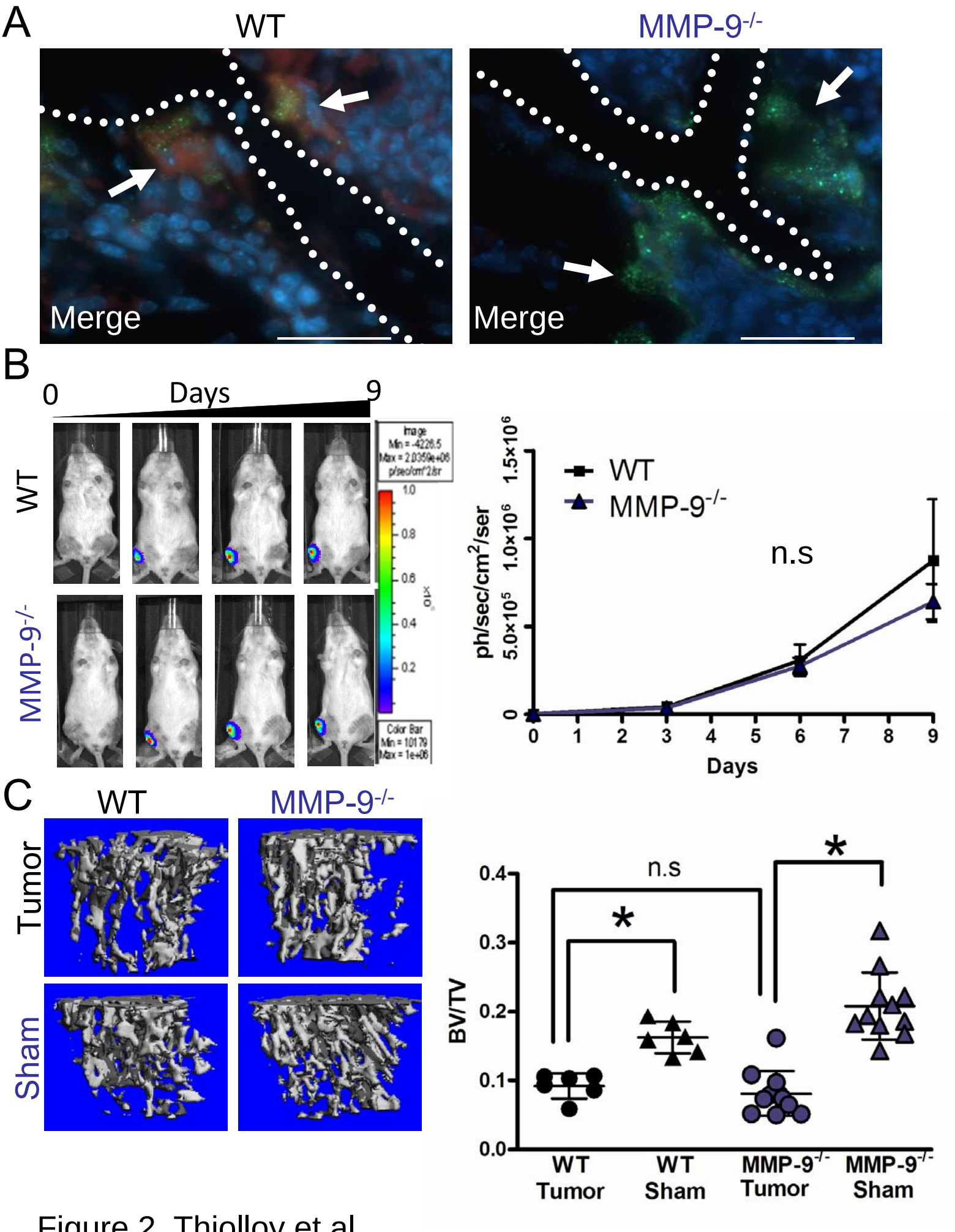

Figure 2. Thiolloy et al

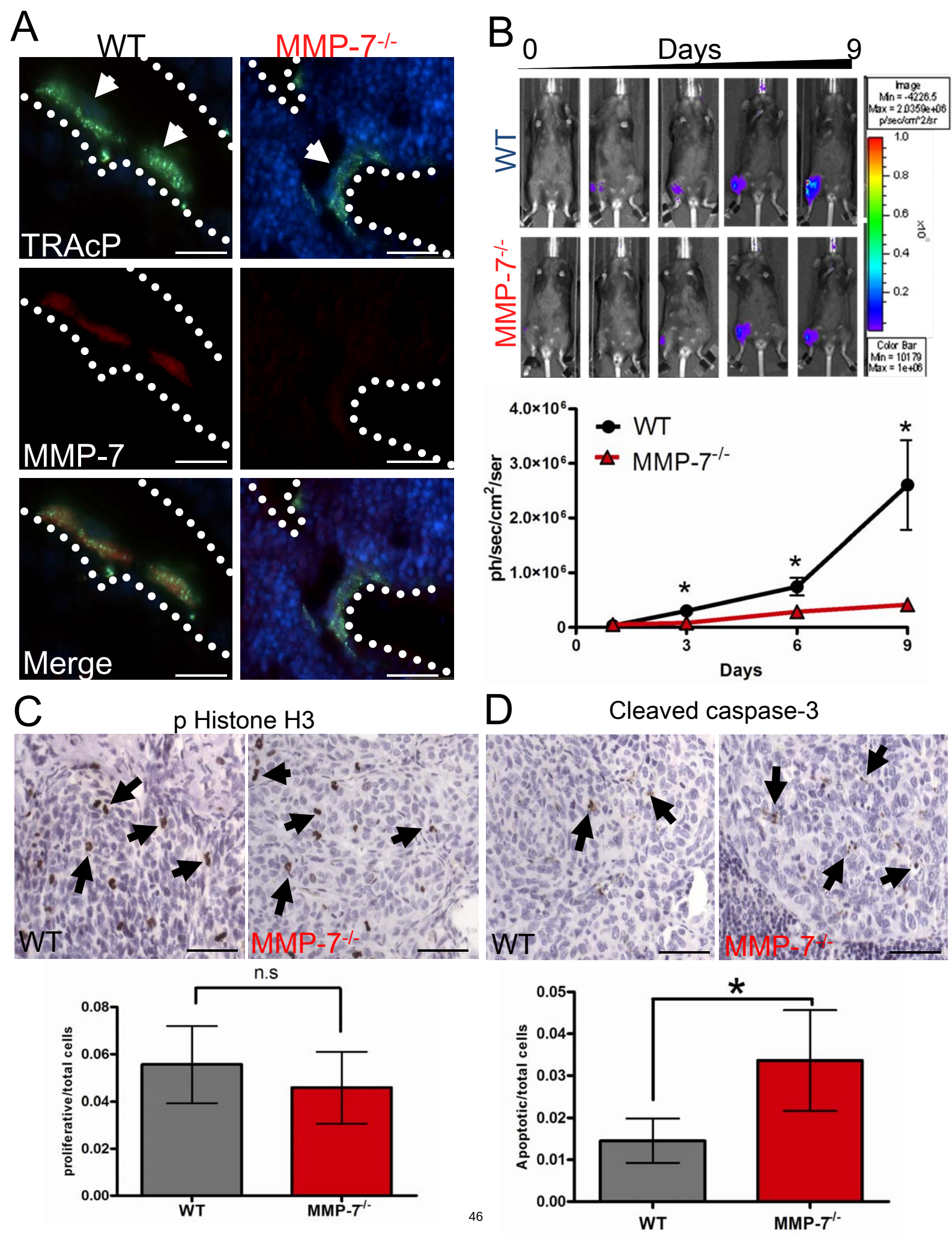

Figure 3. Thiolloy et al

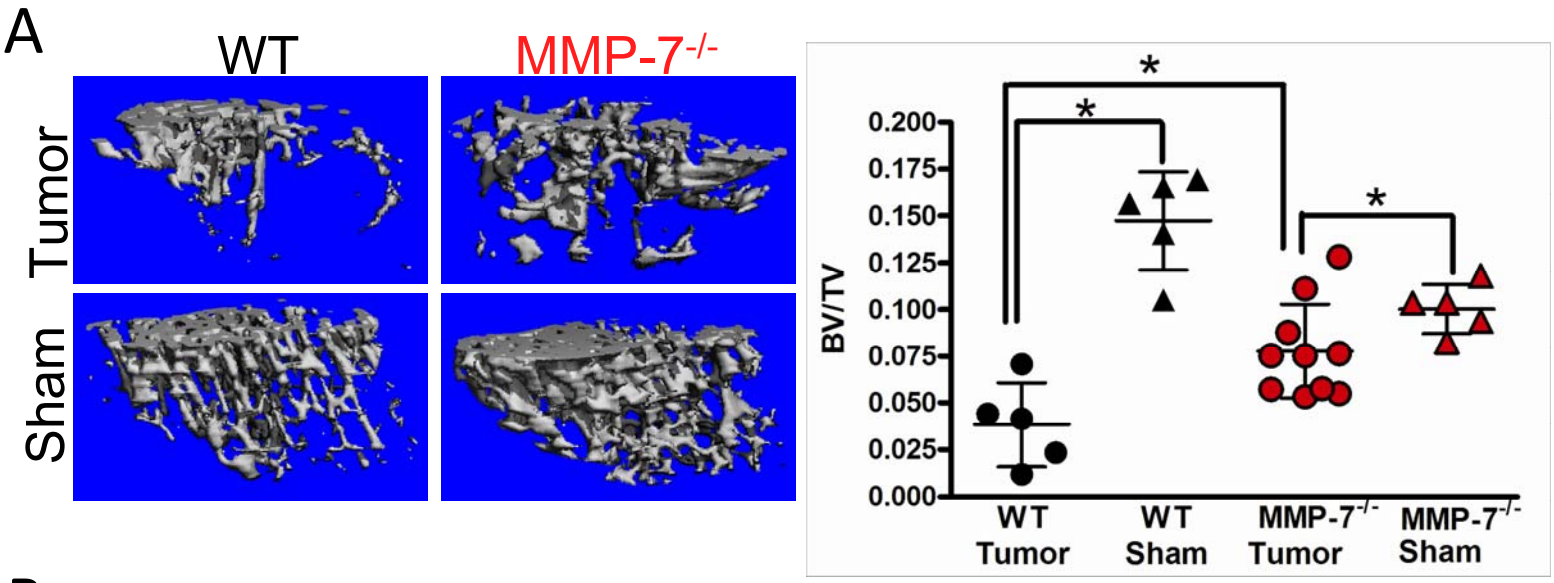
A
WT
MMP-7-/-
Tumor
Sham
BV/TV
0.200
0.175
0.150
0.125
0.100
0.075
0.050
0.025
0.000
*
*
*
WT Tumor
WT Sham
MMP-7-/- Tumor
MMP-7-/- Sham

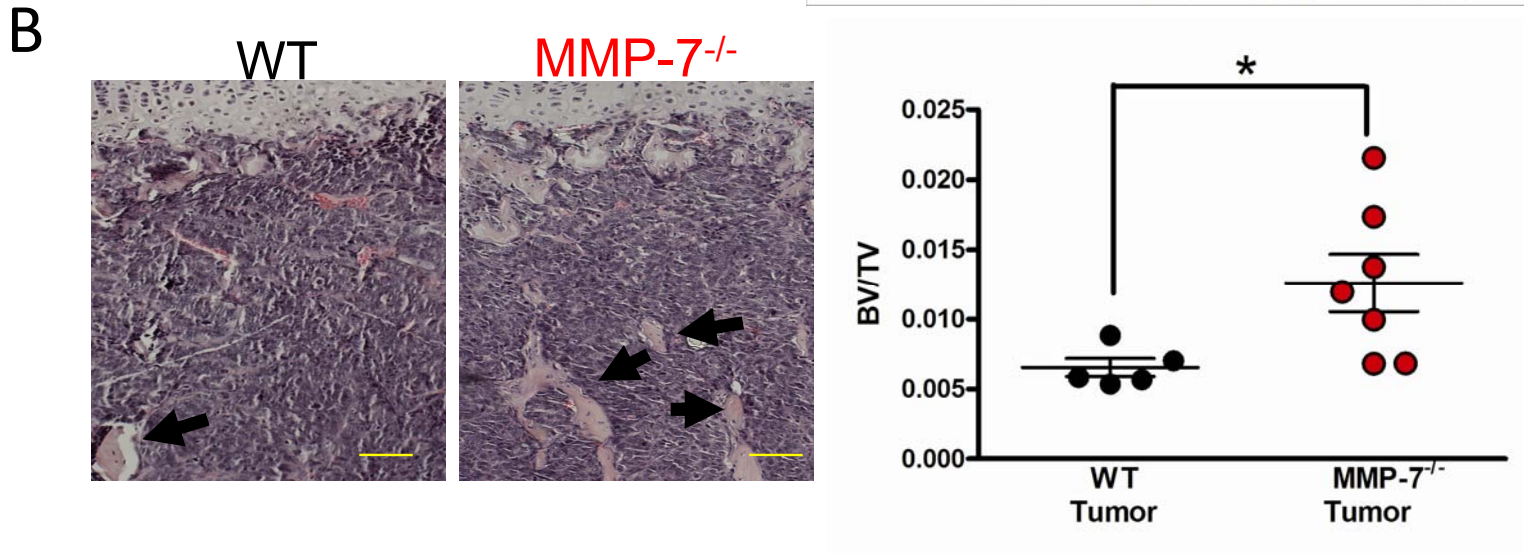
B
WT
MMP-7-/-
BV/TV
0.025
0.020
0.015
0.010
0.005
0.000
*
WT Tumor
MMP-7-/- Tumor

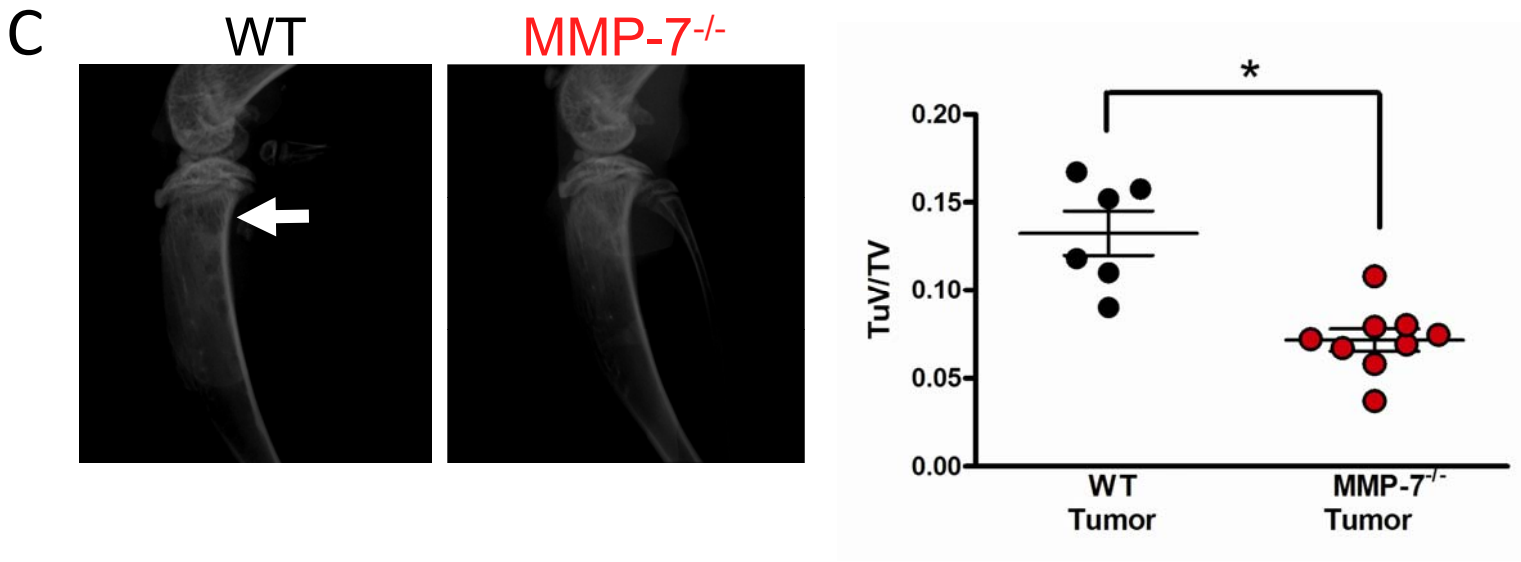
C
WT
MMP-7-/-
TuV/TV
0.20
0.15
0.10
0.05
0.00
*
WT Tumor
MMP-7-/- Tumor

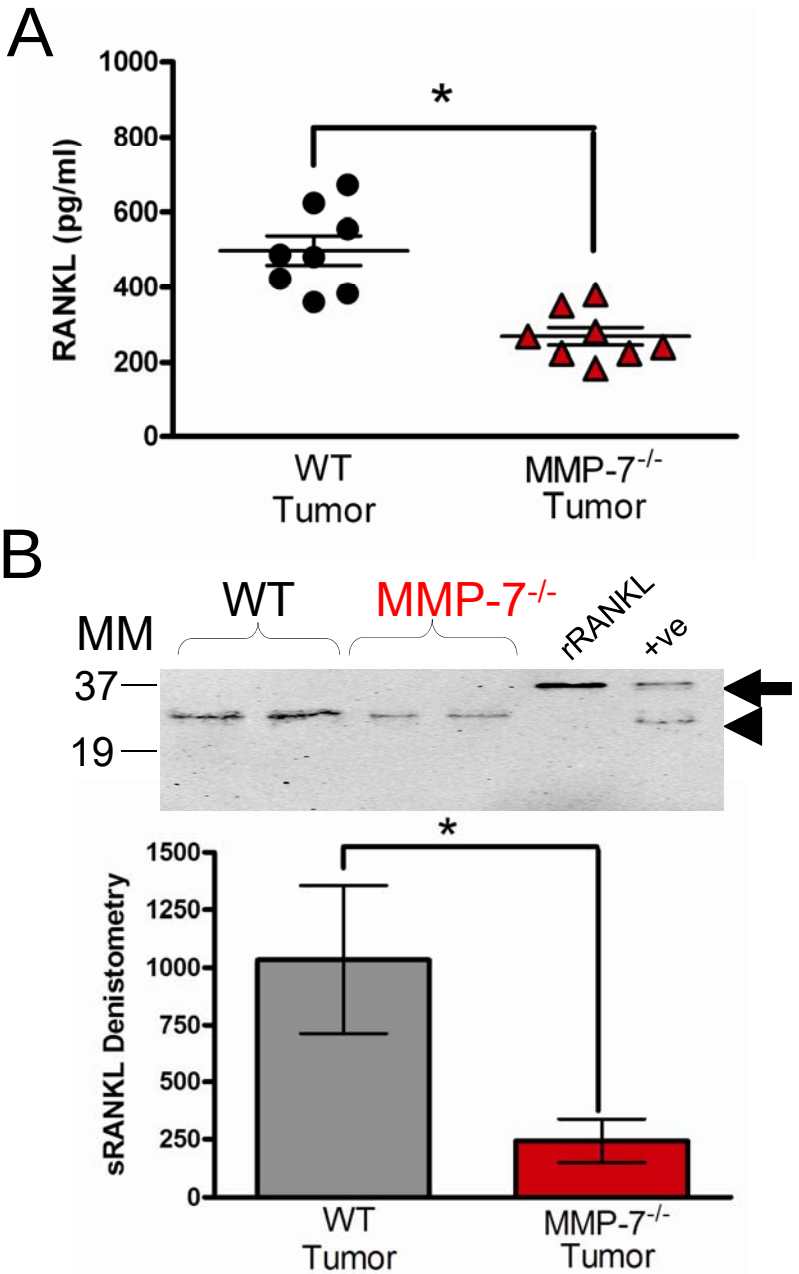

Figure R5. Thiolloy et al

Figure 6. Thiolloy et al

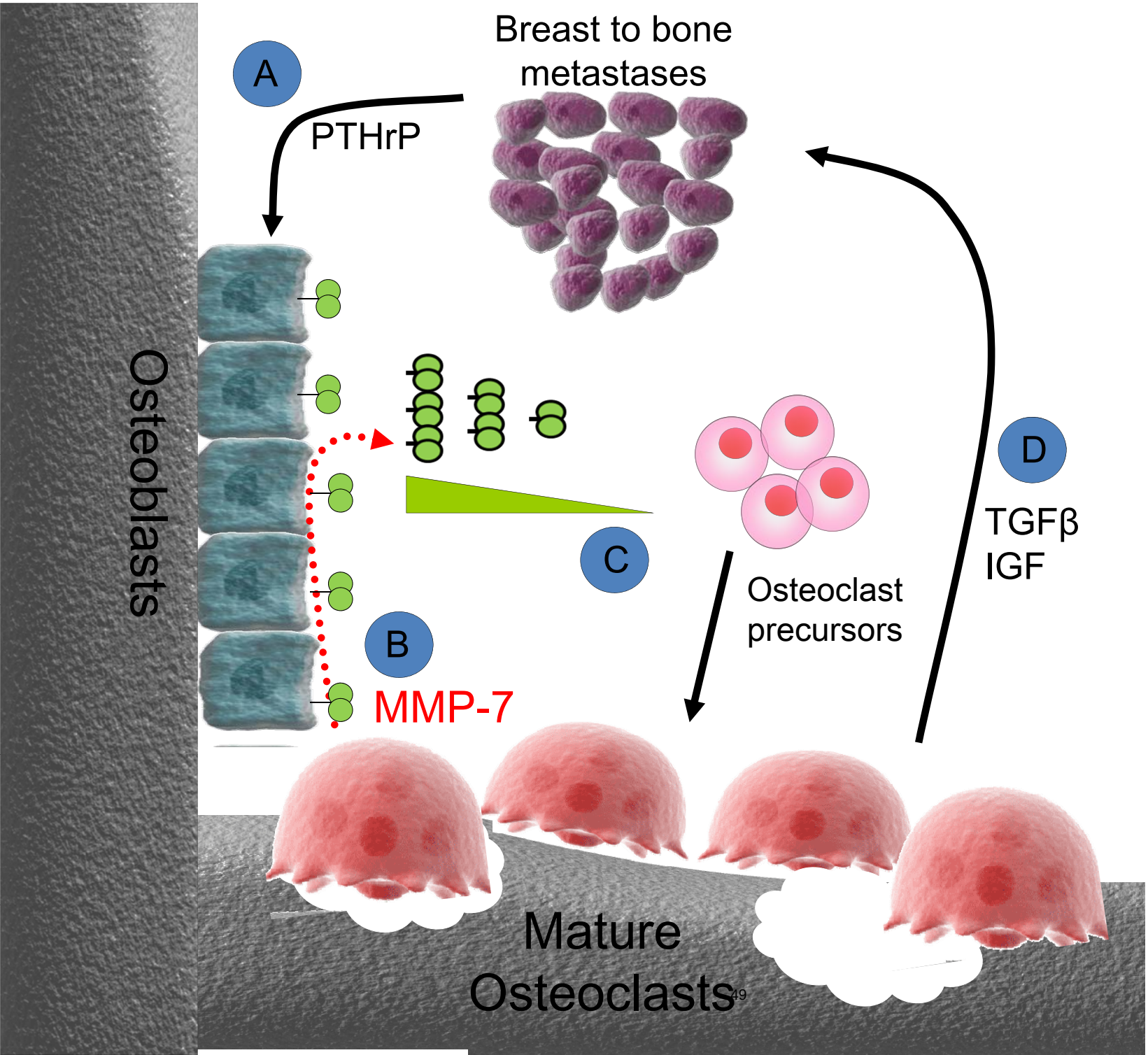

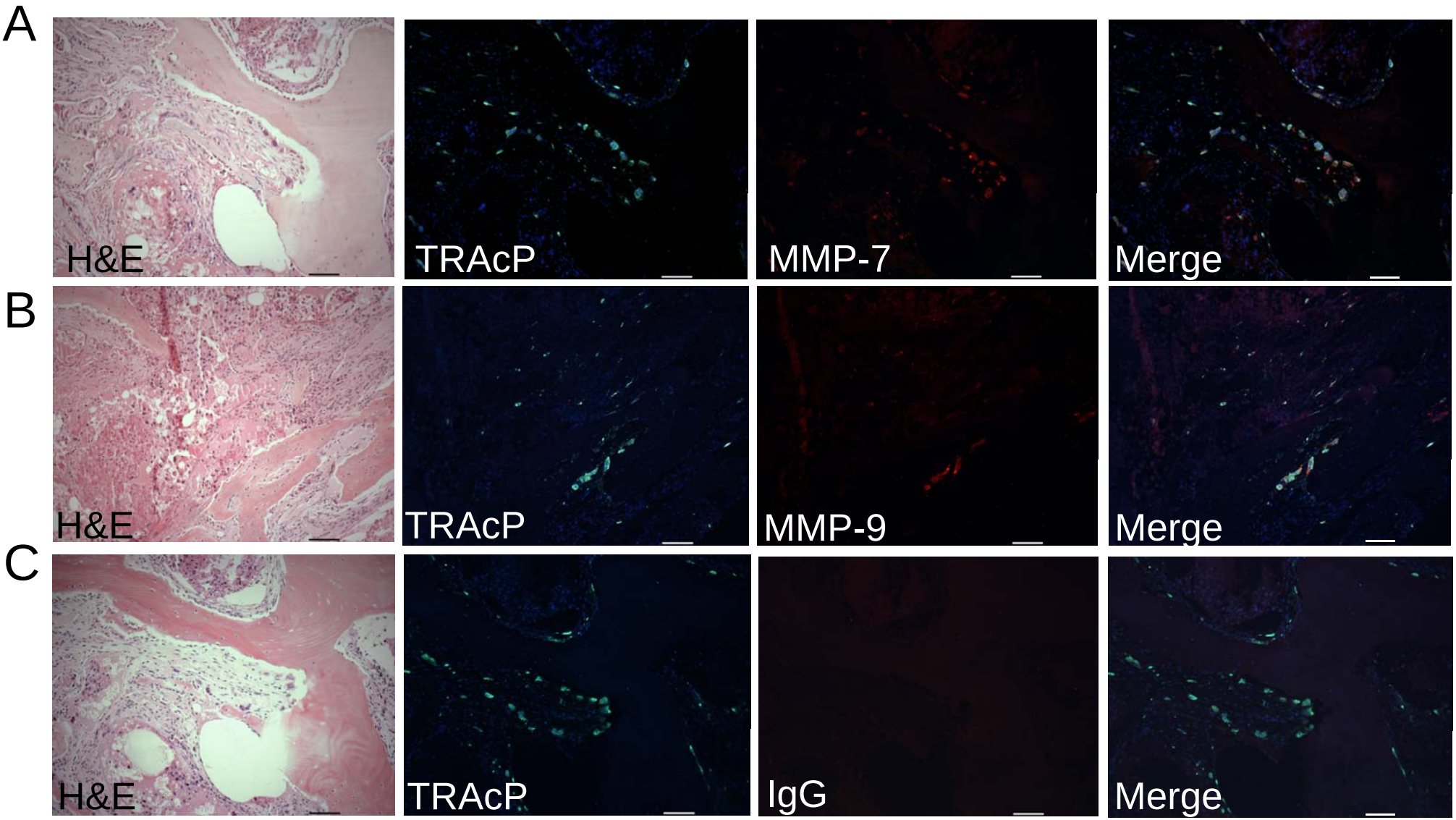

Fig. S1, Thiolloy et al., 2009

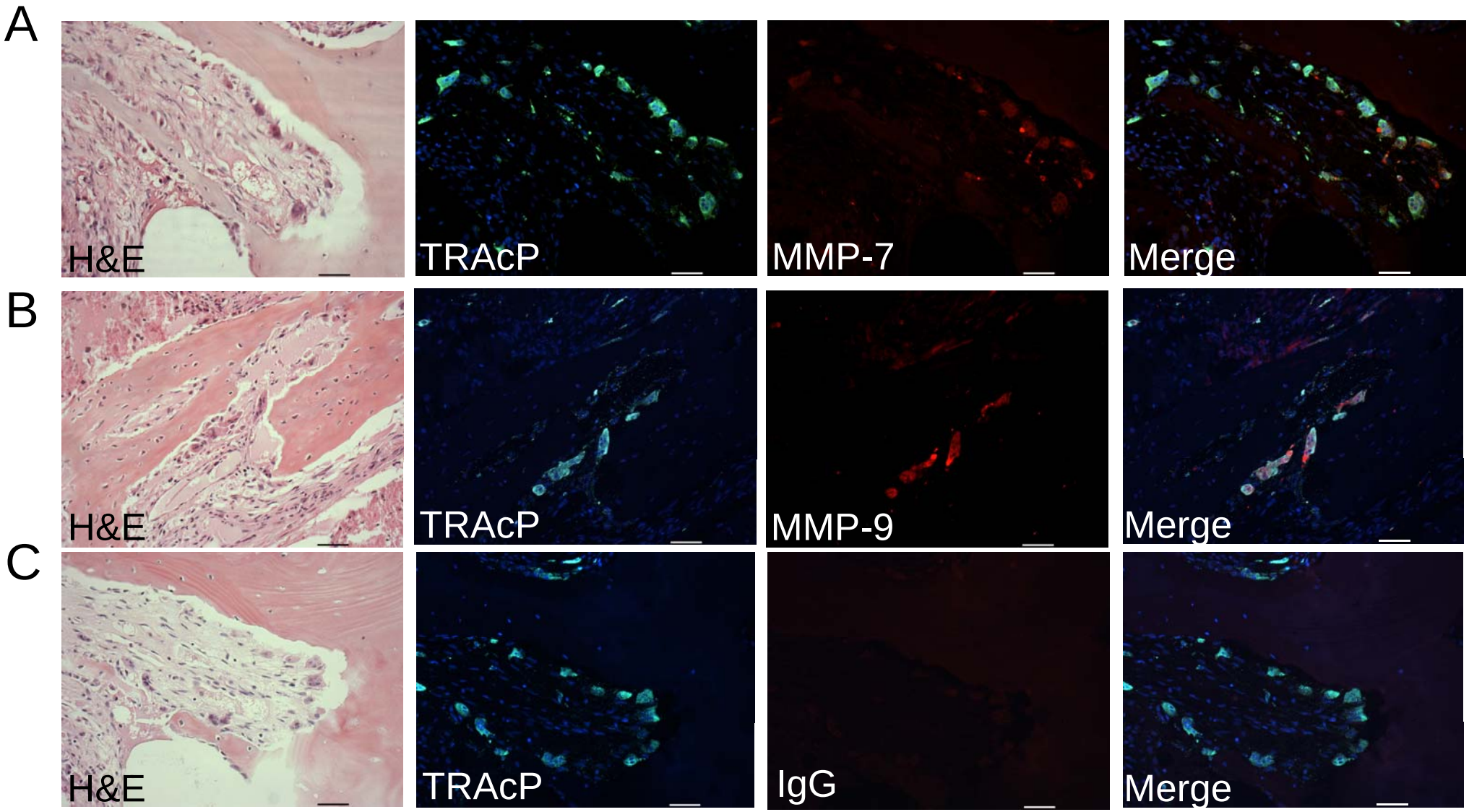

Fig. S2, Thiolloy et al, 2009

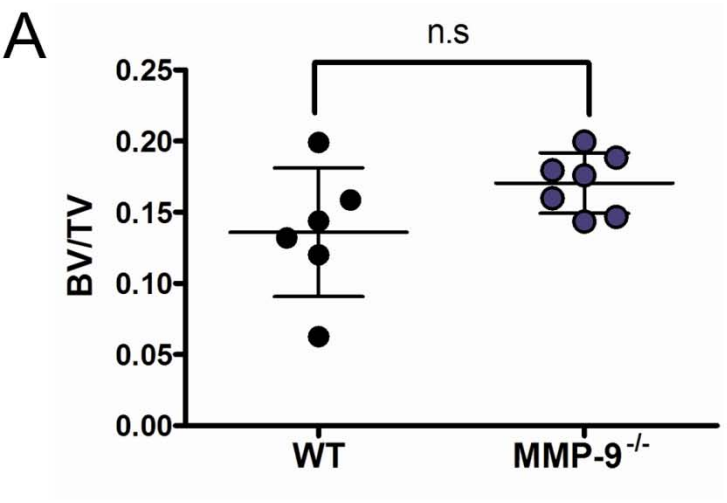

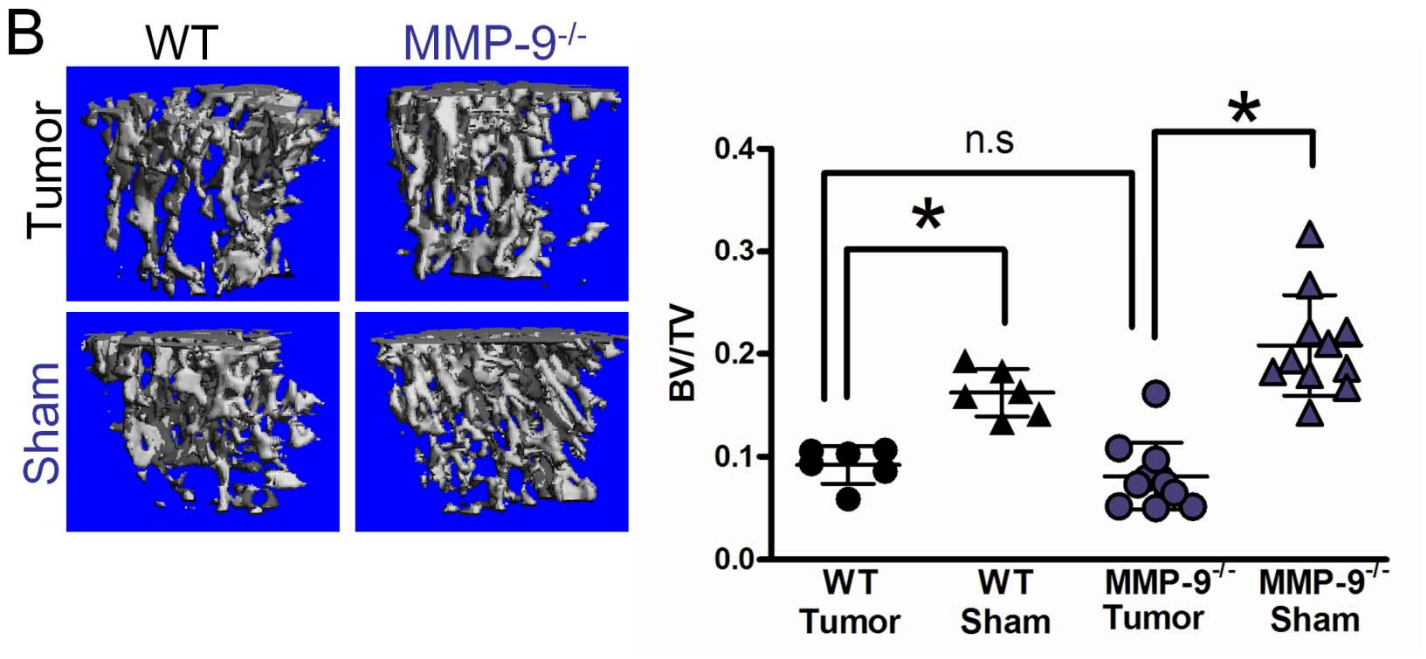

Figure 7. Host MMP-9 does not impact osteolysis in the bone microenvironment. A: The baseline BV/TV ratio immunocompetent 6 week old non-injected WT (n=6) and MMP-9$^{-/-}$ (n=7) mice on an FVB background was assessed by high resolution µCT scan analysis. **B:** Representative µCT scans of trabecular bone from tumor bearing and sham injected limbs of WT and MMP-9$^{-/-}$ animals. µCT was also used to calculate the ratio of trabecular bone volume to tissue volume (BV/TV) for tumor injected and sham injected wild type and MMP-9$^{-/-}$ mice. Data are mean ± SD. Asterisk denotes that $p<0.05$ while n.s. indicates a non-significant p value.

Fig. S3, Thiolloy et al, 2009

A

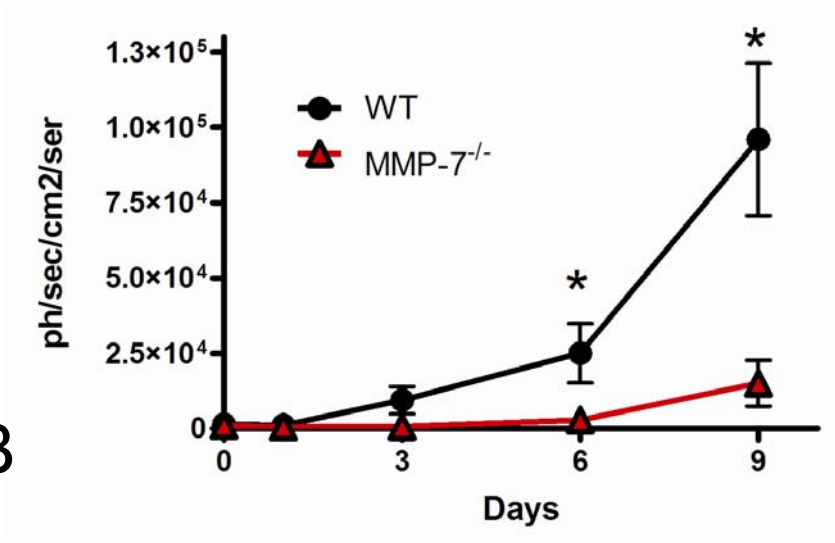

B

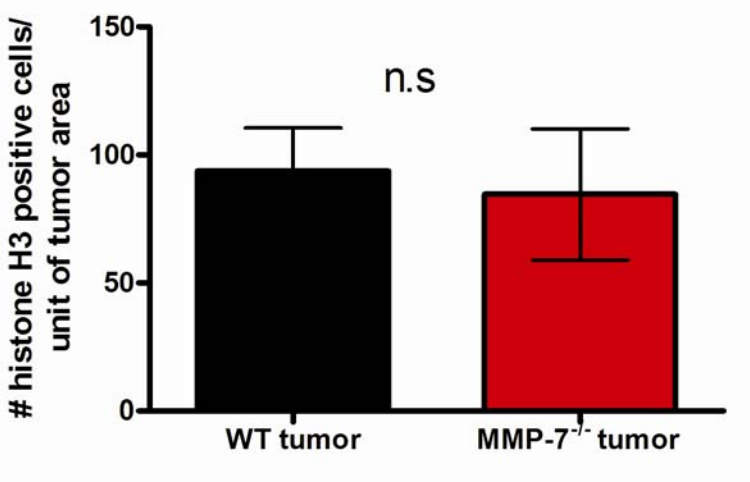

C

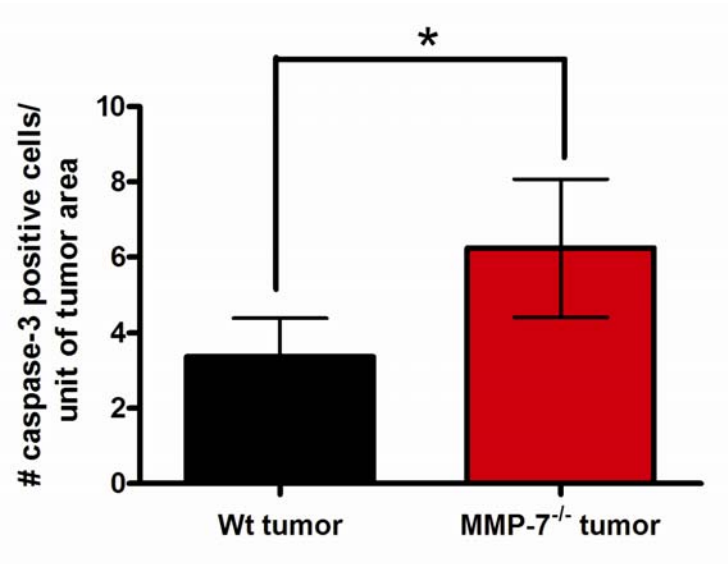

Fg. S4. Thiolloy et al, 2009

A

Fig. S5, Thiolloy et al., 2009

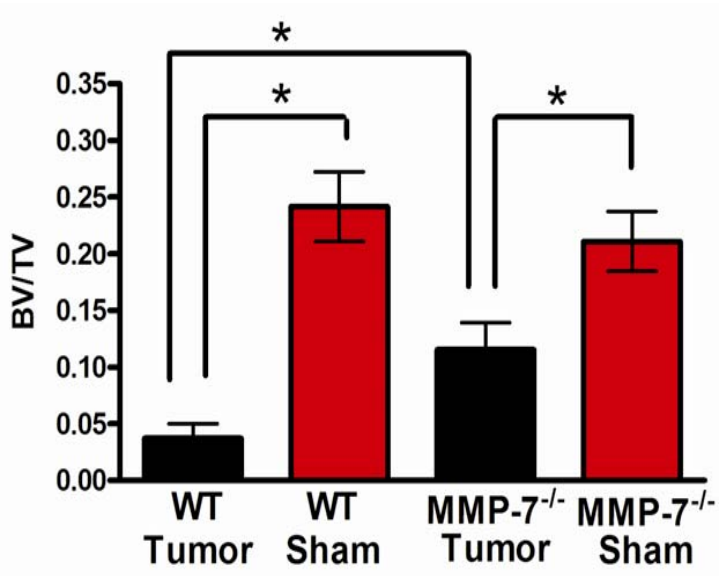

B

WT tumor

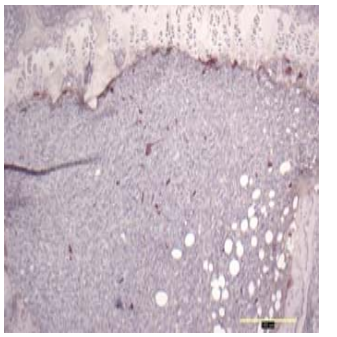

MMP-7$^{-/-}$ tumor

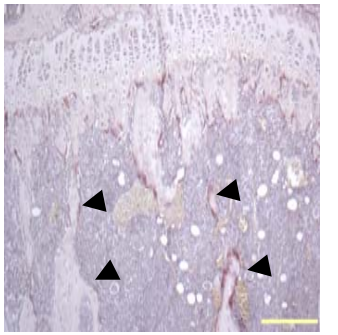

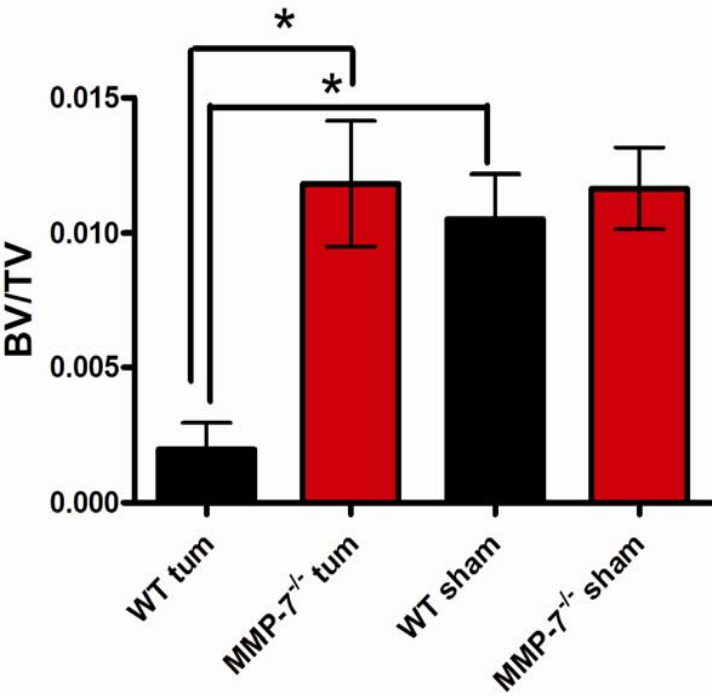

C

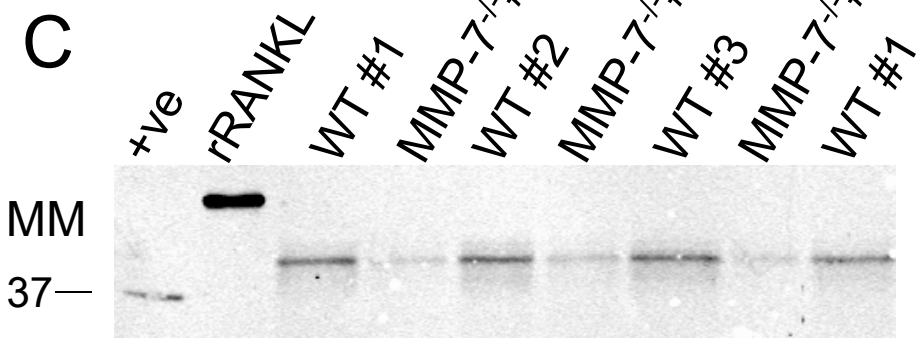

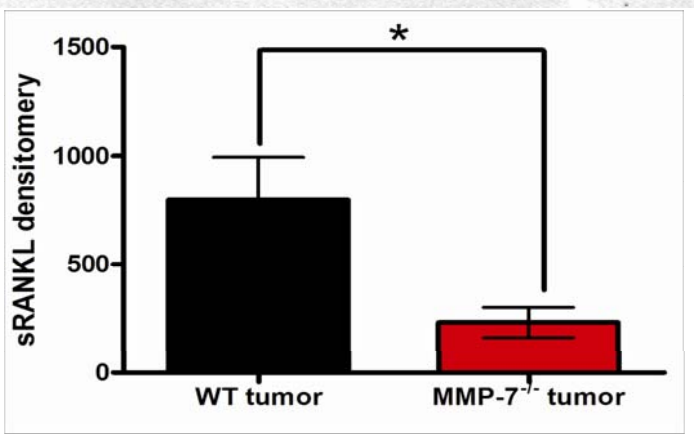

D

WT tumor

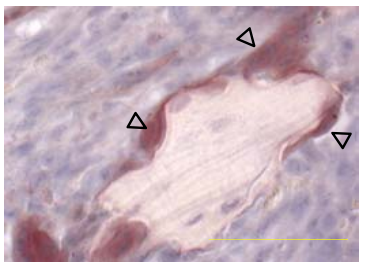

MMP-7$^{-/-}$ tumor

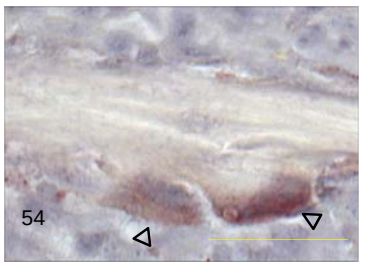

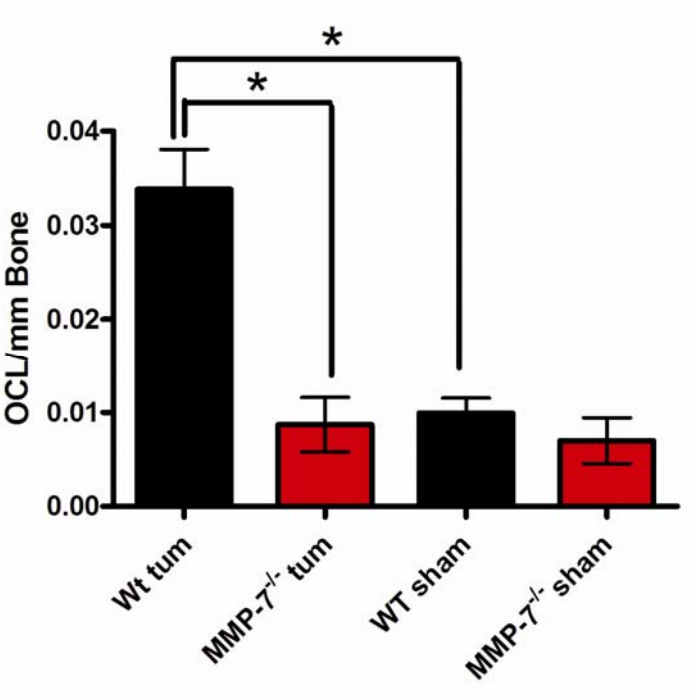

An Osteoblast-derived protease controls TGF-beta release and tumor cell survival in the bone microenvironment.

Thiolloy, S.[1], Edwards J.[2], Fingleton B.[1], Rifkin D.B[4], Mundy G.R.[2], Matrisian, L.M.[1], and Lynch, C.C.[3,1]

[1]Department of Cancer Biology, [2] Vanderbilt Center for Bone Biology, [3]Department of Orthopaedics and Rehabilitation, Vanderbilt University, Nashville, Tennessee and [4]Department of Cell Biology, New York University School of Medicine, New York.

Abstract

Introduction

Osteoblasts are the cells responsible for the production of the bone constituents and the deposition of growth factors such as transforming growth factor-β (TGF-β) and insulin growth factors (IGFs) in the bone matrix. These factors are complexed in latency proteins and therefore, the proteases that govern their release and activation are of great importance. TGF-β and IGFs are crucial player in the vicious cycle as they induced the differentiation of osteoclast precursor cells into multinucleated mature osteoclast (Lacey et al., 1998). By activating osteoclasts, osteoblasts promote osteolysis and the release of growth factors in the tumor-bone microenvironment (Kakonen and Mundy, 2003). Many studies on breast tumor growth in bone have focused on osteoclast function and the inhibition of bone resorption. However, with the exception of tumor stimulation of osteoclastogenic factors by the osteoblasts such as receptor

activator of NF-kappaB ligand (RANKL), little attention has been given to osteoblast contributions of tumor growth *in vivo*.

Matrix metalloproteinases (MMPs) are a family of 23 endopeptidases that can degrade numerous components of the extracellular matrix (ECM). More recently, MMPs have been implicated as important mediators of cell-cell communication by virtue of their ability to process multiple non-matrix molecules such as cytokines and growth factors to soluble forms resulting in either enhanced or attenuated activities (Lynch and Matrisian, 2002). Both osteoclasts and osteoblasts have been reported to express many MMP family members (Bord et al., 1998; Bord et al., 1996; Breckon et al., 1999; Dew et al., 2000; Holmbeck et al., 1999; Kusano et al., 1998; Parikka et al., 2005). Pre-clinical studies using broad spectrum MMPIs such as BB94 and GM6001 demonstrated that treatment of animal bearing breast or prostate tumor with MMPIs can reduce and prevent tumor growth and the development of bone lesions (Bonfil et al., 2006; Lee et al., 2001; Nemeth et al., 2002; Winding et al., 2002). It is generally assumed that the mechanism of action is the inhibition of collagen degradation. However, the MMPs have minimal activity in the acidic environment produced during osteoclast-mediated bone resorption. We have previously demonstrated osteoclast-expressed MMP7 solubilizes RANKL, and genetic ablation of host MMP7 results in a dramatic decrease in osteolysis and prostate tumor growth (Lynch et al., 2005). The contribution of osteoblast-derived MMPs to the vicious cycle remains to be examined.

In assessing MMP expression in human and murine breast-to-bone metastases, we found that one MMP in particular, MMP-2 was localized to osteoblasts, osteocytes and other cell types throughout the tumor/stroma compartment. MMP-2 deficient mice have a significantly slower

growth rate compared to wild type mice (Itoh et al., 1997). More detailed studies have shown that MMP-2 deficient mice also have abnormal cranio-facial defects mirroring those of the nodulis, arthropathy and osteolysis (NAO) syndrome in humans having a mutation in *mmp2* gene (Inoue et al., 2006; Mosig et al., 2007). Thus far, the contribution of MMP-2 in the pathological context of the metastatic tumor-bone microenvironment has not been examined. Given the importance of the osteoblasts in driving the vicious cycle, the current study focused on determining if and how host-derived MMP-2 impacted tumor induced osteolysis.

Results

Expression of MMP-2 in human and mouse samples of breast to bone metastasis

Microarray analysis revealed the high expression of several MMPs (MMP-2, -3, -7, -9 and -13) at the tumor-bone interface in a murine model of tumor growth in the bone (Lynch et al., 2005) In human samples of breast to bone metastasis and tumor bearing limbs of wild type animals, expression of these 5 MMPs were assessed. MMP-7 and MMP-9 were primarily localized in TRAcP positive multinucleated osteoclasts present at the tumor-bone interface (Thiolloy et al., 2009). In contrast, MMP-2 expression appeared more diffuse throughout the tumor/stroma compartment (Figure 1A-2B and data not shown). Osteoblasts and osteocytes were consistently positive for MMP-2 (Figure 1A and 1B). Interestingly, TRAcP positive cells in the tumor-bone microenvironment were rarely positive for MMP-2 (Figure 1A). These observations are in agreement with recent studies reporting osteocyte and osteoblast expression of MMP-2 in normal murine bone (Inoue et al., 2006; Mosig et al., 2007). We examined the potential impact of the ablation of host MMP-2 in a murine model of an osteolytic tumor-bone microenvironment.

Host MMP-2 significantly impacts mammary tumor growth in the bone

As MMP-2 deficient mice have a transient bone phenotype, we determined the baseline of trabecular bone volume/tissue volume (BV/TV) ratios of tibiae of 6 week old wild type and MMP-2 deficient animals corresponding to the age of the mice at the time of introduction of tumor cells. Trabecular bone is the first bone to be resorbed during tumor growth-induced osteolysis, resulting in the release of factors essential for the growth of the tumor (Mastro et al, 2003). High resolution μCT did not show differences in the BV/TV ratios between the wild type and MMP-2 deficient animals (Figure S1A).

To determine the contribution of host derived MMP-2 in mammary tumor growth in the bone, a mammary tumor cell line derived from a transgenic mouse expressing polyoma middle T antigen in the mammary gland, PyMT-Luc (Martin et al., 2008), was injected into the tibia of syngeneic immunocompetent FVB wild type and MMP-2 deficient animals. Quantitation of the bioluminescent signal from the PyMT-Luc tumor cells showed a marked decrease in tumor growth rate in MMP-2 null mice compared to wild type controls from day 3 post-injection onwards (Figure 2A and B). The observed result on tumor growth was confirmed using another independent mammary tumor cell line, 17L3C-Luc cells (Martin et al., 2008) (data not shown). To delineate whether reduced tumor growth was due to survival or slow growth rate *in vivo*, tumors in the MMP-2 deficient animals were imaged for at least 25 days. The bioluminescent signal was never comparable to the signal obtained in the wild type mice (Figure S1A). These data suggested that host MMP-2 was important for the initial survival and establishment of tumor cells.

To further analyze the impact of host MMP-2 to mammary tumor growth in the bone, tumor proliferation and apoptosis were analyzed by immunohistochemical staining for Mcm2 and cleaved caspase-3 respectively. No difference in tumor proliferation was observed between the two groups of animals at different time points (Figure 2C and D). However, MMP-2 deficient mice showed a significant higher level of apoptotic tumor cells as early as 3 days after intratibial injection compared to wild type mice (Figure 2C), despite the fact that the tumor cells express high levels of MMP2 *in vitro* (data not shown). The apoptotic tumor levels remained significantly higher in the MMP-2 deficient animals compared to controls at 6 days post-injection (Figure 2D). These data showed for the first time that host-MMP-2 impacts tumor growth in the bone as a result of a sustained effect on enhancing tumor cell survival.

Host MMP-2 contributes to mammary tumor growth induced osteolysis

Since a decreased in tumor growth was observed, we next assessed whether there was a concomitant decrease in osteolysis in the MMP-2 deficient tumor-bone microenvironment. High resolution μ-CT and histomorphometry analyses of the BV/TV ratio of wild type and MMP-2 deficient mice were performed at the end of the study period. Tumor bearing limbs of wild type mice showed a significant decrease in the trabecular bone content compared to tumor injected tibias of MMP-2 deficient animals (Figure 3A and B). In addition, X-rays analysis revealed that MMP-2 deficient mice present a significant lower tumor burden and less bone resorption compared to the wild type control mice (Figure 3C). As osteoclasts are the bone cells responsible for osteolysis, the number of mature osteoclasts was assessed in both groups of animals by counting the number of TRAcP positive multinucleated osteoclasts in multiple sections of multiple animals. A significant higher number of osteoclast per unit length of bone was

observed in tumor injected tibia of wild type mice compared tumor bearing limbs of MMP-2 deficient animals (Figure 3D). This decrease in osteoclast number in the MMP-2 deficient mice is in agreement with the higher content of trabecular bone and the decreased tumor growth rate i.e. less tumor growth induces less bone resorption therefore a lower number of mature osteoclasts.

Osteoblast-derived MMP-2 and TGF-β mediate to mammary tumor survival in the bone

Given that MMP-2 has been shown to impact osteoblast function and that our human and mouse tissues samples showed an osteoblast localization of MMP-2, we determined if osteoblast-derived MMP-2 could mediate tumor growth and survival. The ability of conditioned media from wild type and MMP-2 deficient primary osteoblast to modulate PyMT-Luc cells growth and survival was assessed using MTT growth and soft agar colony formation assays (Figure 4A and B). Conditioned media derived from wild type primary osteoblasts induced significant higher metabolic activity of tumor cells and a statistical higher number of tumor colonies compared to tumor cells incubated with conditioned media from MMP-2 deficient osteoblasts (Figure 4A). However, no difference was observed in the average size of the colonies between the two conditions, suggesting that the absence of MMP-2 in osteoblasts affects tumor survival but not tumor growth which is in agreement with our *in vivo* data (Figure 4B).

Next we assessed how osteoblast-derived MMP-2 controlled tumor growth and survival. MMP-2 can process numerous growth and survival factors, including TGF-β (Lynch and Matrisian, 2002), TGF-β is a key regulator of the vicious cycle, influencing both osteoblast and osteoclast differentiation and function (Guise and Mundy, 1998; Hauschka et al., 1986). TGF-β

is maintained in a latent form via its complex with the latency associated peptide (LAP) and the latent TGF-β binding protein (LTBP-1-4), and successive proteolytic cleavages induce the release of the active growth factor (Dubois et al., 1995; Saharinen et al., 1999). LTBP-3 deficient mice displayed a distinct cranial phenotype and develop osteopetrosis, therefore suggesting its key role in controlling the bioavailability of TGF-β in the bone (Dabovic et al., 2002; Dabovic et al., 2005). Furthermore, LTBP-3 has been shown to be important for osteogenic differentiation of human mesenchymal stem cells (Koli et al., 2008). Therefore, we investigated if MMP-2 was able to process LTBP-3. To assess the susceptibility of LTBP-3 for proteolytic processing, the conditioned medium of COS-7 cells overexpressing the large latent complex of LTBP-3 and LAP-TGF-β was subjected to digestion with recombinant active MMP-2. The molecular weight of the complex was reduced from ~240 kDa to ~230-220 kDa in the presence of recombinant active MMP-2, a processing event that has been previously reported to be the result of plasmin cleavage (Figure 4C) (Penttinen et al., 2002). Furthermore, ELISA for active TGF-β on conditioned media from COS-7 cells overexpressing LTBP-3-LAP-TGF-β complex revealed significantly increased levels of active TGF-β in presence of recombinant MMP-2 (Figure D). These data demonstrate for the first time that MMP-2 has the ability to process the latency binding protein of TGF-β, LTBP-3, responsible for sequestering TGF-β in the bone matrix.

The ability of TGF-β to promote tumor survival and growth of the PyMT-Luc cells was then assessed in a soft agar colony formation assay. Treatment of the tumor cells with TGF-β significantly increased the number of colonies but not the size of the colonies compared to the control condition (Figure 4E). We evaluated the levels of latent TGF-β *in vivo* by immunoblotting lysates of tumor bearing limbs of wild type and MMP-2 deficient mice 3 days

post-injection for LAP-TGF-β complex. Samples of MMP-2 deficient tibias injected with tumor showed a significant higher level of inactive LAP-TGF-β compared to the controls (Figure 4F). To investigate if higher levels of TGF-β will impact the tumor-bone microenvironment, the status of TGF-β signaling was assessed by immunoblotting for the phospho Smad2, the main intracellular effector of TGF-β receptor II/TGF-β signaling pathway (de Caestecker et al., 1998). Tissue lysates of tumor bearing tibias of MMP-2 deficient mice displayed a significant lower ratio of phospho smad2 over total smad2 compared to wild type controls (Figure 4F and G). Taken together, these data demonstrate that the proteolytic cleavage of LTBP-3 by osteoblast-produced MMP-2 mediates a primary step in the activation of TGF-β in the bone, resulting in tumor cell survival and the vicious cycle of tumor growth and osteolysis.

Osteoblast-derived MMP-2 impacts mammary tumor survival by mediating the release of active TGF-β.

In a bid to determine the molecular mechanism through which MMP-2 and TGF-β mediate their effect on mammary tumor growth, we first assess the possibility that TGF-β could mediate tumor survival in conditioned media from osteoblast. Neutralizing TGF-β antibody, 2G7, was used to treat cell culture media harvested from wild type and MMP-2 deficient primary osteoblasts. Blocking of TGF-β in conditioned media of wild type osteoblasts significantly reduced tumor metabolic activity and tumor cell survival (Figure 5A-C). Furthermore, to confirm that osteoblast-derived MMP-2 mediates tumor survival, recombinant MMP-2 was added to conditioned media from MMP-2 deficient primary osteoblasts prior to treatment of PyMT-Luc cells. Addition of exogenous MMP-2 to conditioned media from MMP-2 deficient osteoblasts rescued the tumor survival phenotype (Figure 5A-C). Interestingly, the presence of recombinant

MMP-2 was not sufficient to rescue the tumor survival phenotype when TGF-β was neutralized by 2G7 antibody (Figure 5A-C). This suggests that osteoblast-derived MMP-2 effect on tumor survival requires active TGF-β. Taken together, these results demonstrate for the first time that osteoblast-derived MMP-2 influences tumor cell survival via a TGF-β-mediated mechanism.

Discussion

Breast to bone metastasis is an incurable disease which affects more than 70 % of patients presenting with advanced breast cancer (Coleman and Rubens, 1987). Lytic bone lesions cause severe complications that greatly affect the quality of life of the patients (Mundy, 1997). Currently, no cure can be offered to patients suffering with bone metastasis, only palliative treatments such as bisphosphonates, surgery, radiotherapy and chemotherapy are available. Therefore, finding new molecular mechanisms underlying cell-cell communication in the tumor-bone microenvironment is key for the development of better therapies. Osteoblasts are important mediators of osteoclastogenesis and bone resorption and in assessing MMP expression in human and murine breast-to-bone metastases, we found that MMP-2 was localized to osteoblasts. To date, the contribution of osteoblast-derived proteases in mammary tumor growth-induced bone resorption has been understudied. We demonstrated that osteoblast-derived MMP-2 is required for tumor growth by enhancing tumor survival in the bone microenvironment. MMP-2 contributes to pathological bone resorption, but without affecting osteoclast precursor cells migration, maturation and differentiation (unpublished data). Our results show that osteoblast-MMP-2 affects on tumor survival in the bone microenvironment are mediated via the

processing of TGF-β latency proteins such as LTBP-3. It is of interest to note that MMTV-PyMT mice deficient for MMP-2 do not show any difference in terms of mammary tumor incidence, onset, growth rate and tumor volume compared to wild type control mice (Fingleton and Matrisian, personal communication), demonstrating that the effect of host MMP-2 are specific to the bone microenvironment.

Our study suggests that osteoblast-derived MMP-2 can modulate the release of TGF-β via the processing of LTBP-3. TGF-β is sequestered in a latency complex comprised of LTBP-1-4 and LAP and that these complexes must be sequentially processed in order to generate active TGF-β (Dallas et al., 1995; Janssens et al., 2005; Maeda et al., 2001; Maeda et al., 2002; Yu and Stamenkovic, 2000). Other members of the LTBP family such as LTBP-1 have been shown to be substrates for MMPs, in particular MMP-2 (Dallas et al, 2002, Maeda et al, 2002, Tatti et al, 2008). In addition, a recent study using a multiplex proteomics approach, identified LTBP-4 as a potential novel substrate for MMP-2 (Dean and Overall, 2007). However, of the four members of the LTBP family, only LTBP-3 deficient mice are reported as having skeletal defects including osteoarthritis and osteopetrosis (Dabovic et al., 2002; Dabovic et al., 2005). MMP-2 has also been shown to process LAP-TGF-β leading to the release of the active form of the growth factor (Dallas et al., 2002). Our study identifies for the first time that osteoblast-derived MMP-2 is responsible for the cleavage of LTBP-3, and we posit that based on other studies that MMP-2 subsequently cleaves LAP-TGF-β to release active TGF-β (Yu and Stamenkovic, 2000). While we suggest that MMP-2 is critical for TGF-β activation, the role of other proteases that can process TGF-β latency complexes, such as plasmin and MMP-9, may also contribute and explain

why residual levels of active TGF-β were identified in the conditioned media of MMP-2 deficient osteoblasts (Sato and Rifkin, 1989; Yu and Stamenkovic, 2000).

MMP-2-mediated activation of TGF-β is the primary mechanism responsible for tumor survival in the bone in our model. However, MMP-2 could impact tumor survival through the processing of other bone factors (Hauschka et al., 1986). IGFs are sequestered in a latent complex through their interactions with IGF binding proteins (IGFBP-1 to -4) (Mohan and Baylink, 1993) and several MMPs, including MMP-2 have been shown to process different members of the IGFBP family resulting in the activation of IGFs (Dunn et al., 1997; Fowlkes et al., 1994; Georgii-Hemming et al., 1996). However, we determined active IGF signaling levels in tissue lysates of tumor bearing limbs from wild type and MMP-2 deficient mice by immunoblotting for phospho IGF-receptor 1 (IGF-1R). No difference between MMP-2 deficient and wild type control animals was observed in terms of the phosphorylation levels of IGF-1R (data not shown). These data further support our conclusion that MMP-2 activation of TGF-β is a major mechanism mediating tumor survival in the tumor-bone microenvironment. However, we acknowledge that other reported substrates of MMP-2 may also contribute to tumor survival.

The majority of the studies examining the osteolytic vicious cycle conducted so far have focused almost exclusively on the 'forward' communication i.e. tumor cell control of osteoblast behavior that in turn impacts osteoclastic bone resorption. For the first time, our study demonstrates the *in vivo* 'reverse' communication i.e. osteoblast control of tumor cells behavior in the vicious cycle. For instance, in the 'forward setting', tumor-derived factors such as parathyroid hormone-related peptide (PTHrP) have been extensively studied as its expression by metastatic breast tumor cells induces osteoclastic bone resorption via osteoblast-dependent

activation of osteoclast precursors (Powell et al., 1991; Thomas et al., 1999). In addition, osteoclast-mediated bone resorption releases TGF-β that in turn affects PTHrP expression by tumor cells (Kakonen et al., 2002; Yin et al., 1999). However, the 'reverse setting' i.e. the direct modulation of the tumor cell behavior by osteoblasts and the molecular mechanisms therein have thus far not been assessed. Our results are the first to demonstrate the importance of osteoblast-derived signals in controlling tumor survival.

Besides its effects on tumor growth, TGF-β has been shown to modulate both osteoblast and osteoclast functions (Erlebacher and Derynck, 1996; Ignotz et al., 1987; Ignotz and Massague, 1985; Marcelli et al., 1990; Noda and Camilliere, 1989). Therefore, MMP-2-mediated release of active TGF-β may also directly affect osteoblast-osteoclast interactions. Our studies revealed a decrease in tumor-induced osteolysis. While our observations ruled out a direct role for MMP-2 in osteoclast maturation and activation, we speculate that osteoblast-derived MMP-2 potentially via the processing of LTBP-3 and activation of TGF-β impacts osteoclastogenesis. TGF-β has been shown be sufficient to induce osteoclastogenesis (Karsdal et al, 2003) but also to support and/or increase osteoclast activation (Lovibond et al., 2003; Takuma et al., 2003). Therefore, it is possible that the release of TGF-β by osteoblast-derived MMP-2 induces an increase in osteoclastogenesis in addition to its effects on tumor survival.

Our study demonstrates that MMP-2 secreted by osteoblasts impacts mammary tumor growth and mammary tumor-induced osteolysis. However, we cannot rule out that MMP-2 derived from other cell types is of importance in mediating tumor survival and bone resorption. For example, immune cells have been shown to express MMPs, including MMP-2 and recent findings demonstrated that T cells (a rich source of MMP-2) modulate tumor-induced bone

resorption (Fournier et al., 2006; Goetzl et al., 1996). Thus, a contribution of MMP-2 secreted by immune cells such as T cells that are present in our syngeneic immunocompetent mice cannot be disregarded. Inoue and coworkers reported the importance of MMP-2 in maintaining proper osteocytic canicular network caused by a defect in osteocyte functions and increased apoptosis (Inoue et al, 2006). Osteocytes are important in controlling bone mass through the modulation of osteoblast/osteoclast function via the secretion of factors such as sclerostin (van Bezooijen et al., 2004). As a consequence, we acknowledge that reduced osteolysis in a tumor setting could be caused by osteocyte function to regulate bone remodeling is a possibility in our model but has not been explored thus far.

In conclusion, this study demonstrates that osteoblast-derived MMP-2 significantly impact mammary tumor growth in the bone microenvironment by enhancing initial tumor survival. We suggest that MMP-2 contributes to mammary tumor survival by controlling the levels of active TGF-β release via the processing of LTBP-3. Our data demonstrate that the development of MMP-2-selective inhibitors have the potential to reduce TGF-β release from bone stores and add a therapeutic agent to the palliative treatments currently offered to patients with breast-to-bone metastasis.

Acknowledgements

We would like to thank Steve Munoz of the Vanderbilt Bone Center for his expertise, Branka Dabovic of The department of Cell Biology, New York University School of Medicine, New York for providing reagents. This research was supported by NIH: 1 R01 CA84360 (LMM) and NCI 1U54-CA126505, CCL and ST are supported by the Department of Defense under award

number W81XWH-07-1-0208 and BC051038 respectively..Views and opinions of, and endorsements by the author(s) do not reflect those of the US Army or the Department of Defense.

MATERIALS AND METHODS

Reagents

All experiments involving animals were conducted after review and approval by the office of animal welfare at Vanderbilt University. De-identified human samples of frank osteolytic breast to bone metastasis (n=11) were collected by curettage with IRB approval from Vanderbilt University from 2005 to 2008. Wild type and MMP-2 deficient mice in the FVB/N-Tg background were kindly provided by Dr. Lisa Coussens, Dept. of Pathology, University of California San Francisco. Two different syngeneic FVB mammary tumor cell lines derived from the mammary tumor virus (MMTV) long terminal repeat-polyoma middle-T antigen (MMTV-PyMT) model of mammary tumorigenesis were isolated in our laboratory and maintained as previously described (Martin et al, 2006). These tumor cells lines were tagged with a luciferase reporter gene and designated, PyMT-Luc and 17L3C-Luc. All reagents were obtained from Sigma-Aldrich except where specified.

Intratibial injection and in vivo quantitation of tumor growth

PyMT-Luc or 17L3C-Luc tumor cells ($2x10^5$) in a 10µl volume of sterile phosphate buffered saline (PBS) were injected into the tibia of anesthetized immunocompetent 6 week old mice that were wild type or deficient in MMP-2. The contralateral limb was injected with 10µl of PBS

alone and acted as a sham injected control for changes in the bone due to the surgical procedure. The IVIS^{TM} system (Caliper Life Sciences) was used to detect luminescence from the PyMT-Luc and 17L3C-Luc tumor cells after intratibial injection. Firefly luciferin (120mg/kg in sterile PBS, Gold Biotechnology, Inc.) was delivered retro-orbitally 1 to 2 minutes prior imaging. Mice were imaged at 24 hours and every 3 days after surgery. Living Image^{TM} software (Calipers Life Sciences) was used to quantify the luminescence intensity in the tumor bearing limb over time. For the histomorphometry, mice were sacrificed at 9 days post-surgery, a time point previously determined to be prior to the breach of the cortical bone by the tumor and both the tumor injected and contralateral control tibiae were harvested. For immunohistochemical staining, mice were injected with PyMT-Luc cells were collected at described time points and both tumor bearing and control tibias were collected. All animal studies were independently repeated at least three times.

Histology

Fresh human breast-to-bone metastases, tumor and sham injected mouse tibiae were fixed overnight in 10% buffered formalin and decalcified for 3 weeks in 14% EDTA at pH 7.4 at 4^{o}C with changes every three days. Tissues were dehydrated through ethanols and embedded in paraffin and 5μm thick sections were cut. For MMP-2 localization (Abcam, cat. No.ab37150), tumor proliferation (anti-Mcm2 Abcam, Cat. No.ab31159) and tumor apoptosis (anti-Caspase-3, Cell Signaling, Cat. No. 9662), the following technique was employed. Sections were rehydrated through a series of ethanols and then rinsed in tris buffered saline (TBS; 10mM Tris at pH 7.4, 150mM NaCl) with Tween-20 (0.05%). Following washing in TBS, tissue sections were blocked using standard blocking criteria for 1 hour at room temperature. MMP-2 (1:150 dilution), Mcm2

(1:200 dilution) and cleaved caspase-3 (1:400 dilution) antibodies at an appropriate dilution of were added in blocking solution to the tissue sections overnight at 4^{o}C. The appropriate IgG control antibodies were used for each antibody to ensure specificity. Slides were washed extensively in TBST prior to the addition of a species specific secondary biotinylated IgG antibody (Vector Laboratories) diluted 1:1,000 in blocking solution for 1 hour at room temperature. Labeled cells were visualized using an avidin-biotin peroxidase complex (Vectastain ABC kit, Vector Laboratories) and 3,3′ –Diaminobenzidine tetrahydrochloride substrate (Sigma, St. Louis, MO). Sections were counterstained with hematoxylin prior to dehydration through ethanols and permanently mounted.

Tartrate-resistant acid phosphatase (TRAcP), a marker of mature osteoclasts, was detected using a colorimetric kit according to the manufacturer's instructions (Sigma-Aldrich, Cat. No. 387A). Gross anatomy of the mouse tibiae was assessed by hematoxylin and eosin (H&E) staining.

Micro computed tomography (µCT) and histomorphometric analyses

For gross analysis of trabecular bone volume, formalin fixed tibiae were scanned at an isotropic voxel size of 12µm using a microCT40 (SCANCO Medical). The tissue volume (TV) was derived from generating a contour around the metaphyseal trabecular bone that excluded the cortices. The area of measurement began at least 0.2mm below the growth plate and was extended by 0.12mm. The bone volume (BV) included all bone tissue that had a material density greater than 438.7 mgHA/cm^3. These analyses allowed for the calculation of the BV/TV ratio. The same threshold setting for bone tissue was used for all samples.

For histomorphometry, three non-serial sections of tumor bearing and sham injected hind limbs were H&E stained to assess the BV/TV ratio or with TRAcP to assess osteoclast number per mm bone at the tumor bone interface using Metamorph® software (Molecular Devices).

Immunoblotting

Tumor and sham injected tibias from wild type or MMP deficient animals were harvested 3 days post-injection and flash frozen in liquid nitrogen. Tissue homogenates were generated by mortar and pestle and total protein was subsequently extracted using a standard protein lysis buffer (0.1 % sodium dodecyl sulfate, 0.5 % sodium deoxycholate, 1 % triton X100, 10 mM Tris pH 7.5, 150 mM NaCl) containing a complete protease inhibitor cocktail (Roche, Cat. No. 11836145001) and phosphatase inhibitor cocktails (Sigma Cat. No. P2850 and P5726). Protein concentration in isolated samples was quantitated using a bicinchoninic acid (BCA) assay as per manufacturer's instructions (Pierce, Cat. No. 23227). Equal concentrations of total protein were loaded on to a denaturing 8% SDS-PAGE gel. The blots were then panned with antibodies directed to latent-associated peptide (LAP) (R&D system, cat. No., 1:1,000 dilution), phospho Smad2 (Millipore, cat. No.AB3849, 1:1000 dilution), total Smad2 (Cell signaling, cat. No.3102, 1:1,000 dilution) and actin (Santa Cruz, Cat. No. sc-1615, 1:1,000) in 5% BSA in 1XTBST (TBS with 0.05% Tween 20) overnight with rocking at 4^{o}C. For latent binding protein-3 (LTBP-3) immunoblotting, equal amounts of protein were loaded on 6 % SDS-PAGE non-denaturing gels respectively. Blots were then incubated with anti-LTBP-3 (anti-L3C, dilution 1:1,000, kindly provided by Dr D. Rifkin, Dept of Cell Biology and Medicine, New York University School of Medicine) (Chen et al, 2002) diluted in standard blocking solution (5 % milk in 1X TBS) overnight at 4^{o}C with rocking. The following day, blots were washed extensively with 1xTBST

prior to the addition of a secondary infra-red labeled antibody (1: 5,000 dilution in 1xTBST, Rockland Inc.) for 1 hour at room temperature with rocking, in the dark. After washing in 1xTBST, blots were developed and bands of interest were quantitated using the Odyssey system (LI-COR Biosciences, Lincoln, NE).

Isolation of primary osteoblasts and osteoclast precursor cells

Calvaria from wild type or MMP-2 deficient 3 to 4 day-old pups were isolated in cold sterile 1X PBS (Phosphate buffered saline) buffer. Calvaria were then subjected to three repetitive digestions (15 min, 30 min and 1 hour) in digestion buffer (α-MEM, GIBCO, cat. No. 12571, 0.025% trypsin, GIBCO, cat. No. 25200, 10mg/ml collagenase P, Roche, cat. No. 11213857001, 100 µg/ml penicillin/streptomycin, Invitrogen, 250 UG/ml fongizon, GIBCO, cat. No. 15290-018) at 37^{o}C with vigorous shaking every 15 min. Isolated primary cells were then maintained in α-MEM and 10% fetal bovine serum (Atlas Biologicals, cat. No. 0500A). Primary osteoblasts were plated at a density of 2x10^{5} cells/well in 6 well-plates and 24 h after seeding; cells were cultured in serum-free α-MEM. After 24 h, conditioned media was collected, centrifuged at 1100 rpm to remove cellular debris and used for the MTT and soft agar colony formation assays described below.

Bone marrow cells from tibias and femurs were isolated from 6 week-old wild type and MMP-2 deficient mice by flushing the cells with 1 ml of cold 1X PBS using a 25G$^{5/8}$ gauge needle. Isolated cells were centrifuges at 1,000 rpm and rinse with 1 ml of 1X PBS. CD11 positive cells were then isolated using a Macs® separation columns (Miltenyi Biotech., MS coloumns) following the manufacturer protocol and plated in α-MEM and 10% fetal bovine

serum (Atlas Biologicals), 100 µg/ml penicillin, streptomycin (Invirogen) and 250 UG/ml fongizon (Gibco, BRL, Long Island, NY) for the migration and differentiation assays.

MTT Assay

Quantitation of viable PyMT-Luc cells treated with conditioned media from primary osteoblast wild-type or MMP-2 deficient mice was assessed by tetrazolium-based colorimetric assay (MTT, Promega Corporation, cat. No. G5421). Tumor cells were plated in 96-well plates at a density of 1000 cells/well and 24 h after seeding, cells were treated with 100 µl either serum-free or conditioned media from primary osteoblasts isolated from either wild type or MMP-2 deficient mice. For the MMP-2 rescue experiment, wild type and MMP-2 deficient osteoblasts were treated overnight in serum starved media with 200 ng human recombinant MMP-2 (Calbiochem, Cat. No.ab 37150-100). For the TGF-β neutralization experiment, conditioned media from wild type and MMP-2 deficient osteoblasts were incubated overnight at 37^{o}C in presence of 50 µg/ml 2G7 (TGF-β neutralizing antibody, kindly provided by Dr Mundy, Vanderbilt Center for Bone Biology, Vanderbilt University). After 24 and 48h of treatment, 20 µl of MTS was added to each well of cells, and the reactions were allowed to run for 3 h at 37°C. Spectrophotometric absorbance of each sample was measured at 490 nm using a MRX revelation microplate reader (Dynex Technologies). Experiments were performed in quadruplicate.

Soft agar colony formation assay

PyMT-Luc cells were plated at a density of $1.5x10^3$ cells/well in 24 well-plates in soft agar containing α-MEM, 5% fetal bovine serum, 0.7% agarose (Fischer, cat. No. BP164). Subsequent to plating, tumor cells were treated with 400 µl of either with 5% serum α-MEM or conditioned media derived from either wild type or MMP-2 null primary osteoblasts supplemented with 5 % serum. As a control, 1ng/ml TGFβ was also added to the 5% serum α-MEM. All media were changed every 3 days. After 10 days of culture, cells were stained overnight with 0.1mg/ml p-iodonitrotatrazolium (Sigma, cat. No. I-8377). Numbers of colonies and average diameter of the colonies for each condition were measured on 100X photomicrographs and analyzed using Meta morph Imaging Software (Molecular Devices). Experiments were performed in quadruplicate.

Expression and processing assays

COS-7 cells were transiently transfected with a full length LTBP-3 cDNA construct and human TGF-β1 cDNA (kindly provided by Dr Rifkin, Dept of Cell Biology and Medicine, New York University School of Medicine) using Superfect kit (QIAGEN). COS-7 cells were plated at a density of 10^5 cells/well in a 6 well plate the day prior the transfection. Cells were then incubated in transfection mix (30 µl of superfect reagent, 0.5 µg of each constructs and 500 µl of DMEM and 10% fetal bovin serum) overnight. The next day, transfected COS-7 cells were incubated for 48 hours in serum starved DMEM media. The conditioned media was then incubated for 3 hours in presence of 300 ng of recombinant human MMP-2 (Calbiochem, Cat. No. PF023) or for 1 hour in presence of 150 ng of plasmin (Sigma-Aldrich Cat. No. P1867) as a positive control (Penttinen et al, 2002). Samples were then analyzed by immunoblotting for LTBP-3 as described above.

Statistical analyses

Statistical analyses were performed using Student's *t* Test and Anova test using GraphPad Prism Software, Inc. A value of $p < 0.05$ was considered significant. Data are presented as mean ± standard deviation (SD).

References

Bonfil, R. D., Sabbota, A., Nabha, S., Bernardo, M. M., Dong, Z., Meng, H., Yamamoto, H., Chinni, S. R., Lim, I. T., Chang, M.*, et al.* (2006). Inhibition of human prostate cancer growth, osteolysis and angiogenesis in a bone metastasis model by a novel mechanism-based selective gelatinase inhibitor 1. International Journal of Cancer *118*, 2721-2726.

Bord, S., Horner, A., Hembry, R. M., and Compston, J. E. (1998). Stromelysin-1 (MMP-3) and stromelysin-2 (MMP-10) expression in developing human bone: potential roles in skeletal development. Bone *23*, 7-12.

Bord, S., Horner, A., Hembry, R. M., Reynolds, J. J., and Compston, J. E. (1996). Production of collagenase by human osteoblasts and osteoclasts in vivo. Bone *19*, 35-40.

Breckon, J. J., Papaioannou, S., Kon, L. W., Tumber, A., Hembry, R. M., Murphy, G., Reynolds, J. J., and Meikle, M. C. (1999). Stromelysin (MMP-3) synthesis is up-regulated in estrogen-deficient mouse osteoblasts in vivo and in vitro. Journal of Bone and Mineral Research *14*, 1880-1890.

Coleman, R. E., and Rubens, R. D. (1987). The clinical course of bone metastases from breast cancer. British Journal of Cancer *55*, 61-66.

Dabovic, B., Chen, Y., Colarossi, C., Zambuto, L., Obata, H., and Rifkin, D. B. (2002). Bone defects in latent TGF-beta binding protein (Ltbp)-3 null mice; a role for Ltbp in TGF-beta presentation. J Endocrinol *175*, 129-141.

Dabovic, B., Levasseur, R., Zambuto, L., Chen, Y., Karsenty, G., and Rifkin, D. B. (2005). Osteopetrosis-like phenotype in latent TGF-beta binding protein 3 deficient mice. Bone *37*, 25-31.

Dallas, S. L., Miyazono, K., Skerry, T. M., Mundy, G. R., and Bonewald, L. F. (1995). Dual role for the latent transforming growth factor-beta binding protein in storage of latent TGF-beta in the extracellular matrix and as a structural matrix protein 6. J Cell Biol *131*, 539-549.

Dallas, S. L., Rosser, J. L., Mundy, G. R., and Bonewald, L. F. (2002). Proteolysis of latent transforming growth factor-beta (TGF-beta)-binding protein-1 by osteoclasts. A cellular mechanism for release of TGF-beta from bone matrix. J Biol Chem *277*, 21352-21360.

de Caestecker, M. P., Parks, W. T., Frank, C. J., Castagnino, P., Bottaro, D. P., Roberts, A. B., and Lechleider, R. J. (1998). Smad2 transduces common signals from receptor serine-threonine and tyrosine kinases. Genes Dev *12*, 1587-1592.

Dean, R. A., and Overall, C. M. (2007). Proteomics discovery of metalloproteinase substrates in the cellular context by iTRAQ labeling reveals a diverse MMP-2 substrate degradome. Mol Cell Proteomics *6*, 611-623.

Dew, G., Murphy, G., Stanton, H., Vallon, R., Angel, P., Reynolds, J. J., and Hembry, R. M. (2000). Localisation of matrix metalloproteinases and TIMP-2 in resorbing mouse bone. Cell and Tissue Research *299*, 385-394.
Dubois, C. M., Laprise, M. H., Blanchette, F., Gentry, L. E., and Leduc, R. (1995). Processing of transforming growth factor beta 1 precursor by human furin convertase. J Biol Chem *270*, 10618-10624.
Dunn, S. E., Hardman, R. A., Kari, F. W., and Barrett, J. C. (1997). Insulin-like growth factor 1 (IGF-1) alters drug sensitivity of HBL100 human breast cancer cells by inhibition of apoptosis induced by diverse anticancer drugs. Cancer Res *57*, 2687-2693.
Erlebacher, A., and Derynck, R. (1996). Increased expression of TGF-beta 2 in osteoblasts results in an osteoporosis-like phenotype. J Cell Biol *132*, 195-210.
Fournier, P. G., Chirgwin, J. M., and Guise, T. A. (2006). New insights into the role of T cells in the vicious cycle of bone metastases. CurrOpinRheumatol *18*, 396-404.
Fowlkes, J. L., Suzuki, K., Nagase, H., and Thrailkill, K. M. (1994). Proteolysis of insulin-like growth factor binding protein-3 during rat pregnancy: a role for matrix metalloproteinases. Endocrinology, 2810-2813.
Georgii-Hemming, P., Wiklund, H. J., Ljunggren, O., and Nilsson, K. (1996). Insulin-like growth factor I is a growth and survival factor in human multiple myeloma cell lines. Blood *88*, 2250-2258.
Goetzl, E. J., Bonda, M. J., and Leppert, D. (1996). Matrix metalloproteinoses in immunity. Journal of Immunology *156*, 1-4.
Guise, T. A., and Mundy, G. R. (1998). Cancer and bone. Endocr Rev *19*, 18-54.
Hauschka, P. V., Mavrakos, A. E., Iafrati, M. D., Doleman, S. E., and Klagsbrun, M. (1986). Growth factors in bone matrix. Isolation of multiple types by affinity chromatography on heparin-Sepharose 2. J BiolChem *261*, 12665-12674.
Holmbeck, K., Bianco, P., Caterina, J., Yamada, S., Kromer, M., Kuznetsov, S. A., Mankani, M., Robey, P. G., Poole, A. R., Pidoux, I*., et al.* (1999). MT1-MMP-deficient mice develop dwarfism, osteopenia, arthritis, and connective tissue disease due to inadequate collagen turnover. Cell *99*, 81-92.
Ignotz, R. A., Endo, T., and Massague, J. (1987). Regulation of fibronectin and type I collagen mRNA levels by transforming growth factor-beta. J Biol Chem *262*, 6443-6446.
Ignotz, R. A., and Massague, J. (1985). Type beta transforming growth factor controls the adipogenic differentiation of 3T3 fibroblasts. Proc Natl Acad Sci U S A *82*, 8530-8534.
Inoue, K., Mikuni-Takagaki, Y., Oikawa, K., Itoh, T., Inada, M., Noguchi, T., Park, J. S., Onodera, T., Krane, S. M., Noda, M., and Itohara, S. (2006). A crucial role for matrix metalloproteinase 2 in osteocytic canalicular formation and bone metabolism. J Biol Chem *281*, 33814-33824.
Itoh, T., Ikeda, T., Gomi, H., Nakao, S., Suzuki, T., and Itohara, S. (1997). Unaltered secretion of beta-amyloid precursor protein in gelatinase A (matrix metalloproteinase 2)-deficient mice. Journal Biological Chemistry *272*, 22389-22392.
Janssens, K., Ten Dijke, P., Janssens, S., and Van Hul, W. (2005). Transforming growth factor-beta1 to the bone 2. EndocrRev *26*, 743-774.
Kakonen, S. M., and Mundy, G. R. (2003). Mechanisms of osteolytic bone metastases in breast carcinoma. Cancer *97*, 834-839.
Kakonen, S. M., Selander, K. S., Chirgwin, J. M., Yin, J. J., Burns, S., Rankin, W. A., Grubbs, B. G., Dallas, M., Cui, Y., and Guise, T. A. (2002). Transforming growth factor-beta stimulates parathyroid hormone-related protein and osteolytic metastases via Smad and mitogen-activated protein kinase signaling pathways. J Biol Chem *277*, 24571-24578.
Koli, K., Ryynanen, M. J., and Keski-Oja, J. (2008). Latent TGF-beta binding proteins (LTBPs)-1 and -3 coordinate proliferation and osteogenic differentiation of human mesenchymal stem cells. Bone *43*, 679-688.

Kusano, K., Miyaura, C., Inada, M., Tamura, T., Ito, A., Nagase, H., Kamoi, K., and Suda, T. (1998). Regulation of matrix metalloproteinases (MMP-2, -3, -9, and -13) by interleukin-1 and interleukin-6 in mouse calvaria: association of MMP induction with bone resorption. Endocrinology *139*, 1338-1345.
Lacey, D. L., Timms, E., Tan, H. L., Kelley, M. J., Dunstan, C. R., Burgess, T., Elliott, R., Colombero, A., Elliott, G., Scully, S.*, et al.* (1998). Osteoprotegerin ligand is a cytokine that regulates osteoclast differentiation and activation. Cell *93*, 165-176.
Lee, J., Weber, M., Mejia, S., Bone, E., Watson, P., and Orr, W. (2001). A matrix metalloproteinase inhibitor, batimastat, retards the development of osteolytic bone metastases by MDA-MB-231 human breast cancer cells in Balb C nu/nu mice. European Journal of Cancer *37*, 106-113.
Lovibond, A. C., Haque, S. J., Chambers, T. J., and Fox, S. W. (2003). TGF-beta-induced SOCS3 expression augments TNF-alpha-induced osteoclast formation. Biochem Biophys Res Commun *309*, 762-767.
Lynch, C. C., Hikosaka, A., Acuff, H. B., Martin, M. D., Kawai, N., Singh, R. K., Vargo-Gogola, T. C., Begtrup, J. L., Peterson, T. E., Fingleton, B.*, et al.* (2005). MMP-7 promotes prostate cancer-induced osteolysis via the solubilization of RANKL. Cancer Cell *7*, 485-496.
Lynch, C. C., and Matrisian, L. M. (2002). Matrix metalloproteinases in tumor-host cell communication. Differentiation *70*, 561-573.
Maeda, S., Dean, D. D., Gay, I., Schwartz, Z., and Boyan, B. D. (2001). Activation of latent transforming growth factor beta1 by stromelysin 1 in extracts of growth plate chondrocyte-derived matrix vesicles. Journal of Bone and Mineral Research *16*, 1281-1290.
Maeda, S., Dean, D. D., Gomez, R., Schwartz, Z., and Boyan, B. D. (2002). The first stage of transforming growth factor beta1 activation is release of the large latent complex from the extracellular matrix of growth plate chondrocytes by matrix vesicle stromelysin-1 (MMP-3). Calcif Tissue Int *70*, 54-65.
Marcelli, C., Yates, A. J., and Mundy, G. R. (1990). In vivo effects of human recombinant transforming growth factor beta on bone turnover in normal mice. J Bone Miner Res *5*, 1087-1096.
Martin, M., Carter, K., Thiolloy, S., Lynch, C. C., Matrisian, L., and Fingleton, B. (2008). Effect of ablation or inhibition of stromal matrix metalloproteinase-9 on lung metastasis in a breast cancer model is dependent on genetic background Cancer Res *68*, E-Pub ahead of print.
Mohan, S., and Baylink, D. J. (1993). Characterization of the IGF regulatory system in bone. Adv Exp Med Biol *343*, 397-406.
Mosig, R. A., Dowling, O., DiFeo, A., Ramirez, M. C., Parker, I. C., Abe, E., Diouri, J., Aqeel, A. A., Wylie, J. D., Oblander, S. A.*, et al.* (2007). Loss of MMP-2 disrupts skeletal and craniofacial development and results in decreased bone mineralization, joint erosion and defects in osteoblast and osteoclast growth. Hum Mol Genet *16*, 1113-1123.
Mundy, G. R. (1997). Mechanisms of bone metastasis. Cancer *80*, 1546-1556.
Nemeth, J. A., Yousif, R., Herzog, M., Che, M., Upadhyay, J., Shekarriz, B., Bhagat, S., Mullins, C., Fridman, R., and Cher, M. L. (2002). Matrix metalloproteinase activity, bone matrix turnover, and tumor cell proliferation in prostate cancer bone metastasis. Journal National Cancer Institute *94*, 17-25.
Noda, M., and Camilliere, J. J. (1989). In vivo stimulation of bone formation by transforming growth factor-beta. Endocrinology *124*, 2991-2994.
Parikka, V., Vaananen, A., Risteli, J., Salo, T., Sorsa, T., Vaananen, H. K., and Lehenkari, P. (2005). Human mesenchymal stem cell derived osteoblasts degrade organic bone matrix in vitro by matrix metalloproteinases. Matrix Biol *24*, 438-447.
Penttinen, C., Saharinen, J., Weikkolainen, K., Hyytiainen, M., and Keski-Oja, J. (2002). Secretion of human latent TGF-beta-binding protein-3 (LTBP-3) is dependent on co-expression of TGF-beta. J Cell Sci *115*, 3457-3468.

Powell, G. J., Southby, J., Danks, J. A., Stillwell, R. G., Hayman, J. A., Henderson, M. A., Bennett, R. C., and Martin, T. J. (1991). Localization of parathyroid hormone-related protein in breast cancer metastases: increased incidence in bone compared with other sites. Cancer Research *51*, 3059-3061.
Saharinen, J., Hyytiainen, M., Taipale, J., and Keski-Oja, J. (1999). Latent transforming growth factor-beta binding proteins (LTBPs)--structural extracellular matrix proteins for targeting TGF-beta action 2. Cytokine Growth Factor Rev *10*, 99-117.
Sato, Y., and Rifkin, D. B. (1989). Inhibition of endothelial cell movement by pericytes and smooth muscle cells: activation of a latent transforming growth factor-beta 1-like molecule by plasmin during co-culture. J Cell Biol *109*, 309-315.
Takuma, A., Kaneda, T., Sato, T., Ninomiya, S., Kumegawa, M., and Hakeda, Y. (2003). Dexamethasone enhances osteoclast formation synergistically with transforming growth factor-beta by stimulating the priming of osteoclast progenitors for differentiation into osteoclasts. J Biol Chem *278*, 44667-44674.
Thomas, R. J., Guise, T. A., Yin, J. J., Elliott, J., Horwood, N. J., Martin, T. J., and Gillespie, M. T. (1999). Breast cancer cells interact with osteoblasts to support osteoclast formation. Endocrinology *140*, 4451-4458.
van Bezooijen, R. L., Roelen, B. A., Visser, A., van der Wee-Pals, L., de Wilt, E., Karperien, M., Hamersma, H., Papapoulos, S. E., ten Dijke, P., and Lowik, C. W. (2004). Sclerostin is an osteocyte-expressed negative regulator of bone formation, but not a classical BMP antagonist. J Exp Med *199*, 805-814.
Winding, B., NicAmhlaoibh, R., Misander, H., Hoegh-Andersen, P., Andersen, T. L., Holst-Hansen, C., Heegaard, A. M., Foged, N. T., Brunner, N., and Delaisse, J. M. (2002). Synthetic matrix metalloproteinase inhibitors inhibit growth of established breast cancer osteolytic lesions and prolong survival in mice. Clinical Cancer Research *8*, 1932-1939.
Yin, J. J., Selander, K., Chirgwin, J. M., Dallas, M., Grubbs, B. G., Wieser, R., Massague, J., Mundy, G. R., and Guise, T. A. (1999). TGF-beta signaling blockade inhibits PTHrP secretion by breast cancer cells and bone metastases development. J Clin Invest *103*, 197-206.
Yu, Q., and Stamenkovic, I. (2000). Cell surface-localized matrix metalloproteinase-9 proteolytically activates TGF-beta and promotes tumor invasion and angiogenesis. Genes and Development *14*, 163-176.

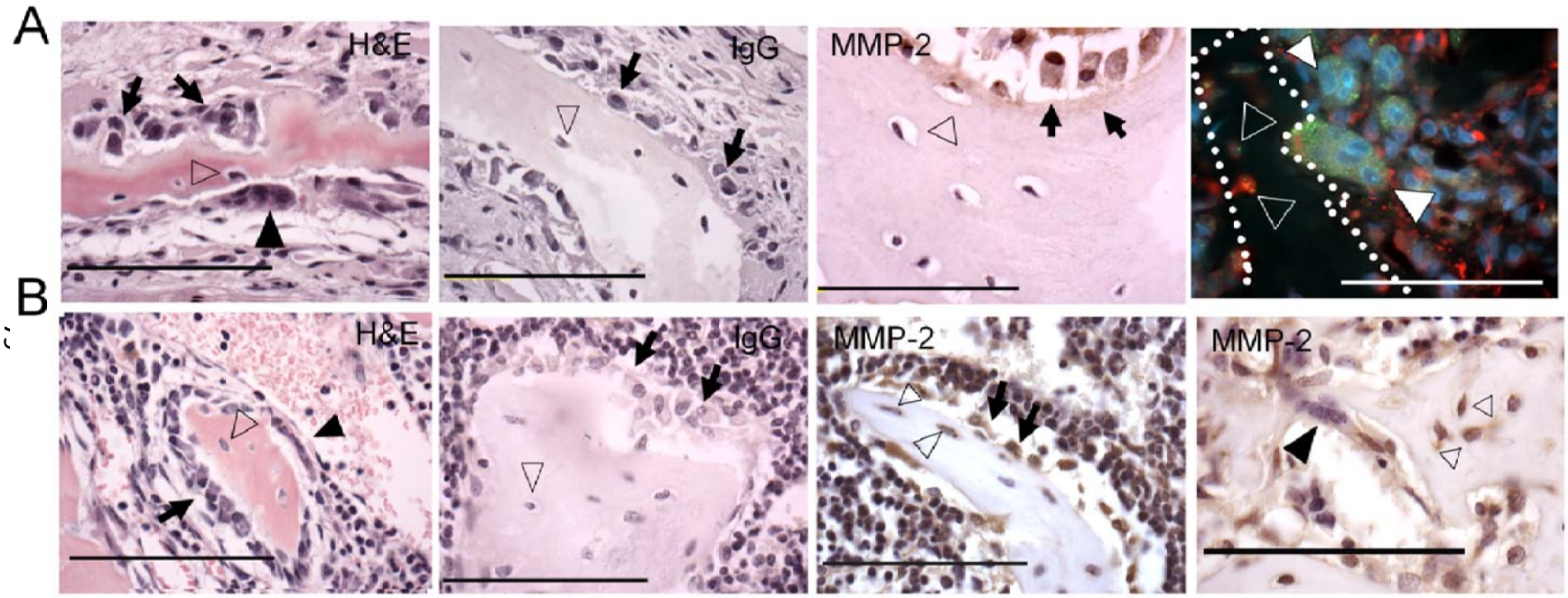

Figure 1. Localization of MMP-2 in human and murine breast-to-bone metastases samples. A-B: Immunohistochemistry for MMP-2. Full arrows indicate osteoblasts, empty arrowheads indicate osteoyctes. Fluorescent TRAP staining (green) was used to localize osteoclasts (full arrowheads arrows) while immunofluorescence was used to localize MMP-2 (red). DAPI (blue) was used as a nuclear stain. Appropriate IgG was used as a negative control . Scale bars are 50μm..

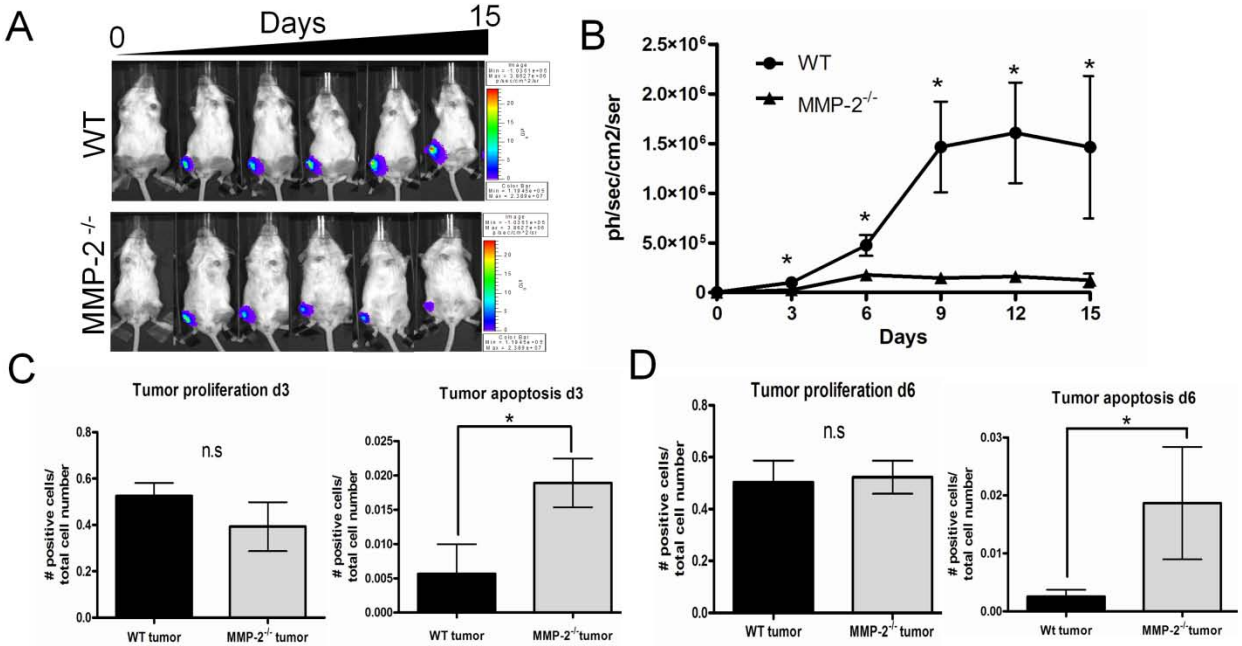

Figure 2. Host-derived MMP-2 impacts mammary tumor growth in the bone microenvironment. A-B: PyMT-Luc cells were intratibially injected into FVB wild type (WT; n=10) or MMP-2 null (MMP-2$^{-/-}$; n=10) mice. The contralateral limb received a sham injection of saline and luciferase activity was assessed as a measure of tumor growth in WT and MMP-2$^{-/-}$ animals. **C:**Tumor proliferation and apoptosis was assessed by immunohistochemical staining for Mcm2 and cleaved caspase-3 respectively, in tumor bearing tibias of WT and MMP-2$^{-/-}$ deficient mice, at 3 days post-surgery. **D:** At 6 days after injection, tumor proliferation and apoptosis was determined by immunohistochemical staining for respectively, MCM2 and cleaved caspase-3 on tumor bearing limbs of WT and MMP-2$^{-/-}$ deficient mice. Data are mean ± SD; n.s. implies a non-significant p value ($p>0.05$).

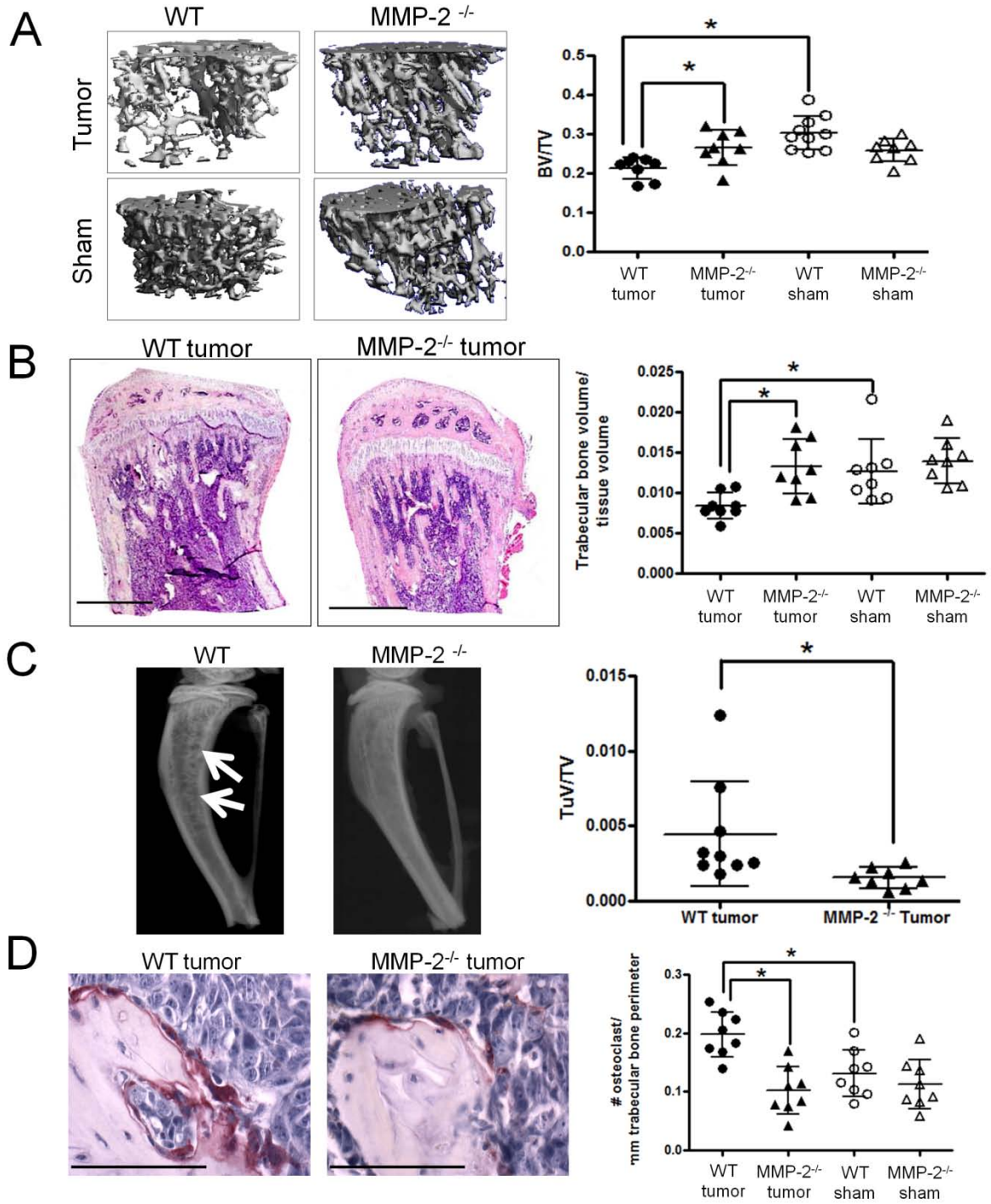

Figure 3. Tumor mediated osteolysis is attenuated in the absence of host derived MMP-2. A: µCT scans of trabecular bone from tumor bearing and sham injected limbs of WT and MMP-2$^{-/-}$ mice allowed for the calculation of the BV/TV ratio. **B:** Representative H&E stained photomicrographs of tumor bearing tibias from WT and MMP-2$^{-/-}$ mice. Scale bars are 1mm. The ratio of trabecular bone volume (BV) to tissue volume (TV) was determined several non-serial sections of tumor injected tibias obtained from WT (n=8) and MMP-2$^{-/-}$ animals (n=8). **C:** Representative radiographic images from tumor injected WT and MMP-2$^{-/-}$ animals at day 9. Arrow indicates lytic tumor lesions in the wild type animals. The tumor volume (TuV) over tissue volume (TV) for tumor injected limbs of WT and MMP-2$^{-/-}$ animals was assessed. Data are mean ± SD. Asterisk denotes that $p<0.05$ while n.s. indicates a non-significant p value.

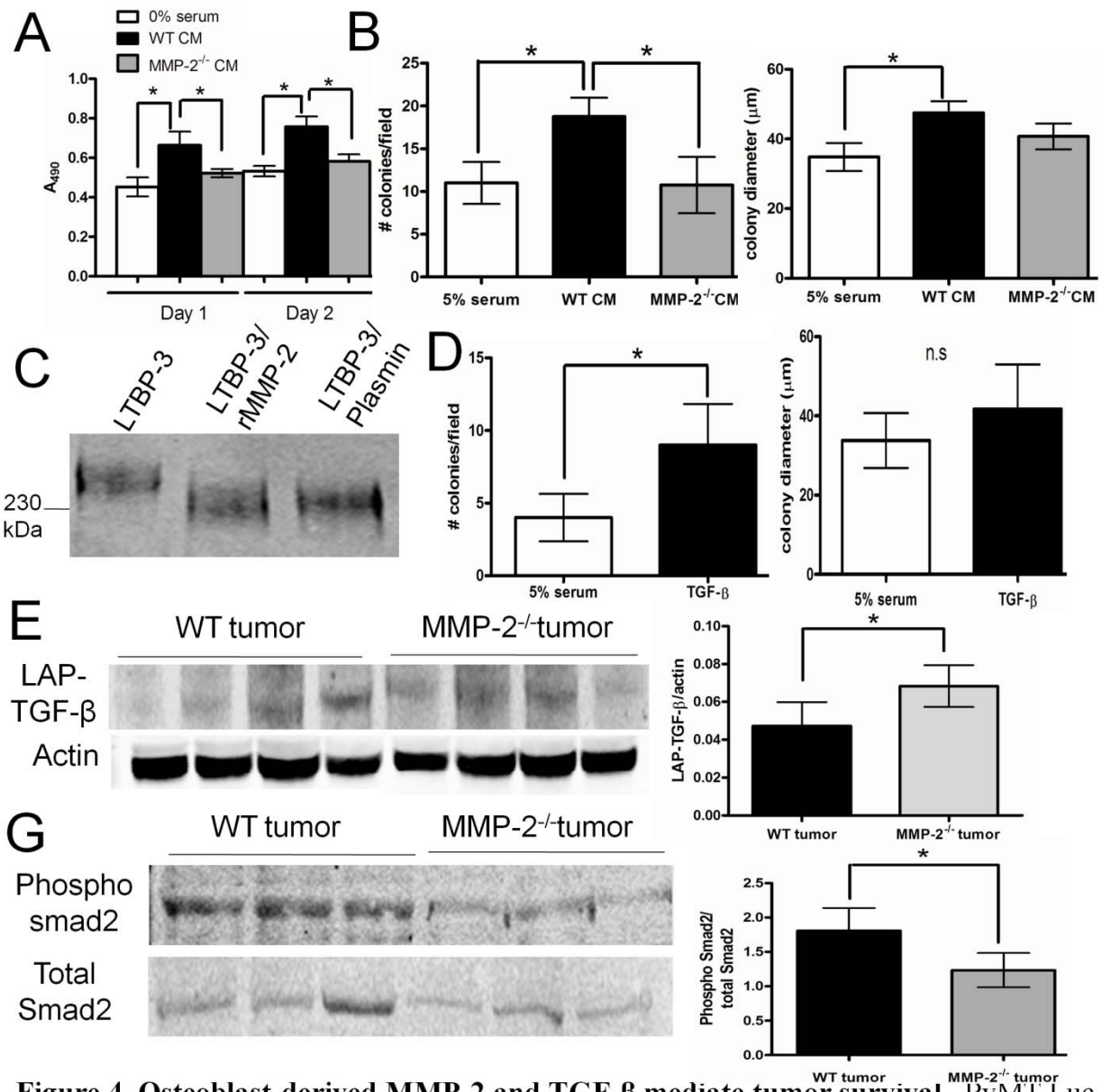

Figure 4. Osteoblast-derived MMP-2 and TGF-β mediate tumor survival. PyMT-Luc cells were treated with conditioned media from wild type (WT CM)or MMP-2 null (MMP-2$^{-/-}$ CM)osteoblasts. **A:** Metabolic activity of PyMT-Luc cells treated with WT CM or MMP-2$^{-/-}$ CM was assessed by MTT assay. **B and D:** Tumor survival and growth in presence of WT CM, MMP-2$^{-/-}$ CM or 1 ng/ml TGF-β was determined by soft agar colony formation assay. **C:** Cleavage assay of LTBP-3 by recombinant MMP-2 or plasmin. **A:** Immunoblotting for LAP-TGF-β and actin in tumor bearing tibias of WT (n=4) and MMP-2 $^{-/-}$ mice (n=4) at 3 days after surgery. **B:** Immunoblotting for phospho and total smad2 tumor injected limbs of wild type (n=3) and MMP-2$^{-/-}$ mice (n=3). Data are mean ± SD. Asterisk denotes that $p<0.05$. Each experiment has been conducted twice on different samples from independent *in vivo* studies. Data are mean ± SD. Asterisk indicates $p<0.05$ and n.s indicates non significance.

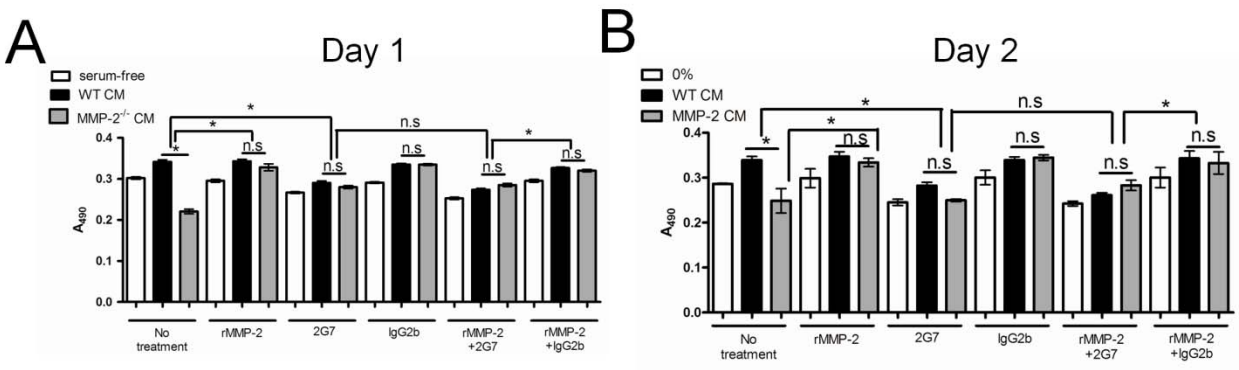

Figure 5. Osteoblast-derived MMP-2 mediates tumor survival via osteoblast-derived TGF-β . PyMT-Luc cells were treated with conditioned media from wild type (WT CM)or MMP-2 null (MMP-2$^{-/-}$ CM)osteoblasts. Ability of the tumor cells to proliferate and survive was assessed by MTT and soft agar colony formation assays. **A and B:** Metabolic activity of PyMT-Luc cells treated with WT CM or MMP-2$^{-/-}$ CM in presence of 2G7 (TGF-β neutralizing antibody), IgG2b (control antibody) or recombinant MMP-2 (rMMP-2) was assessed by MTT assay. Data are mean ± SD. Asterisk indicates $p<0.05$ and n.s indicates non significance.